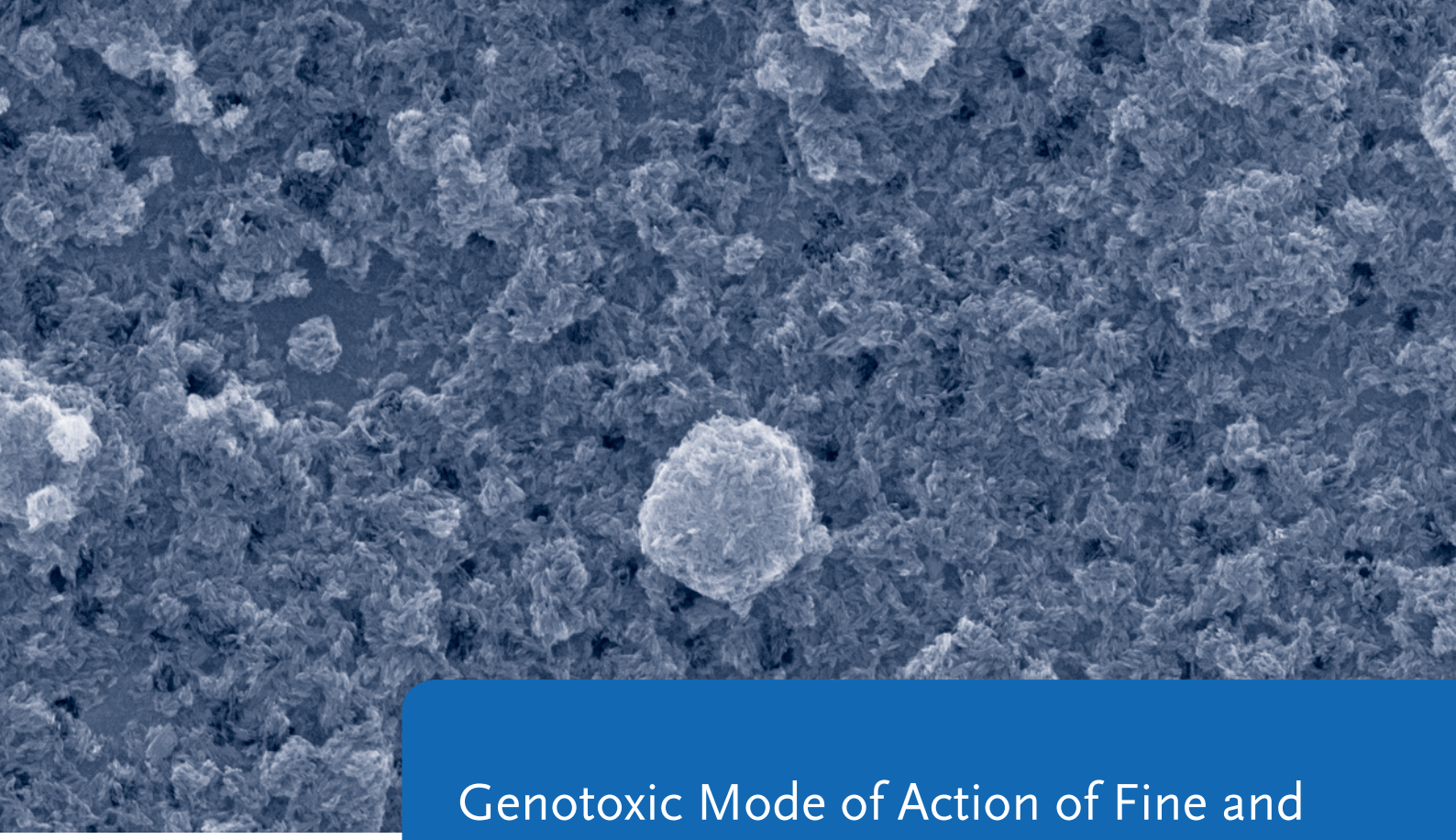

Genotoxic Mode of Action of Fine and Ultrafine Dusts in Lungs

Ch. Ziemann, S. Rittinghausen, H. Ernst, A. Kolling, I. Mangelsdorf, O. Creutzenberg

baua:
Bundesanstalt für Arbeitsschutz
und Arbeitsmedizin

Research
Project F 2135

Ch. Ziemann
S. Rittinghausen
H. Ernst
A. Kolling
I. Mangelsdorf
O. Creutzenberg

Genotoxic Mode of Action of Fine and Ultrafine Dusts in Lungs

Dortmund/Berlin/Dresden 2011

This publication is the final report of the project “Genotoxic Mode of Action of Fine and Ultrafine Dusts in Lungs” – Project F 2135 – on behalf of the Federal Institute for Occupational Safety and Health.
The responsibility for the contents of this publication lies with the authors.

Authors: Dr. Christina Ziemann
Priv.-Doz. Dr. Susanne Rittinghausen
Dr. Heinrich Ernst
Dr. Angelika Kolling
Dr. Inge Mangelsdorf
Dr. Otto Creutzenberg
Fraunhofer Institute for Toxicology and Experimental Medicine (ITEM)
Nikolai Fuchs Str. 1, 30625 Hannover, Germany
Telephone +49 511 5350-461
Fax +49 511 5350-155

Project Manager: Dr. Otto Creutzenberg
Fraunhofer Institute for Toxicology and Experimental Medicine (ITEM)

Cover photo: Sabine Plitzko
Federal Institute for Occupational Safety and Health

Cover design: Rainer Klemm
Federal Institute for Occupational Safety and Health

Publisher: Federal Institute for Occupational Safety and Health
Friedrich-Henkel-Weg 1-25, 44149 Dortmund, Germany
Telephone +49 231 9071-0
Fax +49 231 9071-2454
poststelle@baua.bund.de
www.baua.de

Berlin:
Nöldnerstr. 40-42, 10317 Berlin, Germany
Telephone +49 30 51548-0
Fax +49 30 51548-4170

Dresden:
Fabricestr. 8, 01099 Dresden, Germany
Telephone +49 351 5639-50
Fax +49 351 5639-5210

Contents

Genotoxic Mode of Action of Fine and Ultrafine Dusts in Lungs

Abstract

This project aimed at studying local genotoxicity of fine and ultrafine particles in lung epithelial cells by evaluating the current literature and by using an immunohistochemical approach on existing lung tissue samples from (nano)particle-exposed animals.
Local genotoxicity was assessed by applying immunhistochemical detection and subsequent quantification of different markers for DNA damage in lung tissue samples from a study previously conducted at Fraunhofer ITEM. In this study rats were exposed intratracheally for 3 months to 3 x 2 mg crystalline silica (DQ12, 1300 nm), 3 x 2 mg amorphous silica (Aerosil® 150, 14 nm), or 3 x 6 mg carbon black (PRINTEX® 90, 14 nm). Furthermore, a carcinogenicity study with intratracheal instillation of the same particles (but different particle doses) was available at Fraunhofer ITEM. In parallel, 3-month data concerning bronchoalveolar lavage (BAL) and histological data on inflammation existed allowing correlation of genotoxicity marker expression with the outcome of this carcinogenicity study and with alterations in the lung after 3 month of exposure, respectively. The following genotoxicity markers were selected: Poly(ADP-Ribose) (PAR), phosphorylated H2AX (γ-H2AX), 8-hydroxy-2´-deoxyguanosine (8-OH-dG), and 8-oxoguanine DNA glycosylase (OGG1). PAR indicates early cellular reaction to DNA damage, γ-H2AX DNA double strand breaks (DSB), 8-OH-dG a specific oxidative DNA-base modification (one of several existing), and OGG1 repair capacity related to oxidative damage.
For quartz DQ12 all biomarkers gave statistically significant positive results, indicating profound genotoxic stress, occurrence of DSB, and oxidative DNA damage with subsequent repair activity. The response was less pronounced for PRINTEX® 90 (carbon black), but significant increase in DSB, 8-OH-dG, and OGG1-positive cytoplasm were detected. Finally, for Aerosil® 150 (amorphous silica), only 8-OH-dG levels and repair activity of oxidative DNA damage, as represented by OGG1 expression in the cytoplasm, were statistically significant. The marker which was most sensitive, differentiated best between the three particles, and correlated well with the carcinogenicity data was γ-H2AX. 8-OH-dG correlated best with the inflammation score. The findings also generally correlated with positive or negative results in the *in vitro* and *in vivo* literature data on genotoxicity of these three particles and with carcinogenicity data.
In conclusion, this study demonstrated that using immunohistochemical detection and quantification of different genotoxicity markers in lung tissue samples could be a promising approach for testing local genotoxicity and the genotoxic modes of action of particles in the lung.

Key words:

Nanoparticles, *in vivo* genotoxicity, carbon black, amorphous silica, crystalline silica, oxidative DNA damage, immunohistochemical detection, genotoxicity marker, γ-H2AX, Poly(ADP-Ribose)

Gentoxischer Wirkungsmechanismus von Fein- und Ultrafeinstäuben in der Lunge

Kurzreferat

Im vorliegenden Projekt wurde die lokale Gentoxizität von Fein- und Ultrafeinstäuben in Lungenepithelzellen untersucht. Nach Literaturauswertung wurde experimentell ein immunohistochemischer Ansatz gewählt, um vorhandene Lungengewebsproben von (nano)partikelexponierten Tieren aus einer Fraunhofer ITEM-Studie bezüglich lokaler Gentoxizität analysieren zu können.
Die lokale Gentoxizität wurde durch immunohistochemische Detektion und nachfolgende Quantifizierung von verschiedenen DNA-Schädigungs-Marker im Lungengewebe untersucht. In der Originalstudie wurden die Ratten intratracheal über 3 Monate mit 3 x 2 mg kristallinem Siliziumdioxid (DQ12, 1300 nm), 3 x 2 mg amorphem Siliziumdioxid (Aerosil® 150, 14 nm), oder 3 x 6 mg Testruß (PRINTEX® 90, 14 nm) behandelt. Außerdem standen die Ergebnisse einer Kanzerogenitätsstudie mit intratrachealer Instillation derselben Partikeln (jedoch unterschiedlichen Partikeldosen) im ITEM zur Verfügung und es lagen 3-Monats-Daten bezüglich bronchoalveolärer Lavage (BAL) und Histologie zur Entzündungsreaktion vor, die eine Korrelation der Gentoxizitätsmarker-Expression mit den Ergebnissen der Kanzerogenitätsstudie und mit den Lungenbefunden nach 3 Monaten Exposition ermöglichten. Die folgenden Marker wurden ausgewählt: Poly(ADP-Ribose) (PAR), phosphoryliertes H2AX (γ-H2AX), 8-Hydroxy-2´-desoxyguanosin (8-OH-dG) und 8-Oxoguanin-DNA-Glycosylase (OGG1). PAR zeigt frühe Zellreaktionen bei DNS-Schäden an, γ-H2AX primär DNA Doppelstrangbrüche (DSB), 8-OH-dG eine häufige, prämutagene oxidative DNA-Basenmodifikation und OGG1 die Reparaturkapazität bezüglich oxidativer Schäden.
Bei Quarz DQ12 ergaben alle Biomarker statistisch signifikante positive Ergebnisse, die prägnanten gentoxischen Stress, das Entstehen von DSB und oxidativen DNS-Schäden mit korrespondierender Reparaturaktivität anzeigten. Die gentoxische Antwort auf Partikelexposition war bei PRINTEX® 90 (Testruß) weniger deutlich ausgeprägt, aber es wurden dennoch signifikante Erhöhungen an DSB und 8-OH-dG positiven Kernen und OGG1-positivem Zytoplasma detektiert. Bei Aerosil® 150 (amorphes Siliziumdioxid) waren nur die 8-OH-dG-Werte und die OGG-1 abhängige Reparaturaktivität (angezeigt durch die OGG1-Expression im Zytoplasma) statistisch signifikant erhöht. γ-H2AX war der Marker mit der größten Sensitivität und den besten Differenzierfähigkeiten und korrelierte gut mit den Kanzerogenitätsdaten. 8-OH-dG korrelierte am besten mit dem Entzündungsgrad nach 3 Monaten Exposition. Die Ergebnisse korrelierten generell mit positiven oder negativen Ergebnissen aus der *in vitro* und *in vivo* Literatur zur Gentoxizität dieser drei Partikeltypen und mit entsprechenden Kanzerogenitätsdaten.
Die immunohistochemische Detektion und Quantifizierung verschiedener Gentoxizitätsmarker in Lungengewebsproben könnte ein vielversprechender Ansatz zur Analyse auf Gentoxizität und gentoxische Mechanismen in der Lunge sein.

Schlagwörter:

Nanopartikel, *In-vivo*-Gentoxizität, Carbon Black, amorphes Siliziumdioxid, kristallines Siliziumdioxid, oxidative DNA-Schäden, immunhistochemische Detektion, Gentoxizitätsmarker, γ-H2AX, Poly(ADP-Ribose)

1 Introduction

1.1 Carcinogenicity

Carcinogenicity studies (SAFFIOTTI et al., 1988; WIESSNER et al., 1989; DONALDSON et al., 1998; MUHLE et al., 1989; NIKULA, 2000; ROLLER, 2009) demonstrated that exposure of lungs to various respirable fine and ultrafine particles can lead to the induction of fibrosis and the development of lung tumours, in particular in the rat model. These findings were confirmed by several studies with intratracheal instillation of particles. There are indications that the particle surface is one important factor in determining the carcinogenic potential of particles (OBERDÖRSTER et al., 2005; DUFFIN et al., 2007). Therefore, there is concern, that nanoparticles, based on their proportionally large surface area compared to particle mass, may also be potent carcinogens in the lung. Most recently an extensive study with intratracheal application of insoluble particles of different composition, also including nanoparticles, pointed in this direction (POTT et al., 2003, 2005). However, the mechanisms leading to the development of lung tumours and the contribution of genotoxic effects are not clearly elucidated.
As the induction of genotoxic effects after uptake of particles in the lung follows multifactorial mechanisms, it can only be understood in diverse models. In addition to the physico-chemical properties of the particles, an analysis of the inflammatory situation is crucial which is determined mainly by deposition/retention and clearance of the particles. Various genotoxic endpoints are used to elucidate mechanistic principles of particle-induced inflammation and tumour development. The assessment of the genotoxic potential of particles poses a particular challenge, because, in contrast to chemicals and drugs, low soluble particles do not act as individual molecules or ions, but more likely seem to act in a physico-mechanical (by the particle itself) and/or physico-chemical (due to specific properties of the particle surface) manner, thus rendering elucidation of particle-induced genotoxicity a special discipline in toxicological research.

1.2 Mode of Action

Several modes of action have been discussed to describe and explain the carcinogenic potential of particles, including genotoxicity. Possible genotoxic effects of fine and ultrafine dusts *in vivo* are thought to comprise primary particle-related, and secondary, phagocytosis- and/or inflammation-related mechanisms. Postulated particle-dependent genotoxic modes of action have been summarized earlier by KNAAPEN et al. (2004) and are presented in Fig.1.1:

1. Activation of phagocytic oxidative burst (secondary genotoxicity)
2. Generation of reactive oxygen species (ROS) or reactive nitrogen species (RNS) in the target cells themselves (indirect primary genotoxicity)
    a. *via* activation of NAD(P)H-like enzymes
    b. *via* reactive particle surfaces
    c. *via* mitochondrial activation/disturbance of the respiratory chain
    d. *via* particle-associated soluble (transition) metals (ROS via Haber-Weiss reaction)

3. Adsorbed primary genotoxic compounds (such as PAHs) can be bound to and damage DNA
4. Translocation of ultrafine particle into the nucleus and DNA damage by surfacebound radicals or physical interaction with genomic DNA (direct primary genotoxicity)

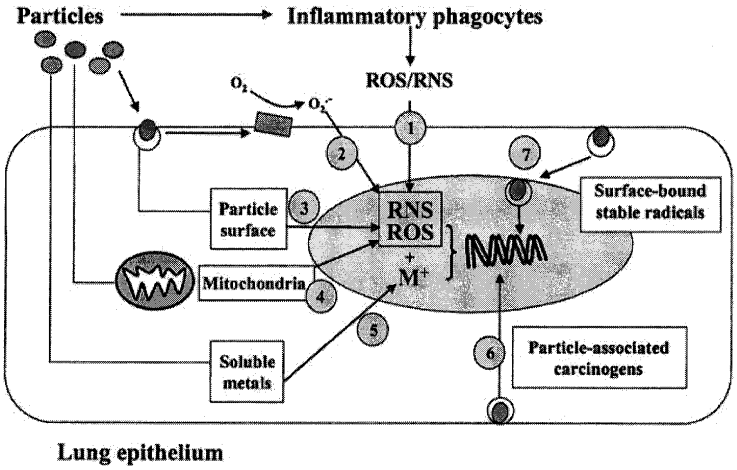

Fig. 1.1 Possible mechanisms of particle-induced DNA damage (adapted from KNAAPEN et al., 2004)

In view of these hypothesized diverse modes of action of fine and ultrafine particles, two approaches have been followed in the present project concerning the (genotoxic) mode of action of fine and ultrafine particles in lungs:

1) An overview was performed of the existing literature on genotoxicity of nanoparticles with focus on selected particles (titanium dioxide TiO_2, C_{60} fullerenes, carbon black, and amorphous as well as crystalline silicon dioxide SiO_2).
2) A novel, experimental *in situ* immunohistochemical approach to analyse and quantify local genotoxicity of particles in lung epithelium of animals treated intratracheally with different fine and ultrafine particles has been developed and checked concerning its feasibility and also concerning its informative value by correlating immunohistochemical data with, e.g., simultaneously obtained histological data on lung inflammation or data from bronchoalveolar lavage (BAL). Data on local genotoxicity could also be compared to tumour development after lifetime exposure of rats to the same types of particles.

2 Evaluation of Literature on Genotoxicity of selected nanoparticles

2.1 Introduction

Several reviews are available, which present an overview and a critical discussion of genotoxicity studies with engineered nanomaterials (GONZALEZ et al., 2008; LANDSIEDEL et al., 2009; SCHINS et al., 2007; SINGH et al., 2009). A comprehensive review paper has recently been issued by GONZALEZ et al. (2008). Regarding carbon black (CB), silica (SiO_2, especially crystalline silica), and titanium dioxide (TiO_2), GONZALEZ et al. (2008) reviewed 11 *in vitro* studies. Other comprehensive review papers were presented by ECETOC (2006) on synthetic amorphous silica and recently on the nanoparticle classes of fullerenes, carbon nanotubes (CNTs), metals and metal oxides (ENRHES REPORT, 2010).
The literature search in the present project focused on updating and completing the literature from 2005 to 2009 on genotoxicity of amorphous and crystalline silica, carbon black, C_{60} fullerenes, and TiO_2, including, in addition, some older studies with nanoparticles not reported by GONZALEZ et al. (2008). The search results summarized below are presented in more detail and in tabular form in Appendix I. To enable a better comparison with the immunohistochemical analyses of the present research project and to allow for a better evaluation of the experimental data on local genotoxicity studies on the genotoxic potential of quartz DQ-12 were also evaluated, even though, due to its larger size (about 1.3 µm), quartz DQ12 does not belong to the group of nanoparticles.
The results of the individual studies are presented in the tables in Appendix I.

2.2 Results and Conclusions

2.2.1 Silica

2.2.1.1 Crystalline Silica (Quartz DQ-12)

Four recent studies on *in vitro* genotoxicity of DQ 12 were identified in the literature search. All studies provided evidence of DQ12-induced genotoxicity (LI et al., 2007; GEH et al., 2006; SCHINS et al., 2002; CAKMAK, 2004). The investigated endpoints in these studies were DNA-strand breaks (comet assays, all studies), increase of 8-OH-dG (LI et al., 2007; SCHINS et al., 2002), and induction of micronuclei (GEH et al., 2006). The tested mass doses ranged from 10 µg/cm^2 to 200 µg/cm^2. With the exception of the study of SCHINS et al. (2002), genotoxicity was observed only at cytotoxic concentrations. In two studies it was further demonstrated that genotoxicity is associated with the generation of ROS, based on the detection of 8-OH-dG (LI et al., 2007; SCHINS et al., 2002). In addition, it was shown that DQ-12 is taken up by cells *in vitro* and is located in the cytoplasm, either encapsulated in membranes or uncovered. The particles were neither found in the nucleus nor in mitochondria. Thus, direct interaction with the DNA was not considered as plausible mechanism for the genotoxic effects (LI et al., 2007). However, DANIEL et al., (1995) could demonstrate nuclear localization of two different α-quartz in FRLE cells (alveolar Type II cell line

derived from fetal lungs) as well as direct interaction of surface silanol groups with the DNA-backbone in acellular experiments with isolated DNA. The positive results observed with quartz DQ12 are supported by studies with other α-quartz preparations. Furthermore, *in vivo* studies indicate a genotoxic potential of α-quartz as well as lung tumour induction following chronic exposure (e.g. after exposure to quartz DQ12). However, other genotoxicity tests *in vitro* like sister chromatid exchange (SCE) and chromosome aberrations (CA) did not show genotoxic effects of such quartz preparations (GREIM, 1999; WHO, 2000).

2.2.1.2 Crystalline Silica Nanoparticles

Only two publications on *in vitro* genotoxicity of nano-sized/ultrafine crystalline silica (quartz) are available. In both studies, the comet assay was performed. In the study of YANG et al. (2009), using primary mouse embryo fibroblasts, DNA-damage was observed at the non-cytotoxic concentration of 10 µg/ml, while in the study of WANG et al. (2007b) the comet assay experiments with a human B-cell lymphoblastoid cell line showed no genotoxic effect at 120 µg/ml, a concentration already cytotoxic, as determined by the MTT assay. A significant genotoxic potential of these particles was however detected in an HPRT-test (lowest effective concentration 30 µg/ml for 24 h) and also in an *in vitro* micronucleus test (at 120 µg/ml for 24 h). In the study of YANG et al. (2009) genotoxicity of crystalline SiO_2 was associated with intracellular oxidative stress as indicated by particle-induced glutathione depletion, malondialdehyde production, inhibition of superoxide dismutase, and intracellular generation of ROS.

2.2.1.3 Amorphous Silica Nanoparticles

Only one study could be identified, where amorphous silica nanoparticles were investigated (BARNES et al., 2008). This study involved 2 different types of nanoparticle amorphous silica which were synthesized for this study. Both were not genotoxic as evaluated in the comet assay with 3T3-L1 fibroblasts in two different laboratories, at dose levels up to 40 µg/mL. In addition, these particles exhibited no cytotoxicity at dose levels up to 40 µg/mL as measured by MTT-, WST-1- and LDH-assays. Cytotoxic particle concentrations, which might have led to genotoxic effects in studies with other particles, were not tested in this study.
In a micronucleus assay with peripheral blood from rats exposed nose only to up to 86 mg/m^3 freshly generated amorphous silica nanoparticles for up to 3 days, no genotoxicity was observed at non cytotoxic concentrations. No effects were also seen in cells and proteins from BAL and lung histopathology up to 2 months after exposure (SAYES et al., 2010).

2.2.2 Carbon Black Nanoparticles

Most of the *in vitro* studies with carbon black (CB) nanoparticles and mammalian cells were conducted with particles of a primary particle size of 14 nm or similar. All these studies used some measures for cytotoxicity ensuring that the assays were performed at non- or marginally cytotoxic concentrations of CB (MROZ et al., 2008; JACOBSEN et al., 2007, 2008; YANG et al., 2009; TOTSUKA et al., 2009). The studies differed in a number of details, mostly the cell type, incubation time, and the incubation conditions. Unfortunately, the agglomeration state of the particles was not well defined. However, these studies provided consistent evidence that CB induces ROS

formation and oxidative stress (JACOBSEN et al., 2008; YANG et al., 2009). The formation of ROS may lead to oxidative DNA damage as indicated by a number of studies which also consistently showed that CB induces *in vitro* DNA single-strand but not double-strand breaks. Fewer data are available regarding the particle-mediated induction of mutations (JACOBSEN et al., 2007) or micronuclei (TOTSUKA et al., 2009) *in vitro.* These *in vitro* observations could be confirmed *in vivo* in lung tissue or BAL cells from animals exposed to CB by intratracheal instillation (DRISCOLL et al., 1997; JACOBSEN et al., 2009; TOTSUKA et al., 2009) or inhalation (JACOBSEN et al., 2009; SABER et al., 2005; DRISCOLL et al., 1996; GALLAGHER et al., 2003). The spectrum of CB-induced *in vivo* effects included the formation of oxidative DNA-damage in lung tissue (GALLAGHER et al., 2003) and DNA single-strand breaks in comet assays with BAL cells (JACOBSEN et al., 2009; SABER et al., 2005) or lung cells (TOTSUKA et al., 2009). The genotoxic effects were observed at concentrations or doses causing lung inflammation. One study showed that the particle size may affect the activity of the CB particle to induce oxidative DNA-damage, with smaller CB particles being more effective than larger ones (GALLAGHER et al., 2003). Furthermore, DNA damage was observed in lungs of C57BL/6J mice by the alkaline comet assay, and the Spi^- mutation frequency in the lung in *gpt* delta mice was increased, after intratracheal instillation of CB particles, but without reaching statistical significance (TOTSUKA et al., 2009).

2.2.3 C_{60} Fullerene

Few data were available regarding the genotoxicity of C_{60} fullerene *in vitro* or *in vivo*. No ROS-, but RNS-formation was observed in two different studies using different assay conditions (JACOBSEN et al., 2008; XU et al., 2009). DNA-single strand breaks were only observed in an enzyme-modified alkaline comet assay (JACOBSEN et al., 2008). TOTSUKA et al. (2009) demonstrated significant and concentration-dependent induction of micronuclei by C_{60} fullerene in the lung epithelial cancer cell line A549 in the absence of growth inhibition. Micronucleus frequency was markedly more pronounced for the fullerene than for CB in the same experiments. In addition, XU et al. (2009) showed dose-dependent increase in mutation frequency in *gpt* delta transgenic mouse primary embryo fibroblasts. Limited data concerning genotoxicity of C_{60} fullerene are available from *in vivo* studies with intratracheal (JACOBSEN et al., 2009) or oral administration (FOLKMANN et al., 2009). The results of these studies indicate some potential of C_{60} fullerene for the induction of oxidative DNA damage, DNA single-strand breaks, mutations or of other parameters, which indicate genetic damage. In addition, TOTSUKA et al. (2009) demonstrated an increase in the mutation frequency in lungs of *gpt* delta mice after intratracheal instillation of C_{60} fullerene. Overall, C_{60} fullerenes seem to possess a genotoxic potential.

2.2.4 Titanium Dioxide (TiO_2) Nanoparticles

Nanosized TiO_2 may induce the formation of ROS (PARK et al., 2008, BATTACHARYA et al., 2008, 2009; KANG et al., 2008), oxidative DNA damage (BATTACHARYA et al., 2009) , DNA single strand breaks in comet assays (GOPALAN et al., 2009; GURR et al., 2005; BATTACHARYA, 2009; KANG et al., 2008; KARLSSON et al., 2008; REEVES et al., 2008; WANG et al., 2007a), mutations in the HPRT test (WANG et al., 2007a) or in cells from gpt delta transgenic mice *in vitro* (XU et al. 2009), and micronuclei (KANG et al., 2008; BATTACHARYA et al., 2008; RAHMANN et al., 2002; WANG et al., 2007a) in

mammalian cells *in vitro*. However, various nanosized TiO_2 particles of different size, crystal modification and coating did not induce chromosome aberrations (CA) in different cell lines (THEOGARAJ et al., 2007, WARHEIT et al., 2007).
The influence of the particle size on genotoxicity was demonstrated in several studies. Nanosized TiO_2 (≤ 20 nm) caused induction of micronuclei in cytokinesis-blocked cells or in assays with kinetochor-staining, while "larger" fine particles (> 200 nm) were inactive (GURR et al., 2005; RAHMANN et al., 2002). Similarly, DNA strand breaking activity as assessed by use of the alkaline comet assay was observed with TiO_2 primary particles ≤ 70 nm (GOPOLAN et al., 2009; GURR et al., 2005; KANG et al., 2008; KARLSSON et al., 2008), but not with obviously "larger" nanoparticles (< 100 nm, > 200 nm) (BHATTACHARYA et al., 2009; GURR et al., 2005).
Studies with 40 – 70 nm sized anatase provided evidence of a photogenotoxic effect of TiO_2, as this effect, observed in blood lymphocytes, was more pronounced when the assay was simultaneously irradiated. This photogenotoxic effect seemed also to be dependent on the cell type, as in the same study (GOPALAN et al., 2009) the material indeed mediated a genotoxic effect in comet assays with human sperm cells, but the effect in this cells was not altered by parallel irradiation. In another study, 200 nm anatase particles induced oxidative DNA damage only in the presence of light (GURR et al., 2005). However, smaller anatase nanoparticles (10 and 20 nm) induced oxidative stress also in the absence of light. Thus, it seems possible that the smaller the particle is, the more effectively it could induce oxidative damage, even without activation by light.
Limited data further indicate that the genotoxicity *in vitro* may be modified by altering the surface characteristics of the particles (BHATTACHARYA et al., 2008).
Very limited *in vivo* data provide no evidence of oxidative DNA damage by inhalation exposure of rats to nanosized TiO_2 (MA-HOCK et al., 2009). Various genotoxic effects (the most sensitive parameter being the induction of γ-H2AX-foci indicating DNA double strand breaks) were observed after oral exposure to nanosized TiO_2 (TROUILLER et al., 2009). However, the effects were mostly weak and the results have to be confirmed in additional studies before further conclusions regarding the *in vivo* genotoxicity of nano-TiO_2 can be drawn from these few data.

2.2.5 Conclusion

In *in vitro* studies, comet assays and micronucleus assays with a thorough investigation of cytotoxicity have been used frequently for assessing the genotoxicity of nanoparticles. The data indicate a genotoxic potential of nanoparticles, with the exception (based on limited data) of amorphous silica. The effects are usually more pronounced for nanoparticles than for larger particles of similar chemical composition and structure.
The existing literature data on *in vivo* genotoxicity of the examined nanoparticles are insufficient for further evaluation. Especially studies investigating local genotoxicity in the lung are missing for most of the nanoparticles.
For conclusion from the literature data concerning the genotoxic potency of the three particle types (crystalline silica, amorphous silica, and carbon black), which were evaluated in the experimental part of this project, see Section 6.5.

3 Immunohistochemical Detection of local Genotoxicity in vivo

3.1 Project Idea

In the present research project, a completely new approach to analyze and quantify the *in vivo* genotoxic potential of fine and ultrafine particles in lungs, especially in lung epithelium, was followed and checked for its feasibility. The project idea was to use *in situ* immunohistochemical detection and quantification of DNA-damage in paraffin-embedded lung tissue samples of existing studies, by using a panel of genotoxicity markers with different informative value. This approach seemed to enable new insights into the genotoxic potential of fine and ultrafine particles in the lung and also into involved mechanisms by correlating genotoxicity data with already existing data on toxicity, inflammation and carcinogenicity. As several carcinogenicity studies with particles were performed at Fraunhofer ITEM, lung tissue samples for examination were available without onset of a new *in vivo* study.
The experimental design was focused on assessment of feasibility and the informative value of immunohistochemical detection and quantification by image analysis of relevant markers for genotoxicity in paraffin-embedded lung tissue samples (with focus on lung epithelial cells) of animals exposed to fine or ultrafine particles. It was decided to base the project on an existing carcinogenicity study conducted at Fraunhofer ITEM, which offered, in addition, adequately fixed lung tissue samples from rat satellite groups that had been subacutely/subchronically exposed for 1, 3, or 9 months to various dusts by intratracheal instillation. In this study one fine dust (crystalline SiO_2: quartz DQ12) with a confirmed carcinogenic potential in rats and humans and two ultrafine, nanoscaled dusts (carbon black: PRINTEX® 90; amorphous SiO_2: Aerosil® 150) were included. The study aimed at inducing comparable overload* scenarios for all three different granular dusts. For this reason, the applied mass doses were not identical for the different particles. Interestingly, within the lifetime part of the study, all particle-treated groups developed tumours, but with differentiated tumour rates, as shown by using standard microscopy (see Table Appendix III-1 and KOLLING et al. 2010, in preparation) and in particular multiple step sections (KOLLING et al., 2008). Within the present research project, however, only the tumour data generated by standard microscopy were considered for comparison of the tumour data with the data on genotoxicity marker expression.
* Note: "Lung overload" of the rat lung has been investigated in a comprehensive study on toner powder (inert dust type) using radioactively tagged aerosols to analyse the retardation of macrophage-mediated particle clearance. In a 10 (low) and 40 mg/m^3 (high) exposure group 0.4 mg and 3.0 mg/lung were retained in lungs after 3 months. A clear overload was found in the high dose group in terms of alveolar clearance as the physiological clearance was substantially retarded with no recovery within a 6-month post-exposure period [Bellmann B et al., Environm Health Persp 97: 189 (1992)].

A huge number of different data were available from this study, comprising:

- Histopathological determination of inflammation (inflammation score) after 3 months of exposure.
- Endpoints of organ damage and inflammation in bronchoalveolar lavage

(BAL)-fluid after 3 months of exposure.
- E*x vivo* reactivity of alveolar macrophages [zymosane or lipopolysaccharide (LPS)-stimulated liberation of reactive oxygen species (ROS) or reactive nitrogen species (NOx) , and TNF-α] after 3 months of exposure.
- Tumour incidences after chronic, lifetime exposure.

These existing data were very encouraging concerning detection of correlations between local genotoxicity in lung epithelium as target tissue for lung tumour development and organ pathophysiology and thus seemed to be one pre-requisite to enable some conclusions concerning the genotoxic mode of action of fine and ultrafine particles in the overload situation, if appropriate methods of local detection and quantification of relevant mechanism-addressed genotoxicity markers would be applied.
The well-established genotoxicity markers poly(ADP-ribose) (PAR, marker for general modifications of genomic DNA), phosphorylated H2AX (γ-H2AX, marker for manifested DNA amage, especially DNA double-strand breaks), and 8-hydroxy-2'-deoxy-guanosine and 8-oxoguanine DNA glycosylase (8-OH-dG and OGG1, markers for oxidative DNA-damage and subsequent DNA-repair activity) were selected for immunohistochemical detection and quantification in the available lung tissue samples (primarily from animals exposed for 3 months to the particles, the 1 and 9 month tissue samples were only stained and roughly screened), with appropriate marker-adapted methods to be set-up at Fraunhofer ITEM.
Establishment of adequate and reliable immunohistochemical methods for the detection of different genotoxicity markers and feasibility of their quantification in paraffin-embedded lung tissue samples would enable, in the future, to re-evaluate existing lung samples of *in vivo* studies with fine and ultrafine particles concerning mechanisms of particle-induced genotoxicity in lung tissue. Providing that the organs are suitably fixed, such methods, in addition, would allow for integration of mechanistically oriented genotoxicity endpoints in *in vivo* toxicity and carcinogenicity studies with particles to further enlarge the body of knowledge concerning the genotoxic modes of action of fine and ultrafine particles.

3.2 Significance of Chosen Markers for Genotoxicity

In the present project poly(ADP-Ribose) (PAR), phosphorylated H2AX (γ-H2AX), 8-hydroxy-2'-deoxyguanosine (8-OH-dG), and 8-oxoguanine DNA-glycosylase (OGG1) were chosen as markers for genotoxicity with mechanistic virtue.

Poly(ADP-ribose) (PAR), a polymer of ADP-ribose**,** is synthesized by dimers of activated poly(ADP-Ribose) polymerases (PARP), in particular PARP-1, and represents a covalent posttranslational modification impacting on acceptor function. Also, non-covalent interactions between PAR and proteins have been reported. Activation of PARP-1 and attachment of PAR to target proteins like histones, topoisomerases, DNA repair proteins, transcription factors, or PARP-1 itself have been described mainly as immediate early reactions on DNA-damage. In general, PARP-activation is in need of free, nicked DNA-ends (DNA-single or -double strand breaks). However, some authors hypothesized that PARP-activation/PAR synthesis may also occur in the absence of DNA-damage and that it is additionally involved in inflammatory processes and also in regulation of cell division, cell cycle progression, and cell proliferation (for review see HAKMÉ et al., 2008). As the ribosylation reaction can consume

substantial amounts of NAD^+ and ATP, over-activation of PARP-1 by oxidative or nitrosative stress may lead to rapid depletion of metabolic substrates, slowing of glycolysis and mitochondrial respiration with resulting energy failure, and finally necrotic cell death. Thus, the catalytic function of PARP-1 may prevent repair of severely damaged cells and surviving with high number of mutations. But PAR seems also to be able to directly trigger cell death and to be important for the decision between life and death. As PAR-synthesis functions in signaling of DNA-damage, initiation of DNA-repair, genotoxic stress resistance, and regulation of genomic stability in cells under genotoxic stress (BÜRKLE, 2001) and seems also to be involved in asthma and other lung diseases (VIRÁG, 2005), PAR was chosen as a general, overall marker for genotoxic stress in the lung.

Phosphorylated H2AX (γ-H2AX) is a nucleosomal core histone, which is phosphorylated by members of the PIKK group of protein kinases (for example ATM, ATR, and DNA-PK) on serine 139 by occurrence of DNA double-strand breaks (DSB, ROGAKOU et al., 1998). Phosphorylated γ-H2AX is then part of complexes with DNA repair proteins and proteins involved in cell cycle regulation at the place of DNA-damage. It is involved in stabilizing the incoherent DNA-ends and in recruiting DNA repair factors. γ-H2AX-containing foci seem to directly correlate with the number of DSB (SEDELNIKOVA et al., 2002). Gamma-H2AX is thus a marker for DSB, but it has to be kept in mind that γ-H2AX can also occur during apoptosis and seemed to be involved in apoptotic DNA fragmentation (SLUSS et al., 2006). Nevertheless, γ-H2AX was shown to be a good and sensitive marker of genotoxicity (WATTERS et al., 2009) and H2AX phosphorylation was demonstrated to occur in SAE and A549 cells after exposure to silica and TiO_2 particles (MSISKA et al., 2009). γ-H2AX was thus chosen as a marker for DNA double-strand breaks.

8-Hydroxy-2'-deoxyguanosine (8-OH-dG) represents an oxidative DNA modification, produced by the attack of double-bonds by reactive oxygen species (ROS) like O_2^-, $OH^\cdot$ (two radicals) or H_2O_2. 8-OH-dG (see Figure 3.1) is perhaps the best-characterized and is thought to be one of the most mutagenic oxidative base modifications (SHIBUTANI et al., 1991). 8-OH-dG is thus a good and well established marker for oxidative DNA-damage (KASAI, 1997). 8-OH-dG is considered to be a pre-mutagenic lesion, because of its tendency to mispair with adenine during replication and such mispairing can lead, if not excised to G:C -> T:A transversions (WALLACE, 1998; CHENG et al.,1992), which are commonly found in human lung tumours (HUSGAFVEL-PURSIAINEN et al., 2000). Persistence of 8-OH-dG in the genome of proliferating cells constitutes a critical event in cancer development, because of the potential mutation-dependent activation of proto-oncogenes or inactivation of tumour-suppressor genes (KAMIYA et al., 1992). Increase in 8-OH-dG had been demonstrated in many studies on adverse effects of particles in the lung.

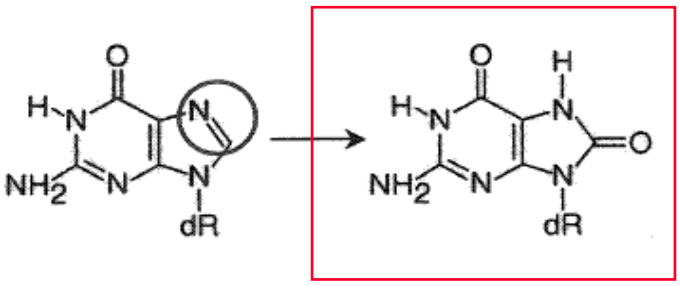

Fig. 3.1 Oxidation of deoxyguanosine to 8-hydroxy-2'-deoxyguanosine (8-OH-dG)

8-Oxoguanine DNA glycosylase (OGG1) belongs to the family of "base-excision repair (BER)" proteins. OGG1 is involved in recognition and excision of the oxidative base modification 8-OH-dG if mispaired with cytosine (DIANOV et al., 1998). The OGG1 enzyme possesses an associated apurinic/apyrimidinic (AP) lyase activity, which enable removal of 8-OH-dG and cleavage of the DNA backbone (ABURATANI et al., 1997; RADICELLA et al., 1997). OGG1 is constitutively expressed but its expression and/or activity can be induced by stimuli or repressed by toxic influences. OGG1 expression in the lung had for example been shown to be repressed by cadmium aerosols in adult male Lewis rats (POTTS et al., 2003) and OGG1 activity was acutely reduced after intratracheal instillation of diesel exhaust particles in female Fisher 344 rats with reactive induction of OGG1 expression 5-7 days after instillation (TSURUDOME et al., 1999). Interestingly, mutations or polymorphisms of the *OGG1* gene (CHEVILLARD et al., 1998; MAMBO et al., 2005) as well as low OGG1 activity (PAZ-ELIZUR et al., 2003) seem to be strongly associated with an increased risk of lung cancer. In humans there exist two OGG1 splice variants which encode for two different isoforms, with α-hOGG1 mainly located in the nucleus and β-hOGG1 located in the inner mitochondrial membrane (NISHIOKA et al., 1999). In mitochondria OGG1 appears to be essential for the maintenance of mitochiondrial DNA (mt-DNA) integrity in mammalian cells (STENSNER et al., 2002), as mt-DNA is of high risk of ROS-mediated damage due to its proximity to the respiratory chain. OGG1 seems to be the only mitochondrial glycosylase for removal of 8-OH-dG in mouse mitochondria (BOHR et al., 2002). In addition, the mitochondrial OGG1 isoform in the absence of glycosylase activity may also function as chaperon protein of aconitase thus preventing oxidant-induced mitochondrial dysfunction and apoptosis (PANDURI et al., 2009) OGG1 was therefore chosen as a marker for oxidative DNA-damage and the related DNA-repair capacity.

Table 3.1 Genotoxicity markers with indicated type of DNA damage

Marker	**Relevance for Genotoxicity**
Poly(ADP-Ribose) (PAR)	Immediate early cellular reaction on DNA damage, overall marker of genotoxic stress
Phosphorylated H2AX (γ-H2AX)	DNA double strand breaks, apoptosis
8-Hydroy-2'-deoxyguanosine (8-OH-dG)	Oxidative DNA damage, pre-mutagenic DNA-base modification
8-Oxoguanine DNA glycosylase (OGG1)	Oxidative DNA damage in both nucleus and mitochondria, related DNA repair capacity

4 Material and Methods

4.1 Lung Tissue Samples for Immunohistochemical Detection of Genotoxicity Markers

For establishment of PAR-, γ-H2AX-, 8-OH-dG- and OGG1-adapted immunohistochemical detection methods and of quantification by image analysis of these genotoxicity markers in lungs of particle-exposed animals, already existing paraffin-embedded lung tissue samples were used. Samples for this feasibility study were available from a German Umweltbundesamt (Federal Environment Agency, UBA) project that has been placed at Fraunhofer ITEM, which was entitled: "Pathogenetische und immunbiologische Untersuchungen zur Frage: Ist die Extrapolation der Staubkanzerogenität von der Ratte auf den Menschen gerechtfertigt?". These lung tissue samples offered the unique possibility to correlate the data on local genotoxicity of repeatedly intratracheally instilled particles in the lungs of female Wistar WU rats (strain: Crl:WI(WU)BR) 1, 3, and 9 months after the first instillation (the present study however mainly focused on the 3 months samples, the 1 and 9 month samples were only stained and roughly screened) with parameters like tissue inflammation (after 3 months), tumour incidences (after lifetime exposure), and also specific pathological findings (ERNST et al., 2002, 2005; KOLLING et al., 2008). In addition, the chosen lung tissue embedded for histology fulfilled the requirements for consecutive immunohistochemistry because the fixation time was limited to 24 hours until embedding. The results of the original study which were relevant for data correlation are listed in Appendix III (see page 91). The histopathology data of the 3-month samples were published by ERNST et al. (2002) (Table 6 of the ERNST publication, see also Table Appendix III-9). There was, however, one drawback concerning correlations with the old study data. Due to the completely different focussing of the original study, the mass doses for the three particle types in the chronic study part were not identical (see Table 4.2), as the study aimed at inducing comparable overload scenarios and grades of chronic inflammation for all three different granular dusts. Applied mass doses thus depended on known particle characteristics. DQ12 (highly reactive crystalline SiO_2, triggering progressive lung injury) and PRINTEX® 90 (carbon black) are low soluble dusts, whereas the amorphous SiO_2, Aerosil® 150, represents a non-biopersistent dust which dissolves relatively fast and triggers acute toxicity and only temporary inflammation in lungs. In addition, in the 3 months satellite study PRINTEX® 90 was administered at three times more particle mass (by error) than the SiO_2-treated animals (DQ12 and Aerosil® 150). For these reason, correlations of the genotoxicity markers with the type of particle and thus the particle material were limited. However, in the 3 months study part crystalline (DQ12) and amorphous SiO_2 (Aerosil® 150) were dosed in the same way (see 5.2.), thus enabling material-based direct comparison of data. As the ratios of doses of the different dusts also varied between the 3 months and lifetime study parts, correlations of genotoxicity marker expression and tumour data should also be handled with care.

4.2 Particle Characteristics and Administration of Particles to the Animals

The origin, preparation, and the properties of the particles used in the 1, 3, and 9 month study parts and in the carcinogenicity lifetime study are depicted in Table 4.1 The preparation of the particle suspensions is also given in that table. At that time (end of the nineties), the physico-chemical characterization of particles, namely ultrafine particles, in an aqueous suspension was generally poor, thus data on hydrodynamic particle diameters or ζ potential are missing.

Table 4.1 Properties of the three investigated dusts and preparation of particle suspensions

Particle	**Crystalline SiO_2** Quartz DQ12	**Amorphous SiO_2** AEROSIL® 150	**Carbon black** PRINTEX® 90
Identity	Dörentrup quartz Ground quartz sand; milling no. 12 Bergbauforschung Essen, Dr. Armbruster (1985) --> for details see Appendix II	Fluffy white powder Hydrophilic fumed silica CAS # 112945-52-5 ex. 7631-86-9 EINECS # 231-545-4 Degussa (1984)	Fluffy black powder High Colour Furnace Black CAS # 1333-86-4 Lot # 8313101 Degussa (1994)
Average primary particle size Arithmetic mean (nm)	1300 geometric mean; mass weighted 560 geometric mean; number weighted	14	14
Specific surface (BET) (m^2/g)	1.5	150 ± 15	approx. 300
Density (g/m^3)	2.2	2.2	1.8-1.9
Preparation of particle suspensions to be administered by intratracheal instillation	Dispersion liquid: physiological saline (0.9% in H_2O)	Dispersion liquid: physiological saline (0.9% in H_2O)	Dispersion liquid: physiological saline (0.9% in H_2O) Detergent: TWEEN 80® (Polyoxyethylen-sorbitanmonooleate)
General procedures	Homogeneity of the particle suspensions was optimised by ultrasonic treatment for 5 min; the suspensions were then kept homogeneous by permanent stirring during the administration period; rats were anesthetised for the intratracheal instillation procedure using CO_2/O_2 65%/35% v/v		

The animals were exposed to the particle suspensions by intratracheal instillation. The animals of the different study parts were dosed as depicted in Table 4.2.

Table 4.2 Dosing schemes: 1-, 3-, and 9-month satellite tests and lifetime carcinogenicity study

Dust	**Crystalline SiO_2** Quartz DQ12 Group 3	**Amorphous SiO_2** AEROSIL® 150 Group 4	**Carbon black** PRINTEX® 90 Group 2
Rats analyzed after 1 month; Dose (per rat)	1 x 2 mg	1 x 2 mg	1 x 6 mg
Rats analyzed after 3 months; Dose (per rat)	3 x 2 mg	3 x 2 mg	3 x 6 mg
Rats analyzed after 9 months; Dose (per rat)	1 x 3 mg	20 x 0.5 mg	10 x 0.5 mg
Carcinogenicity study Dose (per rat)	1 x 3 mg	30 x 0.5 mg	10 x 0.5 mg

Doses were administered at monthly intervals (Note: in the 9-month and the carcinogenicity study the dosing scheme differed: Group 2: 10 x 0.5 mg every 7 days; Group 3: 1 x 3 mg; Group 4: 20 x 0.5 mg/ 30 x 0.5 mg, respectively, every 14 days)

For detection and quantification of the genotoxicity markers in lung tissue, samples of the 3-month test were used. A time period of 3 months seemed to be long enough to guarantee inflammation in the lungs of the particle-treated animals, but was short enough to avoid gross tissue changes which might disturb immunohistochemical staining and quantification of the markers in lung epithelium. For treatment groups and animal numbers see Table 4.3. In addition, slides of rats from the 1- and 9-month studies were stained immunohistochemically and were roughly screened microscopically for suitability for quantification.

Table 4.3 Lung tissue samples used for immunohistochemistry with genotoxicity markers

Treatment **Intratracheal instillation**	**1 Month**[1] **Number of rats**	**3 Months**[2] **Number of rats**	**9 Months**[1] **Number of rats**
Negative control: 0.9% saline	6	6	6
Crystalline SiO_2: Quartz DQ12	6	6	6
Amorphous SiO_2: Aerosil® 150	6	6	6
Carbon black: PRINTEX® 90	6	6	6

[1] Slides were only stained and coarsely screened.
[2] Slides were stained and quantitatively analyzed for occurrence of genotoxicity.

4.3 Immunohistochemical Detection of Genotoxicity Markers

4.3.1 Immune Reactions

For immunohistochemical detection of the chosen genotoxicity markers in lung tissue, 3 µm thin paraffin sections were cut from the selected (see interim report page 10) lung material, using one block of the left lung lobe for each animal, and were mounted on Superfrost Ultra Plus® glass slides (Menzel GmbH & Co KG, Braunschweig, Germany, J3800AMNZ). The paraffin sections were then dewaxed and transferred to DNA hydrolysis with 4N HCl and the respective antigen retrieval methods, which were validated for each of the primary antibodies. Primary antibodies were directed against:
Poly(ADP-Ribose) (PAR): The protein A-column-purified mouse monoclonal antibody 10H (generous gift from Prof. A. Bürkle, University of Konstanz, Germany, dilution 1:50) was used for detection of PAR.
Phosphorylated H2AX (γ-H2AX): A rabbit polyclonal antibody directed against γ-H2AX (phospho S139) "DNA double-strand break marker" (Abcam, Cambridge, UK, ab2893, dilution 1:2000) was used to analyze occurrence of DNA double-strand breaks.
8-Hydroxy-2'-deoxyguanosine (8-OH-dG): Detection of 8-OH-dG was performed with a mouse monoclonal antibody [N45.1] to 8-Hydroxy-2'-deoxyguanosine (Abcam, Cambridge, UK, ab48508, dilution 1:50).
8-Oxoguanine DNA glycosylase (OGG1): The rabbit polyclonal anti-Ogg1 antibody (NOVUS BIOLOGICALS, Littleton, USA, NB100-106, dilution 1:1500) was used to analyze expression of the DNA repair enzyme OGG1 in lung tissue.

Antigen retrieval was performed by Protease (Protease Type XIV bacterial from Streptomyces Griseus, Sigma, St. Louis, MO, USA, P-5147, 5.2 units, 0.25 mg/ml, incubation for 5 minutes at 21 °C) for PAR, for γ-H2AX, 8-OH-dG and OGG1 in a pressure cooker for 2 minutes in citrate-buffered solution. All slides were rinsed with Tris-buffered saline (TBS, pH 7.6) plus 0.01% Tween® 20 (Merck KGaA, Darmstadt, Germany, 8.22184). Slides were incubated for 20 minutes at 21 °C in normal goat serum (Vector Laboratories Inc., CA, USA, S-1000) at a dilution of 1:20 and afterwards incubated with the primary antibody overnight at 4 °C. As secondary antibodies a biotin-SP-conjugated AffiniPure goat-anti-mouse IgG (H+L) with minimal cross reaction to rat (Jackson Immunoresearch, Inc., West Grove, PA, USA, 115-065-100, dilution 1:800) or a biotin-SP-conjugated AffiniPure goat-anti-rabbit IgG (H+L) antibody (Jackson Immunoresearch Inc., West Grove, PA, USA, 111-065-144, dilution 1:3000), both with minimal cross reaction to rat, were applied for 30 minutes incubation time at 21 °C.

Immunostaining was done with a routine method using alkaline phosphatase streptavidin-biotin (Vector Laboratories Inc., CA, USA, S-5100, dilution 1:800, incubation for 30 minutes at 21 °C) and as chromogen Fast Red (Fast Red substrate pack, BioGenex, CA, USA, HK182-5K, incubation time 15 minutes at at 21 °C) in combination with levamisole (Dako Corporation, CA, USA, X3021) for suppressing of non-specific staining due to endogeneous alkaline phosphatase activity. The slides were finally counterstained with Mayer's hematoxylin (Linaris Biologische Produkte GmbH, Wertheim-Bettingen, Germany, EGH3411). Coverslipping was performed using Aquatex® aqueous mounting medium (Merck KGaA, Darmstadt, Germany, 1.08562).

Sample permeabilisation, antibody concentrations, antibody reactions, and staining procedures were optimized for each antibody/marker to get clear and specific immunohistochemical signals.

For set-up and validation of the different marker-specific immunohistochemical methods, lungs of animals treated intratracheally with NaCl (negative control) or quartz DQ12 (positive control) and primary human oral cells, cultured on membranes and treated with appropriate positive controls (γ-H2AX and PAR: Etoposide; 8-OH-dG and OGG1: $KBrO_3$) were used. Like the lung tissue samples, cells on membranes were fixed with formalin and embedded in paraffin for preparation of slides. Immunohistochemical staining with the different antibodies was done accordingly to the staining of lung tissue sections.

4.3.2 Image Analysis and Marker Quantification

Image analysis of the immunohistochemically stained slides was performed using a digital colour camera (ColorView III Soft Imaging System, Olympus Deutschland GmbH, Hamburg, Germany) connected to an automatic driven transmission light microscope (AX70, Olympus Deutschland GmbH, Hamburg, Germany) and the image analysis system AnalySIS Five (Soft Imaging System GmbH, Münster, Germany). From each slide 20 digital images were taken, using a lens with 40-fold magnification. Therefore, in one lung lobe of every rat, 5 bronchioles were selected and images were taken adjacent to the upper, lower, left and right margins (on the working monitor) of the bronchioles. The regions of interest (ROI) were located in every image including as much intact lung tissue as possible. The analyzed tissue areas were calculated by the software. Within the ROIs all epithelial cells with marker-positive nuclei and for OGG1 also the cells with marker-positive cytoplasm were counted interactively on a monitor showing the images in a format of 27.5 x 38.5 cm. (The photographs on pages 25 to 37 are condensed from a format of 27.5 x 38.5 cm to 5 x 7 cm for illustration purposes only and were not used for quantification) Nuclei or cytoplasm were counted as positive if they showed a predominantly red staining. Nuclei with a predominantly blue staining were regarded as negative and were not counted. Nuclei stained violet thus needed to be labelled by a clearly visible portion of red colour to be counted as positive. Macrophages and cells like polymorphonuclear granulocytes freely lying in the analysed alveoli were excluded from the counts.

4.3.3 Data Acquisition

Each image was transferred to a SIS AnalySIS FIVE data base (Soft Imaging System GmbH, Münster, Germany). In addition, all data of the image analysis were entered into the program and stored in this data base.

4.4 Statistics

4.4.1 Statistics of Image Analysis Data

For statistic purposes the image analysis data were exported to an Excel file and then imported into the software packages mentioned below. Data were analyzed by using Analysis of Variance (ANOVA). If the group means differed significantly by

ANOVA the treatment groups were compared with the control group using the Dunnett's test. The Tukey HSD test was used as another post hoc test for comparison among the different treatment groups. Statistical significance was reached if *p ≤ 0.05. Data were judged as highly significant if **p ≤ 0.01 or ***p ≤ 0.001. For statistical purposes the SAS software package (Version SAS Institute, Cary, NC, USA, Release 9.1 on Windows XP Computer) and Statistica (Version 8.0, StatSoft Inc., Tulsa, OK, USA) were used.

4.4.2 Correlations

The data for evaluation of possible correlations between the data for genotoxicity marker expression and for example histopathology, immunobiology, or enzymatic data were extracted from the interim and the final reports of the research projects of the German "Umweltbundesamt" (Federal Environment Agency) „Pathogenetische und immunbiologische Untersuchungen zur Frage: Ist die Extrapolation der Staubkanzerogenität von der Ratte auf den Menschen gerechtfertigt?" (*Ernst et al.,* Umweltforschungsplan des Bundesministeriums für Umwelt, Naturschutz und Reaktorsicherheit Förderkennzeichen: 298 61 273, 2002) and „Pathogenetische und immunbiologische Untersuchungen zur Frage: Ist die Extrapolation der Staubkanzerogenität von der Ratte auf den Menschen gerechtfertigt? Teil II: Histologie" (*Ernst et al.*, Umweltforschungsplan des Bundesministeriums für Umwelt, Naturschutz und Reaktorsicherheit Förderkennzeichen: 203 61 215, 2004, 2005), from the respective publications of these research projects (ERNST et al., 2002; KOLLING et al., 2010 in preparation), and from the raw data of individual animals of the research projects. The study data are listed in Appendix III.
Correlations between the genotoxicity markers and other study parameters like the inflammation score and enzymatic activities or cell counts in the BAL fluids were calculated using the respective group mean values. In the case of the inflammation score, in addition, the individual animal data could be used for determination of correlations, because the identical animals were investigated for both genotoxicity markers and histopathologic evaluation of lung inflammation. The method of "Linear Regression/Pearson Product Moment Correlation" (SAS [Cary, NC, USA] software package Statistica or SigmaStat 3.1) was used to calculate the correlation coefficient (r) and the significance of the correlation (p value). The mean values and correlation coefficients of the different endpoints were transferred to respective tables. Correlation coefficients lacking statistical significance were judged as "correlation without significance" if $r > 0.5$.

5 Results and Discussion of Genotoxicity Marker Detection and Quantification in Lung Tissue Samples

5.1 Poly(ADP-Ribose) (PAR)

In the 3-month test, lung epithelium of the rats treated with crystalline SiO_2 (quartz DQ12, 3 x 2 mg) showed a statistically significant increase ($p<0.01$, Dunnett's test) in the number of PAR-positive nuclei per mm^2, as compared to the negative (saline) control group. In lungs of the carbon black (PRINTEX® 90, 3 x 6 mg) and the amorphous SiO_2 (Aerosil® 150, 3 x 2 mg) treated animals, there was also an increase in PAR-positive nuclei, compared to the saline treated control animals, but the difference did not reach statistical significance (see Table 5.1 and Figure 5.2, and for representative images Figure 5.1). In addition, using the Tukey test, no statistical difference could be demonstrated between the different dust-treated groups. In the present study, PAR, as a general marker for genotoxicity, thus seemed not to be able to provide clear differentiation between the various particle treatments. All particle treatments induced more or less comparable numbers of PAR-positive nuclei, irrespective of the particle type (by comparing crystalline and amorphous SiO_2, same mass dose) and mass dose (by comparing the two low soluble dusts DQ12 and PRINTEX® 90, with 3 times higher mass dose), with slightly higher levels in the DQ12-treated animals.

Table 5.1 Results of image analysis of immunohistochemical detection of PAR as a general marker for genotoxicity in lung tissue of rats of the 3-month test. Data represent counts of cells with labelled nuclei per mm^2.

Marker of genotoxicity: PAR			
Treatment	**3 Months No. of rats**	**Mean** Positive nuclei per mm^2	**Standard deviation**
Negative control: 0.9 % saline	6	290.9	87.8
Crystalline SiO_2: Quartz DQ12	6	**463.6	83.6
Amorphous SiO_2: Aerosil® 150	6	396.3	123.5
Carbon black: PRINTEX® 90	6	409.7	34.0

Significantly different from the negative control group (saline): ** $p<0.01$; Dunnett's test.

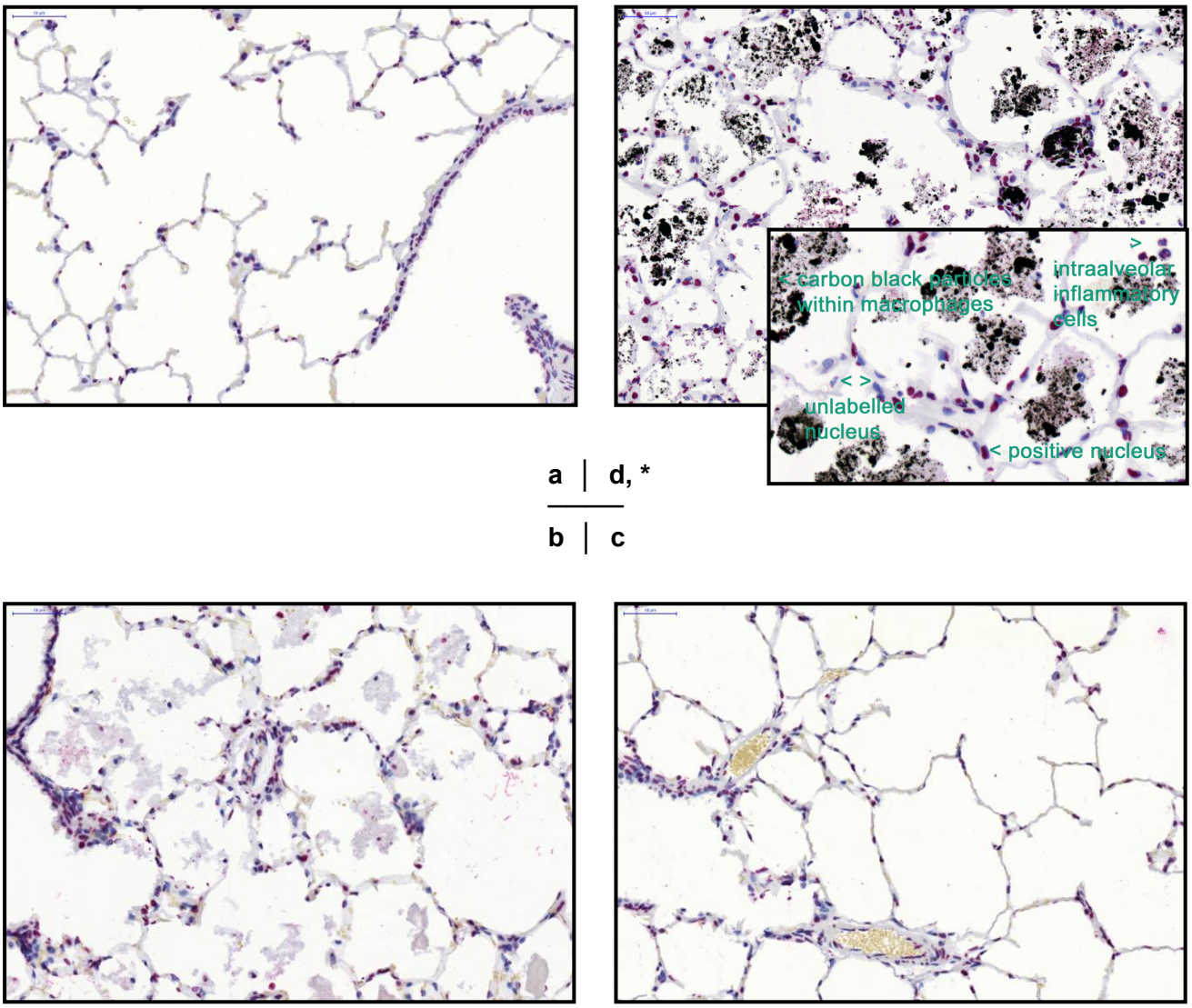

Fig. 5.1 Immunohistochemical detection of PAR as a general marker for genotoxicity in lung tissue of rats of the 3-month time point treated with different dusts. Representative images: a: Negative control: 0.9 % saline; b: Crystalline silica: quartz DQ12; c: Amorphous silica: Aerosil® 150; d: Carbon black: PRINTEX® 90, *: insert showing carbon black within macrophages, intraalveolar inflammatory cells, blue unlabelled nuclei and red positive labelled nuclei. Cells with labelled nuclei were quantified.

Given that particle-induced lung tumour-development involves genotoxic modes of action and based on the lifetime tumour data (see Figure 4.2 and Table Appendix III-1), one would expect that PAR as an overall marker for genotoxic stress would provide clear increase in expression compared to negative control animals and clear differentiation between the animals equally dosed with the crystalline silica, quartz DQ12 (39.6 % rats with lung tumours) or the amorphous silica Aerosil® 150 (9.3 % rats with lung tumours).

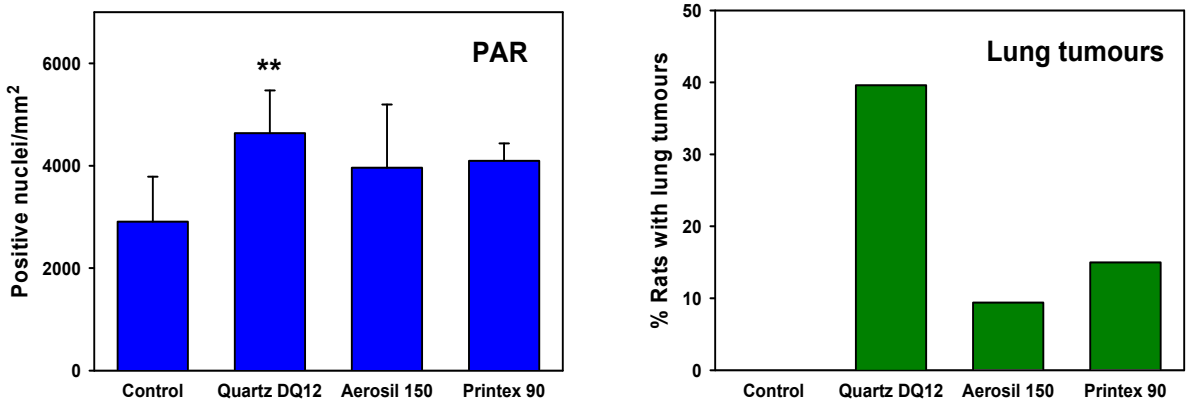

Fig. 5.2 PAR-positive nuclei in lung epithelium after 3 months and lung tumour rates after lifetime exposure.

Unfortunately, PAR was not able to display a significant difference between quartz DQ12 and Aerosil® 150 as expected by considering the tumour and literature data. This unexpected lack in clear particle differentiation through immunohistochemical detection and quantification of PAR may be based on limited sensitivity of the method and/or primary antibody used, but it may also reflect a limited specificity of this endpoint for DNA-damage, because of a growing number of known physiologic as well as pathophysiologic functions of the PARP/PAR system (see HAKMÉ et al., 2008) with in part DNA-damage independent activation. In addition, there is a dynamic equilibrium of PAR synthesis and degradation under conditions of DNA-breakage (ALVAREZ-GONZALEZ et al., 1989) with the present immunostaining only representing a snapshot and perhaps a suboptimal time point for this endpoint. PAR is a very short-lived polymer. For example, in cultured primary rat hepatocytes the PAR-signal in the nucleus was maximal at about 3-5 min after addition of H_2O_2 with a sharp decrease thereafter (ZIEMANN et al., 1999). In the inflamed lung tissue, induction of DNA-strand breaks, as an essential trigger for ongoing polymer synthesis, occurs transiently in an uncoordinated manner, with equilibrium between induction and repair. For this reason accumulation of DNA-damage would only occur in the case of an overwhelmed repair system. In addition, the PARP/PAR system fulfils its tasks through interaction with DNA and proteins, involving most likely on the one hand steric hinderance and electrostatic repulsion, but also recruitement of repair factors to sites of strand breaks (HAKMÉ et al., 2008), with both processes being perhaps sensitive to disturbance by particles (mechanically and through surface charge and other surface characteristics), if the particles are localized in the nuclear compartment. In line with this hypothesis, DANIEL et al. (1995) could demonstrate by electron microscopy and EDX-analyses the presence of small (< 5 µm) Min-U-Sil 5 and Chinese standard □-quartz particles in the nuclei of a foetal rat lung alveolar type II cell line after *in vitro* exposure. They also presented acellular data, generated via infrared spectroscopy, point-

ing to anchoring of the quartz particles via surface silanol groups and hydrogen bonds to the phosphate backbone of DNA. It seems thus possible that the fine and ultrafine particles, used in this study, entered the nuclei of lung epithelial cells and inhibited in part PARP/PAR-dependent activities. In the case of potential, particle-induced disturbance of the PARP/PAR system, the immunohistochemical data for PAR as a genotoxicity marker would not really picture quantitatively particle-induced DNA-damage. One could hypothesize that such particle-mediated disturbance of the PARP/PAR system could also participate, as one primary genotoxicity mechanisms, in the genotoxic and also tumorigenic potential of fine and ultrafine particles in the lung, as the PARP/PAR system is involved in DNA-damage sensing and DNA-damage response and repair, but seems also to participate in the decision between life and death after DNA-damage, in cell division, in cell cycle progression and additionally in cell proliferation, with both covalent and non-covalent binding of PAR to target proteins. Massive PAR production triggers necrosis by energy failure and it also seems to be involved in the initiation of a caspase-independent cell-death pathway by release of apoptosis-inducing factors from mitochondria. Moreover, PARP1 is one of the first substrates cleaved during the execution phase of apoptosis, probably in order to preserve energy for this ATP requiring cell death pathway. If the regulation of genomic stability, cell death and also cell proliferation is disturbed, heavily damaged cells may survive and proliferate with tumour-triggering mutations. For this reason, it would be very interesting to detect and quantify both apoptosis and cell proliferation in the same lung tissue samples for correlation purposes. As the PARP/PAR system is highly energy-dependent, its activity may also be further influenced by a drop in ATP trough disturbance/inhibition of the respiratory chain by fine and ultrafine particles and may thus influence in a primary indirect way the amount of DNA-damage in particle exposed cells, because of higher genomic instability. But in the frame of the present study, a drop in activity of the PARP/PAR system may also lead to underestimation of the real extent of DNA-damage in the particle treated lungs, using PAR as an overall marker for genotoxicity. Interestingly, TAO et al. (2008) could demonstrate inhibition of cellular respiration by mesoporous silica nanoparticles.

5.2 Phosphorylated H2AX (γ-H2AX)

Lungs of rats of the carbon black (PRINTEX® 90, 3 x 6 mg) and of the crystalline SiO_2 (DQ12, 3 x 2 mg) groups showed statistically highly significant (*** $p<0.001$, Dunnett's test) increases in the number of γ-H2AX-positive nuclei per mm^2 after 3 months of exposure, as compared to the negative (saline) control group, pointing to profound induction of DNA double-strand breaks (DSB) by particle treatment, which are potentially mutagenic and, if not repaired adequately, may lead to genomic instability, cell death or cancer (JEGGO et al., 2007). The amorphous SiO_2 (Aerosil® 150, 3 x 2 mg)-treated animals also demonstrated a slight, but not significant increase in γ-H2AX-positive nuclei per mm^2, but induction of DSB was less profound, as compared to the other treatments (see Table 5.2 and Figure 5.3, and for representative images Figure 5.4). Using the Tukey test, there were significant differences between the DQ12- and Aerosil® 150-treated animals (*** $p<0.001$) as well as between the Aerosil® 150- and the PRINTEX® 90-treated animals (** $p<0.01$). There was no statistically significant difference between the DQ12- and the PRINTEX® 90-treated animals. In contrast to PAR, γ-H2AX, a marker for DNA double-strand breaks, seemed to be able to better differentiate the genotoxic potential of various particles/particle

treatments. On the basis of the same mass dose, the low soluble crystalline SiO_2, quartz DQ12 (known to be genotoxic, see 2.2.1.1), induced significantly more DSB than the amorphous, non-biopersistent SiO_2, Aerosil® 150 and, in addition, carbon black (PRINTEX® 90), despite a 3 times higher mass dose, did not mediate the highest induction of γ-H2AX positive nuclei, thus pointing to a profound role of the particle material and the specific particle characteristics, even in the overload situation characterized by lung inflammation.

Table 5.2 Results of image analysis of immunohistochemical detection of γ-H2AX as a marker for DNA double-strand breaks in lung tissue of rats of the 3-month test. Data represent counts of cells with labelled nuclei per mm^2.

Marker of genotoxicity: γ-H2AX			
Treatment	**3 Months No. of rats**	**Mean** Positive nuclei per mm^2	**Standard deviation**
Negative control: 0.9 % saline	6	158.8	25.8
Crystalline SiO_2: Quartz DQ12	6	***388.6	46.6
Amorphous SiO_2: Aerosil® 150	6	217.4	49.7
Carbon black: PRINTEX® 90	6	***334.8	50.3

Significantly different from the negative control group (saline): *** $p<0.001$; Dunnett's test.

Clear differentiation of the genotoxic potential of particles by γ-H2AX quantification was also observed by TSAOUSI et al. (2010). In that study, primary human fibroblasts were incubated for 24 h with 1-10 mg/75 cm^2 flask of alumina (Al_2O_3) ceramic (mean grain size 0,2 nm) or cobalt-chromium metal particles (minimum diameter 0,56 µm) and γ-H2AX formation was quantified after immunocytochemical detection. There was no induction of γ-H2AX foci in the alumina ceramics-treated cells, whereas the cobalt-chrome metal-treated cells demonstrated concentration-dependent enhancement in γ-H2AX foci formation. The better differentiation potential of γ-H2AX, as compared to PAR, may be based on certain aspects. First of all, γ-H2AX foci seem to be a very sensitive marker for DNA-damage (WATTERS et al., 2009), in particular DSB, with one nuclear focus (expanded phosphorylation of H2AX over a megabase region of chromatin surrounding the DSB) representing one DSB (SEDELNIKOVA et al., 2002). In a study of ISMAIL et al. (2007) an γ-H2AX-based flow-cytometric assay for peripheral blood cells detected calicheamicin-induced DNA-damage at levels 100-fold below the detection limit of the alkaline comet assay. In addition, the increase in the γ-H2AX signal was linear over two orders of magnitude in this study, with linear signal increase being also a prerequisite for quantitative differentiation of the genotoxic potential of different particles. The kinetics of γ-H2AX foci formation and γ-H2AX dephosphorylation and thus disappearance of foci seems also to be an important point, as foci rapidly accumulate after DNA-damage, continue to grow up for example in cell lines up to 1 h (BANATH et al., 2004), followed by a decline in foci number, with progression of DNA-repair (BANATH et al., 2004; RÜBE et al., 2010). In the study of

RÜBE et al. (2010) it took several hours for γ-H2AX foci disappearance in lung tissue of ATM$^{+/+}$ wild-type mice after single-dose irradiation with 2 Gy. Repair of irradiation-induced DSB, as determined by disappearance of γ-H2AX, was nearly complete after 24 h and complete after 48 h. Thus, the γ-H2AX signal is less short-lived than the PAR-signal with the possibility of damage-accumulation and more precise damage differentiation.

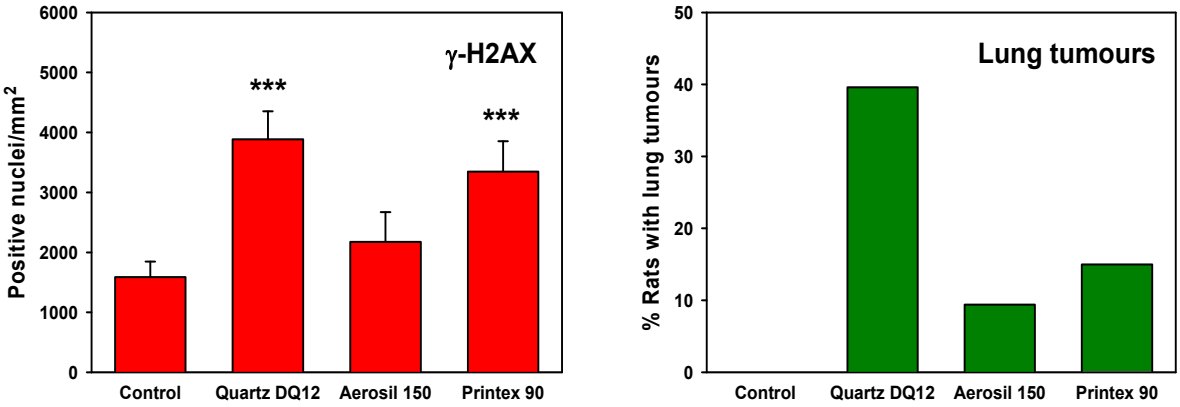

Fig. 5.3 Gamma-H2AX-positive nuclei in lung epithelium after 3 months and lung tumour rates after lifetime exposure.

By comparing the data for γ-H2AX expression with the lifetime tumour data, a similar pattern concerning occurrence of γ-H2AX foci and the number of animals with lung tumours was noted (see Figure 4.3 and Table Appendix III-1). In both cases the effect was highest for DQ12, followed by Printex® 90 (however, no statistical difference to DQ12-treated animals) and Aerosil® 150, indicating an important role of DSB in the development of particle-induced lung tumours. DSB as on type of DNA-damage are difficult to repair, because both templates are damaged and there is no intact template to guide repair. In line with an important role of DSB in particle-induced lung tumour development, γ-H2AX foci expression could not be detected in normal bronchiolar epithelial cells but was found in early hyperplastic preneoplastic regions as well as in advanced preneoplastic regions of lungs in a rat-based silica-induced multistep lung carcinogenesis model driven by inflammation (BLANCO et al., 2007). Gamma-H2AX was still present in tumours but its levels were reduced. Interestingly, γ-H2AX was always co-localized with nitric oxide synthase (iNOS) in the different steps of lung carcinogenesis, pointing to RNS beside ROS as one source of profound DNA-damage in the form of DSB. The authors concluded that silica-induced chronic inflammation leads to chronic exposure of epithelial cells to ROS and RNS, nitro(oxidative)-stress and subsequent DNA-damage with γ-H2AX formation and activation of a p53 response. In line with this model 8-Oh-dG expression was also enhanced in lung tissue of particle-exposed animals in the present project (see Section 5.3).

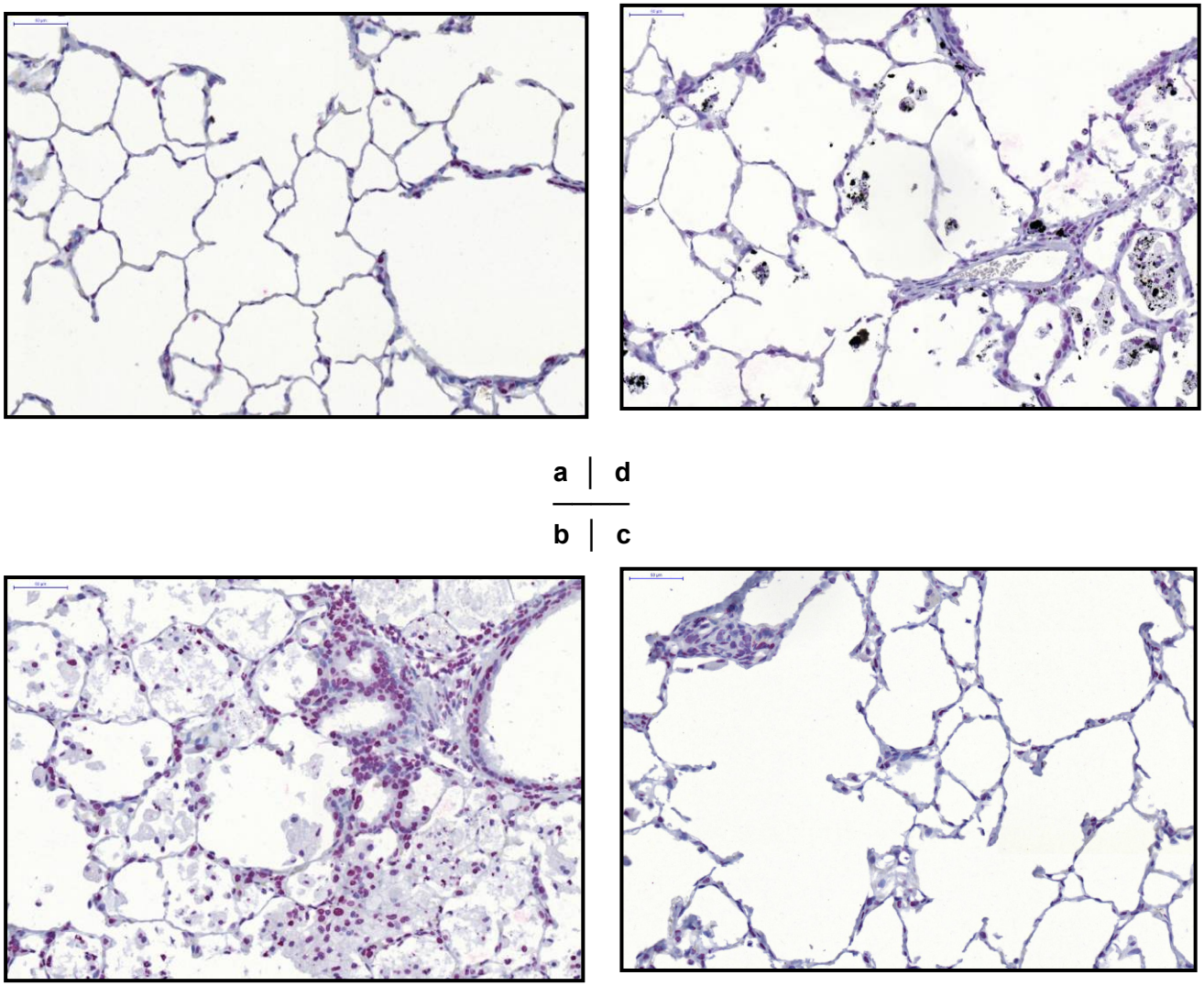

Fig. 5.4 Immunohistochemical detection of γ-H2AX as a marker for DNA double-strand breaks in lung tissue of rats of the 3-month time point treated with different dusts. Representative images: a: Negative control: 0.9% saline; b: Crystalline silica: quartz DQ12; c: Amorphous silica: Aerosil® 150; d: Carbon black: PRINTEX® 90). Cells with labelled nuclei were quantified.

However, besides such secondary ROS-/RNS-driven genotoxic mechanism of particles, there have also to be primary ROS-/RNS-driven genotoxic mechanisms, because for example MSISKA et al. (2010) demonstrated ROS-production and induction of γ-H2AX and thus DSB induction *in vitro* by silica and TiO_2 in normal SAE cells and A549 cells. Gamma-H2AX expression was also induced in a time and concentration-dependent manner by treatment of human embryo lung fibroblasts *in vitro* with silica (ZHANG et al., 2009). Overall, γ-H2AX seems to be a good, sensitive and specific marker with some prognostic value concerning particle-induced carcinogenesis. However, it has to be kept in mind that γ-H2AX may also be involved in apoptosis and γ-H2AX foci may also appear as repair intermediates and may appear during replication. To differentiate the different causes of γ-H2AX in particle-exposed lung tissue it would be very interesting to detect both apoptosis as well as proliferation in the same lung tissue samples.

5.3 8-Hydroxy-2'-Deoxyguanosine (8-OH-dG)

After 3 months of exposure, lung epithelium from rats of the crystalline SiO_2 (quartz DQ12, 3 x 2 mg) group showed a statistically highly significant (***p<0.001, Dunnett's test) increase in the number of 8-OH-dG-positive nuclei per mm^2, as compared to the negative (saline) control. The lung samples of the ultrafine carbon black (PRINTEX® 90, 3 x 6 mg)- and the amorphous silica (Aerosil® 150, 3 x 2 mg)-treated animals also showed significantly enhanced (both **p<0.01), but lower numbers of 8-OH-dG-positive nuclei per mm^2, as compared to the negative (saline) controls and DQ12-treated animals, respectively (see Table 5.3 and Figure 5.5, and for representative images Figure 5.6).

Table 5.3 Results of image analysis of immunohistochemical detection of 8-hydroxy-2'-deoxy-guanosine (8-OH-dG) as a pre-mutagenic base-modification and a marker for oxidative DNA-damage in lung tissue of rats of the 3-month test. Data represent counts of cells with labelled nuclei per mm^2.

Marker of genotoxicity: 8-OH-dG			
Treatment	**3 Months No. of rats**	**Mean** Positive nuclei per mm^2	**Standard deviation**
Negative control: 0.9 % saline	6	131.4	17.7
Crystalline SiO_2: Quartz DQ12	6	***356.1	61.2
Amorphous SiO_2: Aerosil® 150	6	**246.0	50.4
Carbon black: PRINTEX® 90	6	**239.5	60.0

Significantly different from the negative control group (saline): ** p<0.01, *** p<0.001; Dunnett's test.

Using the Tukey test, it could be demonstrated that the DQ12-treated animals exhibited a significantly higher frequency of 8-OH-dG-positive nuclei in lung epithelium (**p<0.01), as compared to the PRINTEX® 90 and Aerosil® 150-treated animals (data not shown). However, there was no significant difference between PRINTEX® 90 and Aerosil® 150-treated animals.
These data indicate, that all particle treatments induced occurrence of the premutagenic oxidative DNA-lesion 8-OH-dG and thus oxidative stress in the rat lung after intratracheal instillation. Oxidative stress in turn might reflect lung particle-mediated lung inflammation, as there was good correlation (see Figure 5.5 and Tables 6.1 and 6.2). Quartz DQ12 is known to induce progressive inflammation in the rat lung and 8-OH-dG expression was indeed most profound in the DQ12-treated group. In addition, 8-OH-dG expression was statistically higher than in animals exposed to the soluble amorphous silica, Aerosil® 150, in the same mass dose, known to induce only temporary inflammation.

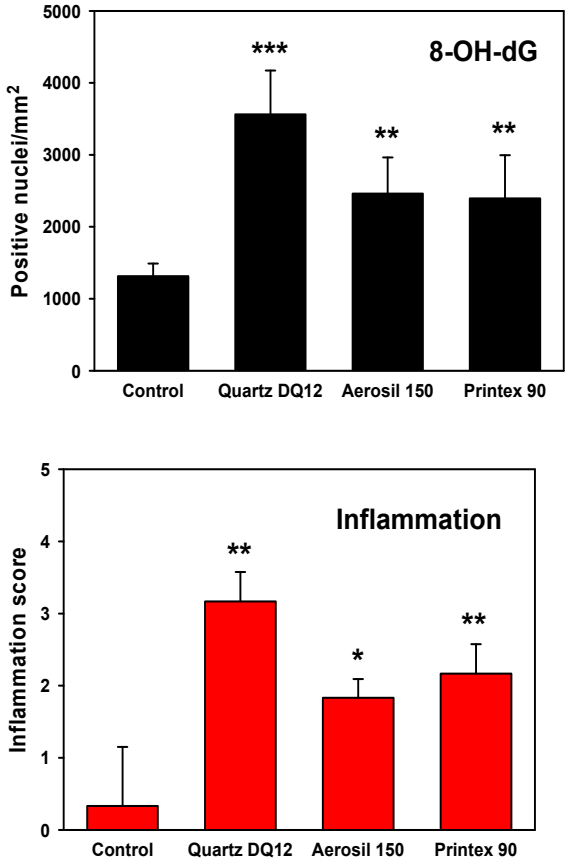

Fig. 5.5 8-OH-dG-positive nuclei in lung epithelium and inflammation score after 3 months of exposure.

By using 8-OH-dG, there was no clear difference between the carbon black and amorphous silica exposed animals, as could be expected by the higher mass dose used for PRINTEX® 90 and by considering the tumour data. This might indicate that 8-OH-dG is not the main oxidative DNA base-lesion in the case of PRINTEX® 90 or that PRINTEX® 90 induced less oxidative stress than expected. Interestingly, TOTSUKA et al. (2009) demonstrated induction of G:C -> C:G transversions at the *gpt*

locus in PRINTEX® 90-treated *gpt* delta transgenic mice. This modification is unable to result from 8-OH-dG lesions, because dG is not incorporated opposite of 8-OH-dG. It is more likely that this type of mutation was based on other oxidative guanine modifications like oxazolone, spiroiminodihydantoin, or guanidinohydantoin, which are thought to be the key molecules causing G:C -> C:G transversions. In addition, increase in G:C -> A:T transistions, but not in 8-OH-dG specific G:C -> T:A transversions were detected. Thus, the spectrum of oxidative DNA lesions may differ, depending on the particle type, and 8-OH-dG, the most typical and best characterised oxidative DNA lesion, is obviously not the only one in the case of particles and especially nanoparticles. This has to be kept in mind, when using and quantifying 8-OH-dG as a marker for particle-induced oxidative stress and as a prognostic marker for the carcinogenicity of particles.
However, it is well established that exposure of animals to fine and ultrafine particles *in vivo* may lead to oxidative stress in the lung (see for example data on colloidal silica particles, KAEWAMATAWONG et al., 2006). This was also demonstrated in the present study by statistically significant increases in 8-OH-dG positive nuclei in all particle-treated groups. The mechanisms of ROS liberation and subsequent oxidative DNA damage may involve phagocytosis of particles by macrophages and leucocytes with subsequent oxidative burst (secondary genotoxicity), but also endocytosis of fine and ultrafine particles in epithelial cells (XU et al., 2009) with generation of ROS for example by iron-catalysed Fenton reaction or other surface-dependent reactions, disturbance or activation of the respiratory chain (LI et al., 2007, XIA et al., 2006), direct interaction with DNA and ROS production directly at the DNA backbone by entering the nucleus (DANIEL et al., 1995), or activation of ROS/RNS-producing enzyme systems like iNOS or cyclooxygenase-2 (BLANCO et al., 2007, XU et al., 2009) (indirect primary genotoxicity). In the present *in vivo* study, originally aiming at producing sustained inflammation, ROS production and increase in 8-OH-dG was most likely based on secondary, inflammation derived mechanisms, as 8-OH-dG expression correlated well with the parallel inflammation score after 3 month of exposure (see Section 6.1 and Figure 5.5). However, the data on OGG1 positive cytoplasm (see Section 5.4) also indicate intracellular generation of ROS and/or RNS, perhaps due to mitochondria-dependent mechanisms.

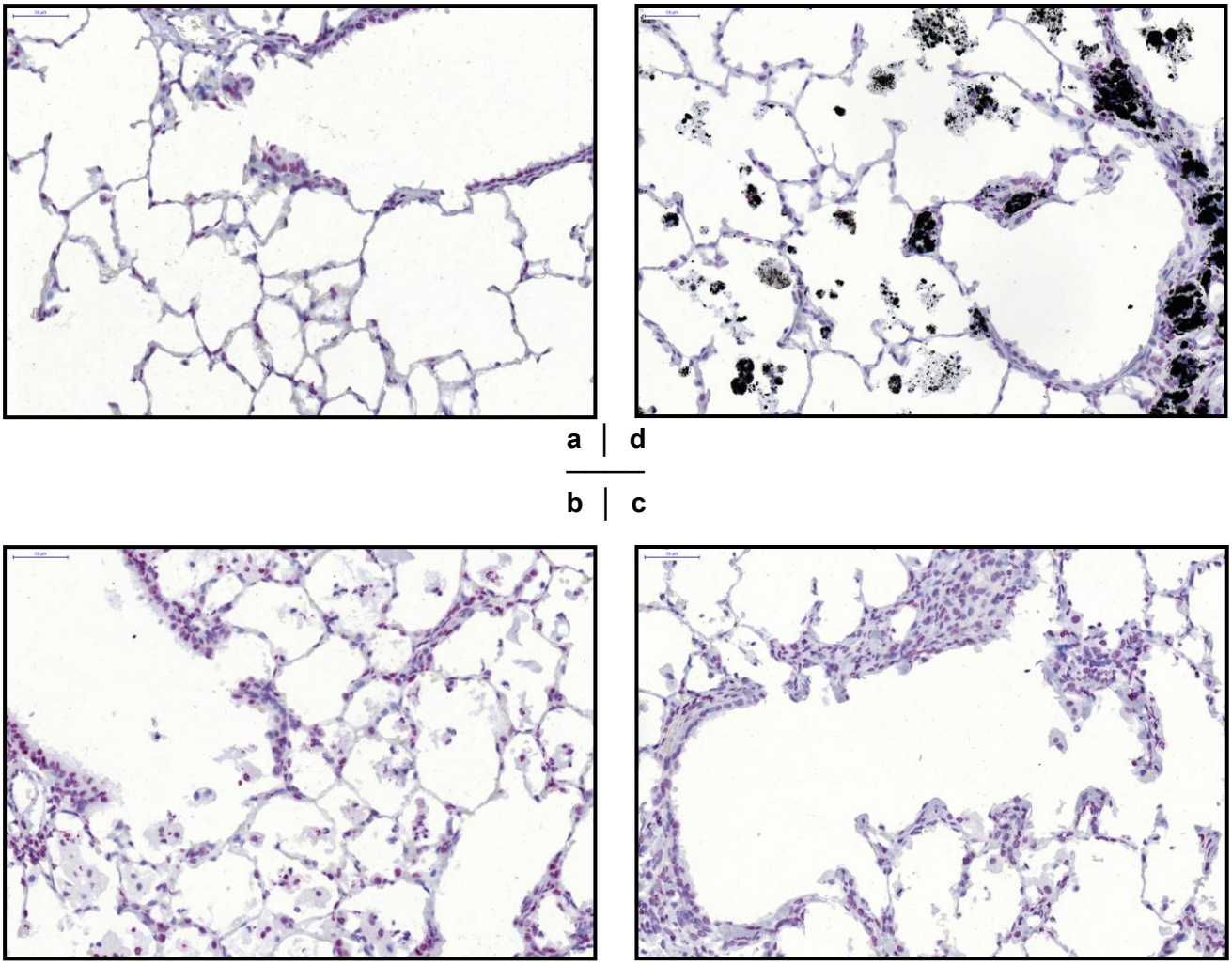

Fig. 5.6 Immunohistochemical detection of 8-hydroxy-2'-deoxyguanosine (8-OH-dG) as a premutagenic DNA-base modification and a marker for oxidative DNA-damage in lung tissue of rats of the 3-month time point treated with different dusts
Representative images: a: Negative control: 0.9% saline; b: Crystalline silica: quartz DQ12; c: Amorphous silica: Aerosil® 150; d: Carbon black: PRINTEX® 90). Cells with labelled nuclei were quantified.

5.4 8-Oxoguanine DNA glycosylase (OGG1)

After 3 months of exposure, only the lungs of rats of the crystalline SiO_2 (quartz DQ12, 3 x 2 mg)-treated group, demonstrated a significant (* $p<0.05$, Dunnett's test) increase in the number of nuclei per mm^2 being positive for OGG1 expression, as compared to the negative (saline) control, (see Table 5.4 and Figure 5.7 and Figure 5.8 for representative images), with OGG1 representing a DNA repair enzyme, mainly dealing with the pre-mutagenic DNA-lesion 8-OH-dG. Increase in OGG1-positive nuclei thus pointed to DQ12-induced oxidative stress with subsequent occurrence of oxidative DNA-lesions in the cell nucleus. This is in line with the parallel increase in 8-OH-dG, also observed in the present study (see Section 5.3). Thereby,

enhanced OGG1-staining in the nucleus might result from induced OGG1 expression, as seen in lungs of Fisher 344 rats 5 - 7 days after intratracheal instillation of diesel exhaust particles (TSURUDOME et al., 1999) or from redistribution from the cytoplasm to the nucleus, as described by CONLON et al. (2003) under nutrient deprivation of cell cultures, associated with oxidative stress.

Table 5.4 Results of image analysis of immunohistochemical detection of 8-oxo-guanine DNA glycosylase (OGG1) as a DNA-repair enzyme and a marker for oxidative DNA-damage in lung tissue of rats of the 3-month test. Data represent counts of cells with labelled nuclei and also labelled cytoplasm per mm^2.

Marker of genotoxicity: OGG1					
Treatment	**No. of rats**	**Mean** Positive nuclei per mm^2	**SD**	**Mean** Cells with positive cytoplasm per mm^2	**SD**
Negative control: 0.9% saline	6	71.8	11.6	57.5	16.1
Crystalline SiO_2: Quartz DQ12	6	*120.4	54.6	***224.4	66.0
Amorphous SiO_2: Aerosil® 150	6	64.1	17.7	**163.4	58.5
Carbon black: PRINTEX® 90	6	62.6	18.9	***237.4	31.9

Significantly different from the negative control group (saline): * $p<0.05$, ** $p<0.01$, *** $p<0.001$; Dunnett's test; SD: Standard deviation.

The frequency of OGG1-positive nuclei in the lungs of carbon black (PRINTEX® 90, 3 x 6 mg) and amorphous SiO_2 (Aerosil® 150, 3 x 2 mg)-treated animals was rather lower than higher, as compared to the control (saline) animals. This unexpected result for PRINTEX® 90 and Aerosil® 150 might perhaps indicate depression of OGG1 expression in these treatment groups, as OGG1 is constitutively expressed and can be induced as well as reduced. Repression of OGG1 expression in lung cells was observed for example in the case of inhalative cadmium exposure of animals (POTTS et al., 2003). This repression phenomenon was also observed in the early phase after intratracheal instillation of diesel exhaust particles (DEP) in lungs of Fisher 344 rats (TSUROME et al., 1999). Interestingly, DEP contains a carbon black nucleus, On the other hand, low OGG1 expression in the carbon black- and amorphous silica-treated animals might also represent low oxidative-stress conditions with no particle-mediated induction of OGG1. However, these animals exhibited significant increase in nuclear 8-OH-dG and thus oxidative DNA lesions (see Section 5.3). Interestingly, low OGG1 expression/activity or polymorphisms may lead to a "mutator phenotype", due to reduced repair of endogenously/metabolically produced ROS, and seem to be linked to an enhanced risk for lung tumour development (PAZ-ELIZUR et al., 2003).
In contrast, all particle-treated groups demonstrated a highly significant increase in the number of cells with OGG1-positive cytoplasm per mm^2 (quartz DQ12 and PRINTEX® 90: ***$p \leq 0.001$; Aerosil® 150: **$p \leq 0.01$), as compared to the control animals

(saline). The frequency of OGG1-positive cytoplasm was comparable for lungs of the DQ12- and the PRINTEX® 90 groups, irrespective of the differing mass doses. Using the Tukey test, there was no statistically significant difference between the lungs of the different dust-treated groups. The occurrence of OGG1-positive cytoplasm, which showed a granular pattern, may represent induction of OGG1-expression in the mitochondrial compartment and may thus point to particle-induced oxidative stress, perhaps generated via mitochondrial activation/ disturbance of the respiratory chain (LI et al., 2007, XIA et al., 2006), which seemed to be one important mechanism of particle-mediated genotoxicity. Interestingly, some studies like the study of XIA et al. (2006) identified nanoparticles within or around mitochondria and LI et al. (2007) demonstrated that inhibition of the mitochondrial respiratory chain function abrogates quartz induced DNA-damage in RLE-6TN rat lung epithelial type II cells. However, LI et al. (2007) could not demonstrate DNA-damage by using inhibitors of the mitochondrial respiratory chain without parallel particle treatment.

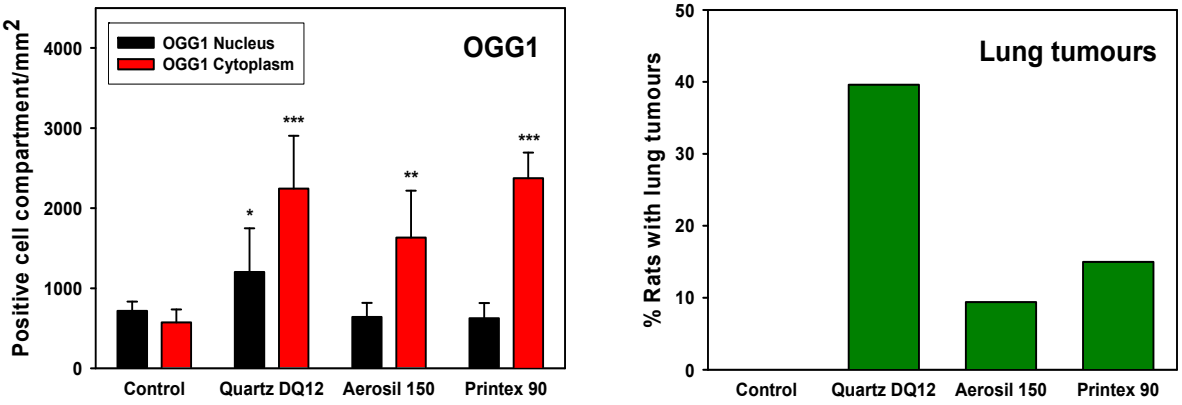

Fig. 5.7 OGG1-positive nuclei and cytoplasm in lung epithelium after 3 months and lung tumour rates after lifetime exposure.

Mitochondria are the major source of endogenous ROS, with much higher levels of 8-OH-dG in mitochondrial DNA than in nuclear DNA (SOUZA-PINTO et al., 2002) and are thus in need of efficient repair of oxidative DNA lesions, with OGG1 being one of the major DNA repair enzymes in mitochondria. Mitochondria also represent a major site for the intracellular formation and reactions with nitric oxide (NO), which represents a relatively long lived RNS. XU et al. (2009) demonstrated production of peroxynitrite anions ($ONOO^-$) by incubation of *gpt* delta transgenic primary mouse embryo fibroblast with TiO_2 and fullerene nanoparticles (ONOO- is generated by reaction of NO with $SO_2^{-\cdot}$). ONOO- besides ROS is also able to hydroxylate DNA and to trigger mutations and tumour development. The mitochondria are thus a central compartment for particle-induced nitro(oxidative) stress and subsequent mutations, with mutations in mitochondrial DNA thought to also contribute to tumourigenesis.

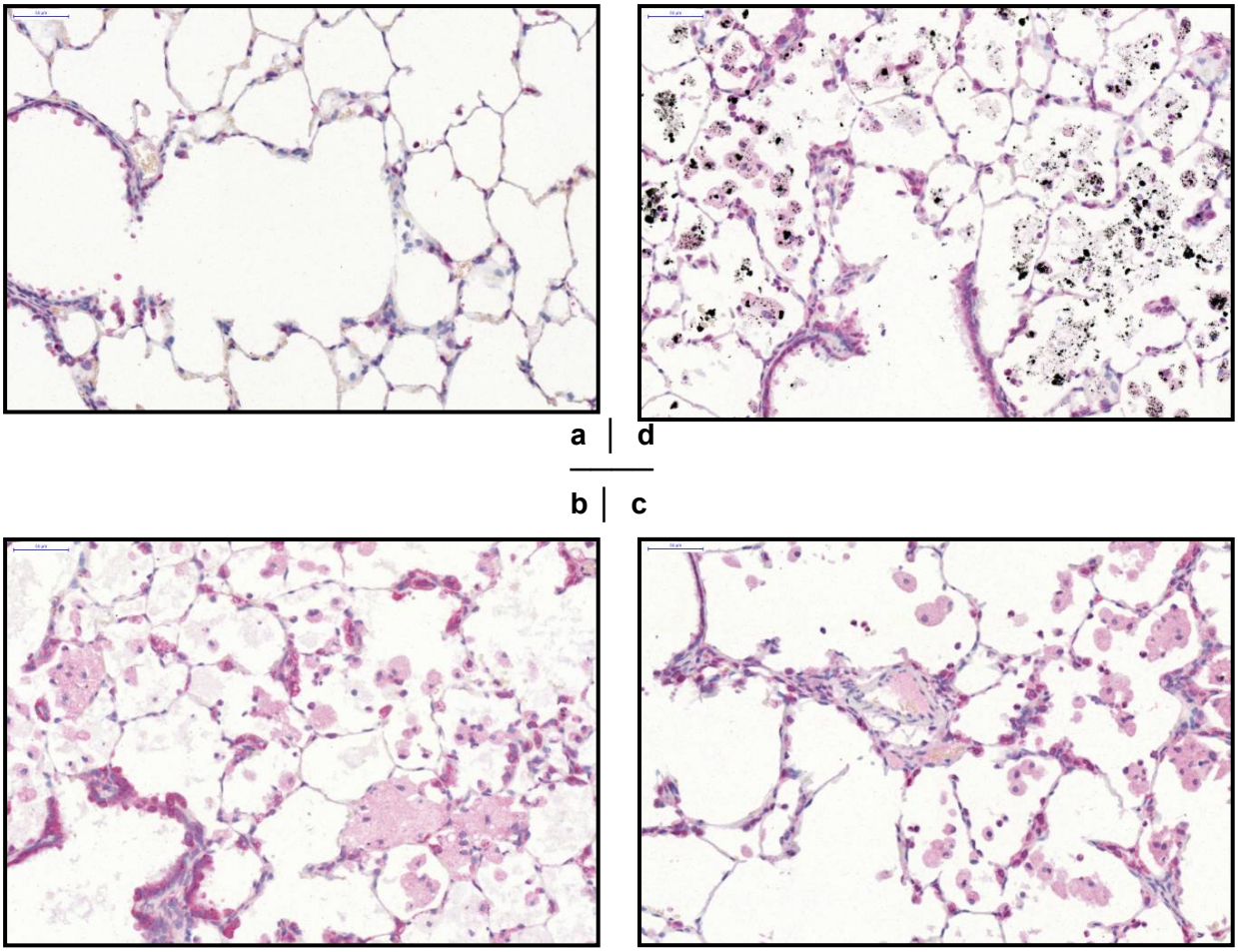

Fig. 5.8 Immunohistochemical detection of 8-oxoguanine DNA glycosylase (OGG1) as a DNA repair enzyme and a marker for oxidative DNA-damage in lung tissue of rats of the 3-month time point treated with different dusts.
Representative images: a: Negative control: 0.9% saline; b: Crystalline silica: quartz DQ 12; c: Amorphous SiO_2: Aerosil® 150; d: Carbon black: PRINTEX® 90). Pictures demonstrated cells with OGG1-positive nuclei and/or cells with OGG1-positive cytoplasm. Labelled nuclei and cytoplasm of cells were quantified separately.

Due to its complex regulation and its roles in both nucleus and mitochondria (see also Section 3.2), together with the specificity for one substrate (8-OH-dG), which is probably induced in varying amounts by the different treatments, OGG1 seems to be a less reliable, less differentiating and perhaps less prognostic (see Figure 5.7) genotoxicity marker than γ-H2AX or 8-OH-dG.

5.5 Microscopic screening of lung tissue slides of the 1- and 9-month studies

Slides of rats from the 1- and 9-month studies, which were stained immunohistochemically accordingly to the slides of the 3-month study, were roughly screened microscopically for suitability for quantification. All slides show positively and negatively stained nuclei in variable amounts and are therefore appropriate for image analysis. Without quantification with the method described above (see 4.3.2) differences between the treatment groups can not be estimated confidentially. Evaluation by image analysis should be performed contemporarily but is not part of this work package.

6 Correlation of Data on Genotoxicity Marker Expression with other Study Data and also with the Literature Data

While in the section before, the results of the individual markers have been presented and discussed, in the following part of the report the results of the markers will be compared to or correlated with the related carcinogenicity study (Section 6.1), with other results obtained from the 3 month study (Section 6.2, 6.3, 6.4), and with literature data (Section 6.5). Concerning more detailed discussion of genotoxic mechanisms see Section 5.

6.1 Correlation with Histopathological Examinations of the Carcinogenicity Study

Correlations of the genotoxicity marker expression after 3 months of exposure with the tumour incidences (lifetime exposure) should be handled with some care due to different dosing ratios concerning particle mass in the two study parts (see Table 4.2). Whereas in the 3-month study part crystalline SiO_2 (quartz DQ12), amorphous SiO_2 (Aerosil® 150), and carbon black (PRINTEX® 90) were applied in a ratio of 1 (6 mg) versus 1 (6 mg) versus 3 (18 mg), respectively, the ratio in the carcinogenicity study part in contrast amounted to 1 (3 mg) versus 5 (15 mg) versus 3.3 (5 mg). The different application ratios were based on an erroneously high application for carbon black in the 3-month study and the intention to induce comparable rate of inflammation for the different particles in the carcinogenicity study. For the methods regarding lung tissue trimming, routine and step section slide preparation see also Appendix III, page 101.

Nevertheless, by comparing the mean group data on genotoxicity marker expression in lung epithelial cells with the group means of the histopathology data of the carcinogenicity study, there were comparable patterns for the tumour incidences based on the standard analysis procedure with 1 slice per lung lobe and in particular γ-H2AX and 8-OH-dG. For PAR, OGG1-positive nuclei, and OGG1-positive cytoplasm the patterns appeared less striking (see Figure 6.1 and Tables Appendix III-1 and Appendix III-11 and KOLLING et al., 2008). Tumour incidences were determined using 6 slides per animal containing two tissue pieces of the two larger lung lobes (dorsal and ventral portion) each and one piece of each of the smaller lung lobes (see page 101) of the carcinogenicity study.

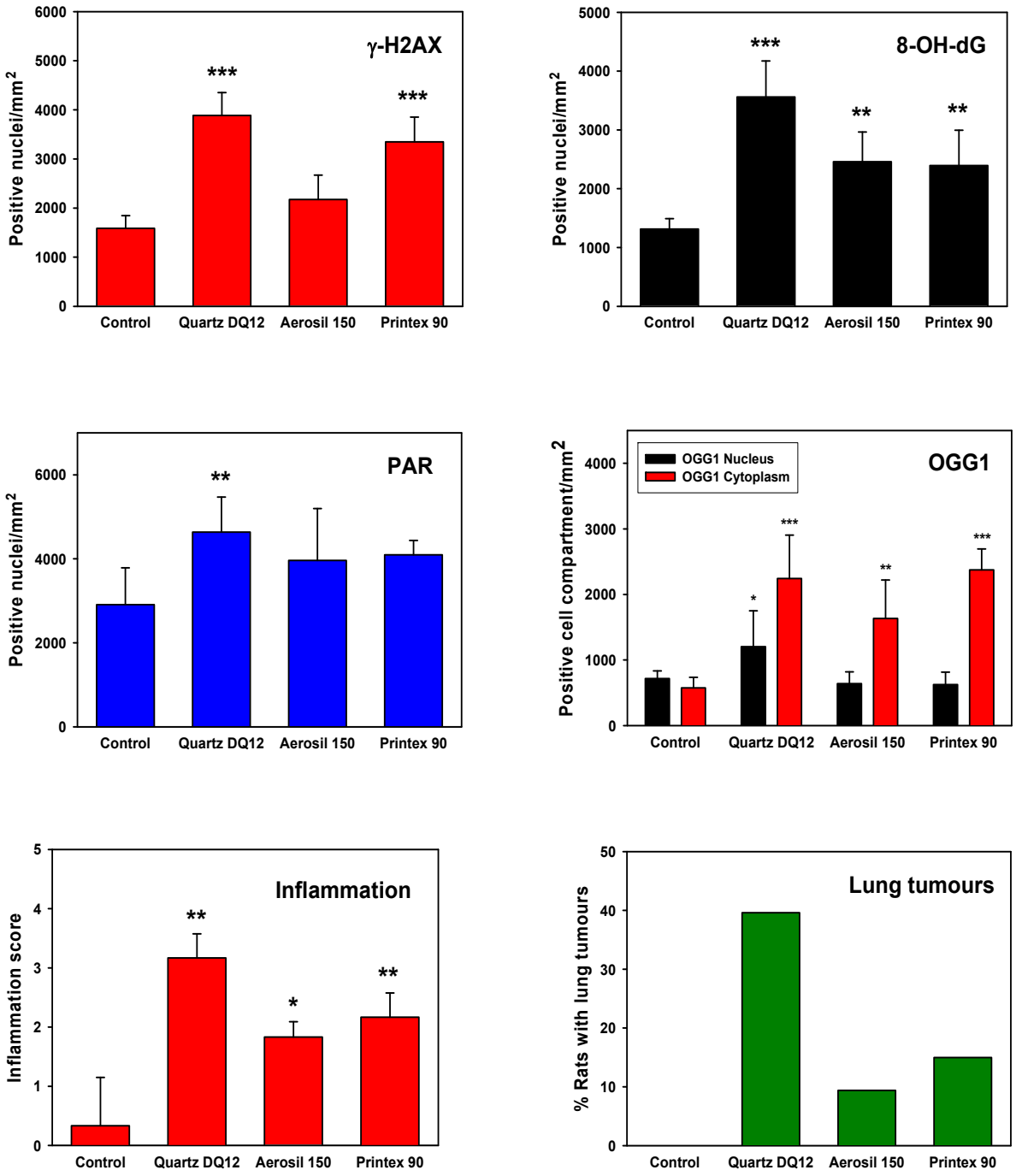

Fig. 6.1 Mean group data for γ-H2AX-, 8-OH-dG, PAR-, and OGG1-positive nuclei, OGG1-positive cytoplasm, and the inflammation score in lung epithelium after 3 months of particle exposure as well as lung tumour rates after lifetime particle-exposure.

Interestingly, using a step section approach with at least 60 slides per animal (20 slides of the left and the right caudal lobe each and 10 sections of the right cranial and right middle, and 10 sections of the accessory lobe each) for tumour analysis, the concordance of the data patterns between marker expression and tumour incidences was even more striking (data not shown). The concordances, irrespective of the different mass dose ratios for the various particles in the two study parts, might point to an important role of genotoxic events in lung epithelial cells in particle-induced lung tumour development, especially of pre-mutagenic oxidative DNA lesions (8-OH-dG) and DNA double-strand breaks (γ-H2AX) (see Sections 5.2 and 5.3 for discussion). In addition, the related patterns indicate that particle type, material, and characteristics might be more important for lung tumour induction than the applied particle mass dose. was Also, there was concordance between the inflammation score data and the tumour incidences, pointing to an important role of chronic inflammation for particle-induced lung tumour development in the overload situation (see Figure 6.1, Tables Appendix III-2 and Appendix III-3).

6.2 Correlation with Histopathological Examinations Concerning Inflammation of the 3-Month Study

In contrast to the tumour data (see 5.1), correlations of the genotoxicity marker expression with the histopathological inflammation score (for raw data see Table Appendix III-2) could be based on identical animals of the 3-month study part and thus the same particle doses. In addition, it was possible to use the group mean as well as the individual animal data (see Table Appendix III-3) for calculation (linear regression/Pearson Product Moment correlation).
Concerning correlations using the group mean data for genotoxicity marker expression and the histopathology data for the inflammation score, there was a significant (*p<0.05) correlation for 8-OH-dG positive nuclei and a highly significant correlation (**p<0.01) for PAR- positive nuclei with the mean inflammation score. Gamma-H2AX positive nuclei, OGG1-positive cytoplasm and OGG1-positive nuclei demonstrated correlations without reaching statistical significance concerning the inflammation score (see Table 6.1).

Table 6.1 Correlation of data on genotoxicity marker expression (group means; n=4) with group means (n=4) of the histopathological mean inflammation score [data from Table 5.1 (PAR), Table 5.2 (γ-H2AX), Table 5.3 (8-OH-dG), Table 5.4 (OGG1) vs. data from Table Appendix III-2 (Inflammation Score Histology)]

Parameter	**PAR** positive nuclei	**γ-H2AX** positive nuclei	**8-OH-dG** positive nuclei	**OGG1** positive nuclei	**OGG1** positive cytoplasm
	r	**r**	**r**	**r**	**r**
Mean Inflammation Score	0.994**	0.939	0.978*	0.626	0.917

Significant correlation: * p<0.05; ** p<0.01; Linear regression/Pearson Product Moment correlation.

Based on the individual animal data (see Table Appendix III-3 for the inflammation score and Appendix IV for marker expression), there were highly significant (***p<0.001) correlations (Pearson Product Moment correlation) of the histopathological inflammation score with the occurrence of 8-OH-dG, and γ-H2AX positive nuclei, and OGG1 positive cytoplasm in the lung epithelium of particle treated animals. A significant (**p<0.01) correlation was noted for PAR positive nuclei. The labelling of the nuclei with OGG1 did not significantly correlate with the mean inflammation score, when using the individual animal data (see Table 6.2). Due to the higher amount of data and thus a higher variance of data by using the individual animal data for calculation of correlations (n = 24), the "r values" are lower than by using the group mean values (n = 4), but nevertheless reach high significance levels, because of direct correlation of genotoxicity marker expression and the inflammation score of the identical animals. These correlation data indicate that lung inflammation and thus secondary mechanisms of genotoxicity are involved in particle-induced DNA-damage induction, with oxidative DNA-lesions like the pre-mutagenic 8-OH-dG. Macrophage- and perhaps granulocyte-derived ROS thus seem to be important for local genotoxicity of fine and ultrafine particles in the lung in an overload situation. Interestingly, there was also high correlation of the mean histopathological inflammation score after 3 months of exposure with the tumour incidences (see Figure 6.1, Table Appendix III-1 and Appendix III-11, and KOLLING et al., 2008), irrespective of the differences in the applied particle mass doses. Correlation amounted to 0.928 for standard tumour analysis and was even statistically significant in the case of the multiple step section procedure for tumour analysis (r = 0.973, * p<0.05; data not shown), thus providing a link between particle exposure, inflammation, induction of DNA-damage, and lung tumour development.

Table 6.2 Correlation of data (individual animals; n=24) on genotoxicity marker expression with histopathological inflammation score of individual animals (n=24) [similar to Table 6.1 with individual data]

Parameter	**PAR** positive nuclei	**γ-H2AX** positive nuclei	**8-OH-dG** positive nuclei	**OGG1** positive nuclei	**OGG1** positive cytoplasm
	r	**r**	**r**	**r**	**r**
Mean Inflammation Score	0.554**	0.771***	0.803***	0.300	0.675***

Significant correlation: *** p<0.001; ** p<0.01; Linear regression / Pearson Product Moment correlation.

6.3 Correlation with Bronchoalveolar Lavage (BAL) Data of the 3-Month Study

The correlation analysis (linear regression/Pearson Product Moment correlation) of the results of the genotoxicity marker immunohistochemistry with data from the BALs of animals of the same treatment groups (see Tables Appendix III-5 to Appendix III-7) demonstrated highly significant correlations (**p<0.01) for γ-H2AX with γ-glutamyl transferase, lactic dehydrogenase, and lung wet-weight, and a significant (*p<0.05) correlation with total protein data. There was no significant correlation of the data for 8-OH-dG, PAR, or the nuclear and cytoplasmic labelling of OGG1 with any of the

BAL endpoints (see Table 6.3). However, for nearly all genotoxicity markers and BAL endpoints there were “r values” which indicated correlation without reaching significance, perhaps due to the use of group means for calculation and not the individual animal data. The good correlation of some BAL markers for lung tissue damage like LDH liberation or total protein with γ-H2AX as a marker for DNA double-strand breaks might indicate a link between tissue damage and occurrence of profound DNA-damage with mutagenic potential. However, increase in γ-H2AX positive nuclei might also reflect, in addition, enhanced apoptosis in lung epithelium due to particle exposure. Analysis of apoptosis in lung tissue samples of the particle-exposed animals could clarify this point.

Table 6.3 Correlation of data (group means; n=4) on genotoxicity markers with group means (n=4) of bronchoalveolar lavage (BAL) data of the 3-month study [raw data see Appendix III: Table 5.1 (PAR), Table 5.2 (γ-H2AX), Table 5.3 (8-OH-dG), Table 5.4 (OGG1) vs. data from Table Appendix III-4 (BAL Leucocytes, BAL Polymorphonuclear Granulocytes), Table Appendix III-5 (BAL γ-Glutamyl Transferase, BAL Alkaline Phosphatase, BAL Lactic Dehydrogenase), Appendix III-6 (BAL Total Protein), Table Appendix III-7 (Lung Wet-Weight)]

Parameter	**PAR** positive nuclei	**γ-H2AX** positive nuclei	**8-OH-dG** positive nuclei	**OGG1** positive nuclei	**OGG1** positive cytoplasm
	r	**r**	**r**	**r**	**r**
BAL γ-Glutamyl Transferase [U/l]	0.907	0.994**	0.854	0.540	0.946
BAL Alkaline Phosphatase [U/l]	0.677	0.740	0.497	-0.062	0.906
BAL Lactic Dehydrogenase [U/l]	0.877	0.996**	0.833	0.573	0.917
BAL Leucocytes [No./ml]	0.779	0.858	0.875	0.937	0.610
BAL Polymorphonuclear Granulocytes [No./ml]	0.826	0.944	0.875	0.842	0.737
BAL Total Protein [mg/l]	0.821	0.983*	0.774	0.554	0.886
Lung Wet-Weight [g]	0.906	0.998**	0.861	0.569	0.935

Significant correlation: * $p<0.05$; ** $p<0.01$; Linear regression / Pearson Product Moment correlation.

6.4 Correlation with *ex vivo* TNF-α Liberation Data of the 3-Month Study

TNF-α liberation (immunobiology) data were generated using re-suspended and cultivated cells from the BAL fluids, which consisted predominantly of alveolar macrophages. Genotoxicity marker data, however, were obtained from histological slides, with predominant analysis lung epithelial cells and exclusion of macrophages from the marker expression counts. Strong correlations of data were therefore not ex-

pected. Nevertheless, decrease in macrophage functionality can reflect lung tissue damage and might lead to enhanced susceptibility of the lung to toxic insults.
Nevertheless, after 3 months of particle exposure, significant negative correlations (*p<0.05; linear regression/Pearson Product Moment correlation) were evident for TNF-α concentrations in culture supernatants of unstimulated BAL cells or BAL cells from particle exposed animals, which were stimulated with 0.1 and 1 ng/ml LPS and lung epithelial cells with γ-H2AX-positive nuclei. Significant negative correlations were also noted for TNF-α-concentrations in supernatants of unstimulated BAL cells and BAL cells from particle exposed animals, which were stimulated with 1 ng/ml LPS and lung epithelial cells with OGG1-positive cytoplasm. Except for OGG1-positive nuclei, there were, in addition, some "r values" which indicate negative correlations, without reaching statistical significance (see Table 6.4 and Table Appendix III-8). These negative correlations might indicate reduced functionality and reactivity of alveolar macrophages after 3 months of (nano)particle exposure with reduced capacity to react on external stimuli with cytokine production. This might be due to particle induced lung and lung cell damage. Interestingly, there was negative correlation for γ-H2AX, as a marker for DNA double-strand breaks and thus profound DNA-damage, with TNF-α-liberation, and on the other hand significant positive correlations of the same genotoxicity marker with markers for tissue damage in the BAL.

Table 6.4 Correlation of data (group means; n=4) on genotoxicity markers with group means (n=4) of tumour-necrosis-factor-α (TNF-α) concentration of 3-month study [raw data see Appendix III: Table 5.1 (PAR), Table 5.2 (γ-H2AX), Table 5.3 (8-OH-dG), Table 5.4 (OGG1) vs. data from Table Appendix III-8 (TNF-α)]

Parameter	**PAR** positive nuclei	**γ-H2AX** positive nuclei	**8-OH-dG** positive nuclei	**OGG1** positive nuclei	**OGG1** positive cytoplasm
	r	**r**	**r**	**r**	**r**
TNF-α concentration [pg/ml], Control	-0.851	-0.976*	-0.776	-0.454	-0.941*
TNF-α concentration [pg/ml], 0.1 ng/ml LPS	-0.808	-0.969*	-0.736	-0.461	-0.909
TNF-α concentration [pg/ml], 1 ng/ml LPS	-0.873	-0.963*	-0.781	-0.391	-0.970*

Significant correlation: * p<0.05; Linear regression / Pearson Product Moment correlation.

6.5 Correlation with Literature Data on *in vitro* and *in vivo* Genotoxicity

In the following those studies have been selected from the literature review, which correspond most closely to the particles investigated in our study. As DQ12 is a commonly used reference dust, data are included for this comparison. Also studies with PRINTEX® 90 are available in the literature. No studies could be detected for Aerosil® 150, which has been examined in our *in vivo* studies. Therefore other studies with amorphous silica have been selected.

Table 6.5 presents the results of *in vitro* studies with selected particles, including the lowest dose level with a positive result. If the study was negative, the maximum dose tested and a statement on cytotoxicity was included, because it is well known that in many cases genotoxicity studies with particles are only positive at or near cytotoxic concentrations. Thus, this information allows an estimate whether a "negative" result (no genotoxic effect observed) is likely to be a “true negative" one.

Table 6.5 *In vitro* genotoxicity of selected nanoparticles

Assay	**Particle**		
	Crystalline Silica: Quartz DQ12	Amorphous Silica	Carbon Black: PRINTEX® 90
Comet assay	**++** 156 µg/ml Lı et al. 2007 125 µg/ml SCHINS et al., 2002 625 µg/ml CAKMAK et al., 2004	**-** max. concentration tested: 40 µg/ml ; no cytotoxicity BARNES et al., 2008	**+** 100 µg/ml; MROZ et al., 2008 75 µg/ml; JACOBSEN et al., 2007
Micronucleus assay	**+** 31 µg/ml GEH et al., 2006	not reported	**+** 3,4 µg/ml, TOTSUKA et al., 2009
HPRT	not reported	not reported	**+** 75 µg/ml; JACOBSEN et al., 2007
8-OH-dG	**++** 300 µg/ml; Lı et al., 2007 240 µg/ml SCHINS et al., 2002	not reported	not reported
ROS	not reported	**-** up to 200 µg/ml ; YU et al., 2009	**+** 6,5 µg/ml JACOBSEN et al., 2008; 20 µg/ml YANG et al., 2009

Particle concentrations for the *in vitro* studies were provided in the publications as µg/cm² or µg/ml. The concentrations per area, i.e. µg/cm², is probably more relevant from a toxicological point of view, because the particles sediment on the cells, irrespective of the volume above the cells. However, concentration per volume (µg/ml) is the more commonly used dose measure. Therefore, to allow comparison between the studies, concentrations of the nanoparticles in µg/cm² have been converted to µg/ml by using the amount of medium used and the size of the petri dish. If not stated in the publications, a volume of 300 µl medium/cm² was assumed.
No study was available, where all of the 3 particles have been tested simultaneously, hampering a direct comparison of the results. Test results may depend on the parti-

cle investigated, but also on the test system (cell type, endpoint investigated) or on the concentration levels tested.

Quartz DQ 12 is clearly genotoxic at similar test concentrations (125-625 µg/ml) in all test systems using the comet assay (CAKMAK et al., 2004; LI et al., 2007; SCHINS et al., 2002) and the micronucleus assay (31 µg/ml, GEH et al., 2006), and it induces oxidative DNA damage as indicated by 8-OH-dG formation (LI et al., 2007; SCHINS et al., 2002). Positive results, however, have been obtained mainly at or near cytotoxic concentrations (Table 6.5). This corresponds to the results of our immunohistochemical *in vivo* investigation, where quartz DQ12 generated a strong positive response for all DNA damage endpoints investigated, including PAR and γ-H2AX (DSB) formation, induction of 8-OH-dG formation and expression of OGG1 in both nucleus and cytoplasm under overload conditions.

Amorphous silica had the lowest genotoxic potency in our tests as no significant genotoxicity was observed, based on the markers PAR and γ-H2AX. This is supported by the few publications available up to now: A comet assay *in vitro* was negative at 40 µg/ml (BARNES et al., 2008). No *in vitro* ROS generation by amorphous silica could be detected at concentrations up to 200 µg/ml (YU et al., 2009) and no increase in micronuclei was found in peripheral blood of rats after inhalation of high concentrations (up to 86 mg/m^3) of amorphous silica nanoparticles (SAYES et al., 2010). There are, however, some open questions. The highest concentration of amorphous silica, tested in the publication of BARNES et al. (2008), is rather low, as compared to the studies with quartz DQ12, and it is not clear whether higher, cytotoxic concentrations, might have generated genotoxic effects. The absence of ROS in the study of YU et al. (2009) is in contrast to our *in vivo* findings, where significant positive results were obtained for 8-OH-dG formation and OGG1 expression in the cytoplasm. The *in vivo* response with respect to 8-OH-dG formation in our study was even higher for amorphous silica than for carbon black, which, however had a higher carcinogenic potency in the lifetime part of our study. This may indicate that the generation of ROS is not the sole determinant of carcinogenicity of the particles.

For **PRINTEX® 90** a comprehensive database of *in vitro* studies is available. All test results concerning genotoxicity and generation of ROS are positive, which corresponds to the findings of our *in vivo* study. However, based on the concentrations tested (3.4 – 100 µg/ml for the *in vitro* genotoxicity studies) it might even have a higher genotoxic potency than DQ12. This may be related to the smaller particle size of the PRINTEX ® 90 particles, as compared to DQ 12, but also to particle/material-specific genotoxicity. In contrast, in our *in vivo* study, PRINTEX® 90 was less potent than DQ12 in almost all parameters investigated. *In vivo,* only studies with PRINTEX® 90 are available, which confirm the genotoxicity of PRINTEX® 90 in the lung, as observed in our investigation. DNA damage was found after intratracheal instillation in a comet assay in lung cells (TOTSUKA et al., 2009). Furthermore, mutations were found in the lungs of gpt delta transgenic mice (TOTSUKA et al., 2009). Another study detected 8-OH-dG in lung tissue after inhalation of PRINTEX® 90 (GALLAGHER et al., 2003). The publication from TOTSUKA et al. (2009) provides also important mechanistic insights. From the prominent mutation spectra in the *gpt* gene, it was suggested that oxidative DNA damage might be commonly involved in the mutagenicity of particles. The most typical lesion of oxidative damage, 8-OH-dG, which, by pairing with dA leads to G:C -> T:A transversions, however, was only rarely detected. Instead of

G:T transversions, the most prominent mutation type induced by particles used was a G:C to C:G transversion. This mutation type only rarely occurred in unexposed cells, but was observed in particle treated animals, irrespective of the particle type. A variety of oxidative lesions of guanine other than 8-OHdG, e.g. oxazolone formation, are known to cause such transversions. Therefore, it might be interesting to develop antibodies detecting specifically these particle-associated lesions.
Overall, the investigations on genotoxicity and ROS generation from the *in vitro* as well as *in vivo* studies in the literature correlate well with the results of our study concerning qualitative effects. There are, however, quantitative differences. The ranking of the genotoxic potency and of the ROS generating potential of the three particles, based on the lowest effective dose in the *in vitro* literature studies, would be PRINTEX® 90 > DQ12 > amorphous silica. In contrast, the ranking based on our *in vivo* study was DQ12 > PRINTEX® 90* > Aerosil® 150. This ranking correlates, however, better to the ranking of the carcinogenic potency in the lifetime carcinogenicity study than does the ranking derived from the *in vitro* literature studies.

* Note: PRINTEX® 90 was dosed 3 times higher than DQ12 and Aerosil® 150, however, it was less genotoxic than DQ12.

7 Summary and Conclusions

This project aimed at studying whether different particles including nanoparticles can induce genotoxicity *in vivo* in lung epithelial cells. Genotoxicity was assessed by applying immunhistochemical detection and quantification of different markers for DNA damage. Furthermore, it was analysed how the results of this study correspond to those of other studies in the literature concerning the genotoxicity of similar or the same particles *in vitro* and *in vivo,* and whether the observed effects may be suitable early indicators to determine a possible carcinogenic potential of low soluble dusts.
Lung tissue samples of a subchronic study with different dusts were available from an experiment previously conducted at the Fraunhofer ITEM. In this study, rats were exposed intratracheally for 3 months to 3 x 2 mg crystalline silica (DQ12, 1300 nm), 3 x 2 mg amorphous silica (Aerosil® 150, 14 nm) or 3 x 6 mg carbon black (PRINTEX® 90, 14 nm), respectively, to induce an overload scenario. Furthermore, a carcinogenicity study with intratracheal instillation of the same particles (however, different doses) is available at Fraunhofer ITEM, which allows comparisons of genotoxicity marker expression with the outcome of this carcinogenicity study. The purpose of this chronic study was to analyse the toxicity of the particles also under overload conditions. Therefore, different amounts of the three particles (with only one dose per particle type) have been applied.
The markers for DNA damage have been selected based on existing experience with *in vitro* and *in vivo* genotoxicity studies with particles as well as the proposed mode of action of particles via oxidative stress. PAR indicates early cellular reaction to DNA damage, γ-H2AX DNA double strand breaks (DSB), 8-OH-dG a specific oxidative DNA-base modification (one of several existing), and OGG1 repair capacity related to oxidative damage.
As demonstrated in Table 7.1, for quartz DQ12 all biomarkers gave statistically significant positive results, indicating profound genotoxic stress, occurrence of DSB, and oxidative DNA damage with subsequent repair activity. The response was less pronounced for PRINTEX® 90 (carbon black), but nevertheless significant increase in DSB, 8-OH-dG, and OGG1-positive cytoplasm were detected. Finally, for Aerosil® 150 (amorphous silica), only 8-OH-dG levels and repair activity of oxidative DNA damage, as represented by OGG1 expression in the cytoplasm, were statistically significant. This indicates that these markers react differently to different types of particles and particle doses. The marker which was most sensitive, differentiated best between the three particles, and correlated well with the carcinogenicity data was γ-H2AX. 8-OH-dG correlated best with the inflammation score after 3 months of exposure. The findings also generally correlated with positive or negative results in the *in vitro* and *in vivo* literature data on genotoxicity of the three particles. However, concerning genotoxic potency, in the present *in vivo* study DQ12 exhibited the highest strength (DQ12 > PRINTEX® 90 > Aerosil® 150) whereas in the *in vitro* literature PRINTEX® 90 seems to be more potent. Further, differences in the genotoxic potency of the various particles seem to be more pronounced with our biomarkers *in vivo* than in the *in vitro* literature studies. The ranking of genotoxicity of the three particles detected with the different markers also correlated with the inflammation scores of the histopathological examinations (Table 7.1), where quartz DQ12 also produced the highest response, followed by PRINTEX® 90 (carbon black) and Aerosil® 150 (amorphous silica).

A comparison with the carcinogenicity study has to consider the different dose levels applied in both studies (Table 7.1). In the carcinogenicity study the highest dose was applied for Aerosil® 150 (amorphous silica, 15 mg), followed by PRINTEX® 90 (carbon black, 5 mg) and quartz DQ12 (crystalline silica), as the purpose of the study was to produce significant inflammation. For the quickly eliminated Aerosil® 150 persistent inflammation could be only maintained by 30-fold renewal of lung dosing (special design of repeated "acute dosing" making Aerosil® 150 to a "secondary" carcinogen). The carcinogenic potency, as determined in the lifetime study, demonstrated the following order for the three particle types: quartz DQ12 (crystalline silica) > PRINTEX® 90 (carbon black) > Aerosil® 150 (amorphous silica). Due to the different dose levels used for the three particles in the carcinogenicity study, the difference in the carcinogenic potency of the particles may, however, be underestimated, because in the case of equal dose levels for the different particles (for example 3 mg/rat as applied for quartz DQ12) the percentage of rats with lung tumours would be quite low for Aerosil® 150 (amorphous silica).
This sequence in tumourigenic activity of the three particles after intratracheal application corresponded more or less (depending on the DNA damage marker used) to the data on local genotoxicity in the lung, indicating that the genotoxicity markers indeed may be predictors of carcinogenicity. Interestingly, quantification of γ-H2AX expression as a marker for DSB, led to nearly the same order like the tumour incidences, thus pointing to an important role of DSB in particle-induced lung tumour development and a potentially high prognostic value of this marker. As patterns of inflammation, oxidative DNA damage, DSB formation, and carcinogenicity were highly related in this study, the findings are consistent with the view that, in the overload situation, chronic inflammation leads to chronic exposure of epithelial cells to ROS, nitro(oxidative)-stress and subsequent oxidative DNA-damage including DSB formation, which may lead to mutations and lung tumour development, but also cell death.

In conclusion this study demonstrated that different genotoxic events are involved in particle-induced lung tumour development, and that local *in vivo* genotoxicity of particles can be detected and quantified immunohistochemically in lung epithelial cells already after 3 months of exposure using lung tissue samples. The use of immunohistochemical detection and quantification of different genotoxicity markers in lung tissue samples could thus be a promising approach for testing in the future the genotoxic modes of action of particles (or also non-particulate compounds) *in vivo* in relevant target cells. In addition, some genotoxicity markers may be sensitive predictors of carcinogenicity, as their early expression seems to correspond in the present study to the carcinogenic potency of the particles and they also responded to compounds (for example amorphous silica), showing low tumour yield in carcinogenicity studies.

Table 7.1 Comparison of results: Marker significance found for various particle types

	Genotoxic relevance	**Control**	**Crystalline SiO_2** Quartz DQ12	**Amorphous SiO_2** Aerosil® 150	**Carbon black** PRINTEX® 90
Particle size [nm]			**1300**	**14**	**14**
Subchronic study					
Dose [mg/rat]		**0**	**3 x 2**	**3 x 2**	**3 x 6**
		Positive nuclei per mm^2			
PAR	Overall marker for genotoxic stress	**290.9** ± 87.8	**463.6**** ± 83.6	**396.3** ± 123.5	**409.7** ± 34.0
γ-H2AX	DNA double-strand breaks	**158.8** ± 25.8	**388.6***** ± 46.6	**217.4** ± 49.7	**334.8***** ± 50.3
8-OH-dG	Oxidative DNA damage	**131.4** ± 17.7	**356.1***** ± 61.2	**246.0**** ± 50.4	**239.5**** ± 60.0
OGG1 – Nuclei	Oxidative DNA damage and related DNA repair capacity	**71.8** ± 11.6	**120.4*** ± 54.6	**64.1** ± 17.7	**62.6** ± 18.9
OGG1 – Cytoplasm		**57.5** ± 16.1	**224.4***** ± 66.0	**163.4**** ± 58.5	**237.4***** ± 31.9
Inflammation score		**0.3** ± 0.8	**3.2** ± 0.4	**1.8** ± 0.3	**2.2** ± 0.4
Carcinogenicity study					
Dose [mg/rat]		**0**	**1 x 3**	**30 x 0.5**	**10 x 0.5**
% of rats with lung tumours*)		**0**	**39.6**	**9.3**	**15**

PAR Poly(ADP-Ribose)
γ-H2AX Phosphorylated H2AX
8-OH-dG 8-Hydroy-2'-deoxyguanosine
OGG1 8-Oxoguanine DNA glycosylase

*** statistically significant increase ($p < 0.001$)
** statistically significant increase ($p < 0.01$)
* statistically significant increase ($p < 0.05$)

*) Data from ERNST et al. (1999) and KOLLING et al. (in preparation)

8 Recommendations

This study has demonstrated that 3 months after particle exposure is a suitable time point for evaluation of genotoxicity in lung tissues by using immunohistochemical detection and quantification of genotoxicity marker expression. Screening analyses of the slides from rats exposed to 1 and 9 months showed positive and negative stained nuclei, indicating a relevant response also at these time points. However, quantification of marker expression at this timepoints was beyond the scope of the project. It should, however, be performed in order to evaluate the best time point for future immunohistochemical investigations. Of special interest is the question, if genotoxicity can be reliably detected already after 1 month, which would allow inclusion of local in vivo genotoxicity analyses in subacute toxicity studies.

The results of this project have been gained from animals that were dosed at clear lung overload conditions, i.e. total lung loads of rats amounted to > 3 mg/lung. Consequently, a strong and persisting inflammation has been induced in the lungs of exposed animals. Therefore, these results cannot conclusively answer if only a secondary inflammation-dependent mechanisms or also particle-specific primary mechanisms of genotoxicity may be responsible for tumour induction by fine and ultrafine particles in the lung. At severe overload, secondary mechanisms will overwhelm and confuse potentially existing primary mechanisms, thus preventing a clear distinction between the different mechanisms.

To better evaluate a potential impact of primary genotoxic mechanisms on lung tumour induction by fine and ultrafine particles, an experiment under non-overload conditions should be designed, or samples of potentially existing studies with appropriate sample fixation could be used. These experiments should include a well-known (human) carcinogenic and a well-known non-carcinogenic dust, and the inflammatory reaction in the lung should not exceed a very slight level (< 10% PMNs). Otherwise the experiments could generate equivocal data.

Only one dose level for each particle type (crystalline silica, amorphous silica, and carbon black) was available in the present study, thus preventing analysis of dose responses concerning marker expression. Further studies should therefore analyse, in addition, different dose levels of particles.

Finally, for better characterisation of the specificity of the used genotoxicity markers, it would be interesting to determine both marker expression, apoptosis and proliferation in the same tissue samples. Besides the genotoxicity markers tested in our study, additional endpoints might be investigated immunohistochemically with suitable markers. This holds especially for oxidative DNA damage, where 8-OHdG may not be the most relevant marker of particle-induced oxidative DNA damage.

9 References

Aburatani H, Hippo Y, Ishida T, Takashima R, Matsuba C, Kodama T, Takao M, Yasui A, Yamamoto K & Asano M (1997) Cloning and charaterization of mammalian 8-hydroxyguanine-specific DNA glycosylase/apurinic, apyrimidinic lyase, a functional mutM homologue. Cancer Res. 57:2151-2156

Alvarez-Gonzalez R & Althaus FR (1989) Poly(ADP-ribose) catabolism in mammalian cells exposed to DNA-damaging agents. Mutat. Res. 218:67-74

Banáth JP, Macphail SH & Olive PL (2004) Radiation sensitivity, H2AX phosphorylation, and kinetics of repair of DNA strand breaks in irradiated cervical cancer cell lines. Cancer Res. 64(19):7144-7149

Barnes CA, Elsaesser A, Arkusz J, Smok A, Palus J & Lesniak A (2008) Reproducible comet assay of amorphous silica nanoparticles detects no genotoxicity. Nano Lett. 8(9):3069-3074

Bhattacharya K, Cramer H, Albrecht C, Schins R, Rahman Q, Zimmermann U & Dopp E (2008) Vanadium pentoxide-coated ultrafine titanium dioxide particles induce cellular damage and micronucleus formation in V79 cells. J. Toxicol. Environ. Health A 71(13-14):976-980

Bhattacharya K, Davoren M, Boertz J, Schins RPF, Hoffmann E & Dopp E (2009) Titanium dioxide nanoparticles induce oxidative stress and DNA adduct formation but not DNA breakage in human lung cells. Part. Fibre Toxicol. 6:17, 36p

Blanco D, Vicent S, Fraga MF, Fernandez-Garcia I, Freire J, Lujambo A, Esteller M, Ortiz-de-Solorzano C, Pio R, Lecanda F & Montuenga LM (2007) Molecular analysis of a multistep lung cancer model induced by chronic inflammation reveals epigenetic regulation of p16 and activation of the DNA damage response pathway. Neoplasia 9(10):840-852

Bohr VA, Stevnsner T & Souza-Pinto NC (2002) Mitochondrial DNA repair of oxidative damage in mammalian cells. Gene 286:127-134

Bürkle A (2001) Physiology and pathophysiology of poly (ADP-ribosyl)ation. BioEssays 23:795-806

Cakmak GD, Schins RP, Shi T, Fenoglio I, Fubini B & Borm PJ (2004) In vitro genotoxicity assessment of commercial quartz flours in comparison to standard DQ12 quartz. Int. J. Hyg. Environ. Health 207(2):105-113

Cheng KC, Cahill DS, Kasai H, Nishimura S & Loeb LA (1992) 8-Hydroxyguanine, an abundant form of oxidative DNA damage, causes G->T and A->C substitutions. J. Biol. Chem. 267:166-172

Chevillard S, Radicella J, Levalois C, Lebeau J, Poupon MF, Oudard S, Dutrillaux B & Boiteux S (1998) Mutations in OGG1, a gene involved in the repair of oxidative

DNA damage, are found in human lung and kidney tumors. Oncogene 16:3083-3086
Conlon KA, Zharkov DO & Berrios M (2003) Immunofluorescent localization of the murine 8-oxoguanine DNA glycosylase (mOGG1) in cells growing under normal and nutrient deprivation conditions. DNA Repair 2:1337-1352

Daniel LN, Mao Y, Williams AO & Safiotti U (1995) Direct interaction between crystalline silica and DNA - a proposed model for silica carcinogenesis. Scand. J. Work Environ. Health. 21(Suppl. 2):22-26

Dianov G, Bischoff C, Piotrowski J & Bohr VA (1998) Repair pathways for processing of 8-oxoguanine in DNA by mammalian cell extracts. J. Biol. Chem. 273:33811-33816

Donaldson K & Borm PJA (1998) The quartz hazard: A variable entity. Ann. Occup. Hyg. 42(5):287-294

Driscoll KE, Carter JM, Howard BW, Hassenbein DG, Pepelko W, Baggs RB & Oberdörster G (1996) Pulmonary inflammatory, chemokine, and mutagenic responses in rats after subchronic inhalation of carbon black. Toxicol. Appl. Pharmacol. 136:372-380

Driscoll KE, Deyo LC, Carter JM, Howard BW & Hassenbein DG (1997) Effects of particle exposure and particle-elicited inflammatory cells on mutation in rat alveolar epithelial cells. Carcinogenesis 18(2):423-430

Duffin R, Tran L, Brown D, Stone V & Donaldson K. (2007) Proinflammogenic effects of low-toxicity and metal nanoparticles in vivo and in vitro: Highlighting the role of particle surface area and surface reactivity. Inhal. Toxicol. 19(10):849-856

ECETOC (2006) Synthetic amorphous silica, JACC no. 51, Brussels, Sept. 2006

ENRHES (2010) Engineered nanoparticles: Review of Health and Environmental Safety, Coordinator: V. Stone, Project website address: http://nmi.jrc.ec.europa.eu/project/ENRHES.htm

Ernst H, Rittinghausen S, Bartsch W, Creutzenberg O, Dasenbrock C, Görlitz BD, Hecht M, Kairies U, Muhle H, Müller M, Heinrich U & Pott F (2002) Pulmonary inflammation in rats after intratracheal instillation of quartz, amorphous SiO_2, carbon black, and coal dust and the influence of poly-2-vinylpyridine-N-oxide (PVNO). Exp. Toxicol. Pathol. 54(2):109-126

Ernst H, Kolling A, Bellmann B, Rittinghausen S, Heinrich U & Pott F (2005) Pathogenetische und immunbiologische Untersuchungen zur Frage: Ist die Extrapolation der Staubkanzerogenität von der Ratte auf den Menschen gerechtfertigt? Teil II: Histologie. Abschlussbericht. Umweltforschungsplan des Bundesministeriums für Umwelt, Naturschutz und Reaktorsicherheit. November 2005. < http://www.umwelt-daten.de/publikationen/fpdf-1/3033.pdf >

Folkmann JK, Risom L, Jacobsen NR, Wallin H, Loft S & Moller P (2009) Oxidatively damaged DNA in rats exposured by oral gavage to C60 fullerenes and single-walled carbon nanotubes. Environ. Health Perspect. 117(5):703-708

Gallagher J, Sams R, Inmon J, Gelein R, Elder A, Oberdörster G & Prahalad AK (2003) Formation of 8-oxo-7,8-dihydro-2'-deoxyguanosine in rat lung DNA following subchronic inhalation of carbon black. Toxicol. Appl. Pharmacol. 190(3):224-231

Gonzalez L, Lison D & Kirsch-Volders M (2008) Genotoxicity of engineered nanomaterials: A critical review. Nanotoxicology 2(4):252-273

Gopalan RC, Osman IF, Amani A, De Matas M & Anderson D (2009) The affect of zinc oxide and titanium dioxide nanoparticles in the comet assay with UVA photoactivation of human sperm and lymphocytes. Nanotoxicology 3:33-39

Greim H (1999) Siliciumdioxid, kristallin Quarz-, Cristobalit-, Tridymitstaub. In: DFG - Gesundheitsschädliche Arbeitsstoffe. Toxikologisch-arbeitsmedizinische Begründungen von MAK-Werten (29.Lfg.). Weinheim , Wiley - VCH, 66p.

Gurr JR, Wang AS, Chen CH & Jan KY (2005) Ultrafine titanium dioxide particles in the absence of photoactivation can induce oxidative damage to human bronchial epithelial cells. Toxicology 213(1-2):66-73. Cited in Gonzalez et al. (2008).

Hakmé A, Wong H-K, Dantzer F & Schreiber V (2008) The expanding field of poly(ADP-ribosyl)ation reactions. Protein Modifications: Beyond the Usual Suspects Review Series. EMBO Rep. 9(11):1094-1100

Henderson RF, Mauderly JL, Pickrell JA, Hahn FF, Rebar AH & Muhle H (1987) Comparative study of bronchoalveolar lavage fluid - effect of species, age, and method of lavage. Experimental Lung Res. 13:329-342

Husgafvel-Pusiainen K, Boffeta P, Kannio A, Nyberg F, Pershagen G, Mukeria A, Constantinescu V, Fortes C & Benhamou S (2000) p53 mutations and exposure to environmental tobacco smoke in a multi-center study on lung cancer. Cancer Res. 60:2906-2911

Ismail IH, Wadhra TI & Hammarstein O (2007) An optimized method for detecting gamma-H2AX in blood cells reveals a significant interindividual variation in the gamma-H2AX response among humans. Nuclei Acids Red. 35(5):e36. Epub 2007 Feb 6.

Jacobsen NR, Saber AT, White P, Moller P, Pojana G, Vogel U, Loft S, Gingerich J, Soper L & Douglas GR & Wallin H (2007) Increased mutant frequency by carbon black, but not quartz, in the lacZ and cII transgenes of muta mouse lung epithelial cells. Environ Mol Mutagen 48(6):451-461. Cited in Gonzalez et al. (2008).

Jacobsen NR, Pojana G, White P, Moller P, Cohn CA, Korsholm KS, Vogel U, Marcomini A, Loft S & Wallin H (2008) Genotoxicity, cytotoxicity, and reactive oxygen species induced by single-walled carbon nanotubes and C(60) fullerenes in the FE1-MutaTMMouse lung epithelial cells. Environ. Mol. Mutagen. 49(6):476-487

Jacobsen NR, Moller P, Jensen KA, Vogel U, Ladefoged O, Loft S & Wallin H (2009) Lung inflammation and genotoxicity following pulmonary exposure to nanoparticles in ApoE-/- mice. Part. Fibre Toxicol. 6:2, 17p.

Jeggo PA & Lobrich M (2007) DNA double-strand breaks: their cellular and clinical impact? Oncogene 26:7717-7719

Kamiya H, Miura K, Ishikawa H, Inoue H, Nishimura S & Ohtsuka E (1992) c-Ha-*ras* containing 8-hydroxyguanine at codon 12 induces point mutations at the modified and adjacent positions. Cancer Res. 52:3483-3485

Kang SJ, Kim BM, Lee YJ & Chung HW (2008) Titanium dioxide nanoparticles trigger p53-mediated damage response in peripheral blood lymphocytes. Environ. Mol. Mutagen. 49:399-405

Karlsson HL, Cronholm P, Gustafsson J & Möller L (2008) Copper oxide nanoparticles are highly toxic: a comparison between metal oxide nanoparticles and carbon nanotubes. Chem. Res. Toxicol. 21:1726-1732

Kasai H (1997) Analysis of a form of oxidative DNA damage, 8-hydroxy-2'-deoxyguanosine, as a marker of cellular oxidative stress during carcinogenesis. Mutat. Res. 387:147-163

Knaapen AM, Borm PJA, Albrecht C & Schins RPF (2004) Inhaled particles and lung cancer. Part A: mechanism. Int. J. Cancer 109:799–809

Kolling A, Ernst H, Rittinghausen S, Heinrich U & Pott F (2008) Comparison of primary lung tumor incidences in the rat evaluated by the standard microscopy method and by multiple step sections. Exp. Toxicol. Pathol. 60: 281-288. Epub 2008 May 2.

Kolling A, Ernst H, Rittinghausen S & Heinrich U (2010 in preparation) Pulmonary toxicity and carcinogenicity of intratracheally instilled granular dusts in a rat bioassay.

Landsiedel R, Kapp MD, Schulz M, Wiench K & Oesch F (2009) Gentoxicity investigations on nanomaterials: methods, preparation and characterization of test material, potentail artifacts and limitations - many question, some answers. Mutat. Res. 681:241-258

Li H, Haberzettl, Albrecht C, Höhr D, Knaapen AM, Borm PJA & Schins RPF (2007) Inhibition of the mitochondrial respiratory chain function abrogates quartz induced DNA damage in lung epithelial cells. Mutat. Res. 617:46-57

Ma-Hock L, Burkhardt S, Strauss V, Gamer AO, Wiench K, van Ravenzwaay B & Landsiedel R (2009) Development of a short-term inhalation test in the rat using nano-titanium dioxide as a model substance. Inhal. Toxicol. 21(2):102-118

Mambo E, Chatterjee A, de Souza-Pinto NC, Mayard S, Hogue BA, Hoque MO, Dizdaroglu M & Bohr VA (2005) Oxidized guanine lesions an hOgg1 activity in lung cancer. Oncogene 24:4496-4508

Mroz RM, Schins RP, Li H, Jimenez LA, Drost EM, Holownia A, MacNee W & Donaldson K (2008) Nanoparticle-driven DNA damage mimics irradiation-related carcinogenesis pathways. Eur. Respir. J. 31(2):241-251. Cited in Gonzalez et al. (2008).

Msiska Z, Pacurari M, Mishra A, Leonard SS, Castranova V & Vallyathan V (2010) DNA double strand breaks by asbestos, silica and titanium dioxide:Possible biomarker of carcinogenic potential? Am. J. Cell. Mol. Biol. 43(2):210-219 [Epub 2009 Sep 25]

Muhle H, Takenaka S, Mohr U, Dasenbrock C & Mermelstein R (1989) Lung tumor induction upon long-term low-level inhalation of crystalline silica. Am. J. Ind. Med. 15:343-346

Nikula KJ (2000) Rat lung tumors induced by exposure to selected poorly soluble nonfibrous particles. Inhal. Toxicol. 12 (1-2): 97-119

Nishioka K, Ohtsubo T, Oda H, Fujiwara T, Kang D, Sugimachi K & Nakabeppu Y (1999) Expression and differential intracellular localization of two major forms of human 8-oxoguanine DNA glycosylase encoded by alternatively spliced *OGG1* mRNAs. Mol. Biol. Cell 10:1637-1652

Oberdörster G, Maynard A, Donaldson K, Castranova V, Fitzpatrick J, Ausman K, Carter J, Karn B, Kreyling W, Lai D, Olin S, Monteiro-Riviere N, Warheit D & Yang H (2005). Principles for characterizing the potential human health effects from exposure to nanomaterials: elements of a screening strategy. Part. Fibre Tox. 2:8

Panduri V, Liu G, Surapureddi S, Kondapalli J, Soberanes S, de Souza-Pinto NC, Bohr VA, Budinger GR, Schumacker PT, Weitzman SA & Kamp DW (2009) Role of mitochondrial hOGG1 and aconitase in oxidant-induced lung epithelial cell apoptosis. Free Radic Biol Med. 47(6):750-759 [Epub 2009 Jun 12].

Park EJ, Yi J, Chung KH, Ryu DY, Choi J & Park K (2008) Oxidative stress and apoptosis induced by titanium dioxide nanoparticles in cultured BEAS-2B cells. Toxicol. Lett. 180:222-229

Paz-Elizur T, Krupsky M, Blumenstein S, Elinger D, Schechtman E & Livneh Z (2003) DNA repair activity for oxidative damage and risk of lung cancer. J. Natl. Cancer Inst. 95:1312-1319

Pott F & Roller M (2003) Untersuchungen zur Kanzerogenität granulärer Stäube an Ratten - Ergebnisse und Interpretationen, 1. Auflage. 2003. 60 Seiten, Projektnummer: F 1843

Potts RJ, Watkin RD & Hart BA (2003) Cadmium exposure down-regulates 8-oxoguanine DNA glycosylase expression in rat lung and alveolar epithelial cells. Toxicology 184:189-202

Radicella JP, Dherin C, Desmaze C, Fox MS & Boiteux S (1997) Cloning and characterization of *hOGG1*, a human homolog of the *OGG1* gene of *Saccharomyces cerevisiae*. Proc. Natl. Acad. Sci. USA 94:8010-8015

Rahman Q, Lohani M, Dopp E, Pemsel H, Jonas L, Weiss DG & Schiffmann D (2002) Evidence that ultrafine titanium dioxide induces micronuclei and apoptosis in Syrian hamster embryo fibroblasts. Environ. Health Perspect 110(8):797-800. Cited in Gonzalez et al. (2008).

Reeves JF, Davies SJ, Dodd NJ & Jha AN (2008) Hydroxyl radicals (OH) are associated with titanium dioxide (TiO(2)) nanoparticle-induced cytotoxicity and oxidative DNA damage in fish cells. Mutat. Res. 640(1-2):113-122. Cited in Gonzalez et al. (2008).

Rehn B, Seiler F, Rehn S, Bruch J & Maier M (2003) Investigations on the inflammatory and genotoxic lung effects of two types of titanium dioxide: untreated and surface treated. Toxicol. Appl. Pharmacol. 189(2):84-95

Rogakou EP, Pilch DR, Orr AH, Ivanova VS & Bonner WM (1998) DNA double stranded breaks induce histone H2AX phosphorylation on serine 139. J. Biol. Chem. 273:5858-5868

Roller M (2009) Carcinogenicity of inhaled nanoparticles. Inhal. Toxicol. 21(S1):144-157

Rübe C, Fricke A, Wendorf J, Stützel A, Kühne M, Mei Fang Ong, Lipp P & Rübe C (2010). Accumulation of DNA double-strand breaks in normal tissues after fractionated irradiation. Int. J. Radiation Oncology 76(4):1206-1213

Saber AT, Bornholdt J, Dybdahl M, Sharma AK, Loft S, Vogel U & Wallin H (2005) Tumor necrosis factor is not required for particle-induced genotoxicity and pulmonary inflammation. Arch. Toxicol. 79(3):177-182

Saffiotti U & Stinson SF (1988) Lung cancer induction by crystalline silica: Relationships to granulomatous reactions and host factors. J. Environ. Sci. Health 6(2):197-212

Sayes CM, Reed KL, Glover KP, Swain KA, Ostraat ML, Donner EM & Warheit DB (2010) Changing the dose metric for inhalation toxicity studies: short-term study in rats with engineered aerosolized amorphous silica nanoparticles. Inhalation Toxicology 22, 348-354

Sedelnikova OA, Rogakou EP, Panyutin IG & Bonner WM (2002) Quantitative detection of (125)IdU-induced DNA double-strand breaks with gamma-H2AX antibody. Radiat. Res. 158:486-492

Schins RP & Knaapen AM (2007) Genotoxicity of poorly soluble particles. Inhal. Toxicol. 19(Suppl.1):189-198

Shibutani S, Takeshita M & Grollman AP (1991) Insertion of specific bases during DNA synthesis past the oxidant-damaged 8-oxodG. Nature 349:431-434

Singh N, Manshian B, Jenkins GJS, Griffiths SM, Williams PM, Maffeis TGG, Wright CJ & Doak SH (2009) NanoGenotoxicology: The DNA damaging potential of engineered nanomaterials. Biomaterials 30(23-24):3891-3914

Sluss HK & Davis RJ (2006) H2AX is a target of the JNK signalling pathway that is required for apoptotic DNA fragmentation. Molecular Cell 23(2):152-153

Souza-Pinto NC & Bohr VA (2002) The mitochondrial theory of aging: involvement of mitochondrial DNA damage and repair. INt. Rev. Neurobiol. 53:519-534

Stensner T, Thorslund T, Souza-Pinto NC & Bohr VA (2002) Mitochondrial repair of 8-oxoguanine and changes with aging. Exp. Gerontol. 37:1189-1196

Tao Z, Morrow MP, Asefa T, Sharma KK, Duncan C, Anan A, Penefsky HS, Goodisman J & Souid A-K (2008) Mesoporous silica nanoparticles inhibit cellular respiration. Nano Letters 8(5):1517-1526

Theogaraj E, Riley S, Hughes L, Maier M & Kirkland D (2007) An investigation of the photo-clastogenic potential of ultrafine titanium dioxide particles. Mutat Res 634(1-2):205-219. Cited in Gonzalez et al. (2008).

Totsuka Y, Higuchi T, Imai T, Nishikawa A, Nohmi T, Kato T, Masuda S, Kinae N, Hiyoshi K, Ogo S, Kawanishi M, Yagi T, Ichinose T, Fukumori N, Watanabe M, Sugimura T & Wakabayashi K (2009) Gentoxicity of nano/microparticles in in vitro micronuclei, in vivo comet and mutation assay systems. Part. Fibre Toxicol. 6:23, 11p.

Trouiller B, Reliene R, Westbrook A, Solaimani P & Schiestl RH (2009) Titanium dioxide nanoparticles induce DNA damage and genetic instability *in vivo* in mice. Cancer Res. 69 (22):8784-8788

Tsaousi A, Jones E & Case EP (2010) The in vitro genotoxicity of orthopaedic ceramic (Al2O3) and metal (CoCr alloy) particles. Mutat. Res. 697(1-2):1-9

Tsurudome Y, Horano T, Yamamoto H, Tanaka I, Sagai M, Hirano H, Nagata N, Itoh H & Kasai H (1999) Changes in levels of 8-hydroxyguanine in DNA, its repair and *OGG1* mRNA in rat lungs after intratracheal administration of diesel exhaust particles. Carcinogenesis 20(8):1573-1576

Virág L (2005) Poly(ADP-ribosyl)ation in asthma and other lung diseases. Pharmacol. Res. 52:83-92

Wallace SS (1998) Enzymatic processing of radiation-induced free radical damage in DNA. Radiat. Res. 150:S60-S79

Wang JJ, Sanderson BJ & Wang H (2007a) Cyto- and genotoxicity of ultrafine TiO_2 particles in cultured human lymphoblastoid cells. Mutat. Res. 628(2):99-106. Cited in Gonzalez et al. (2008).

Wang JJ, Sanderson BJ & Wang H (2007b) Cytotoxicity and genotoxicity of ultrafine crystalline SiO_2 particulate in cultured human lymphoblastoid cells. Environ. Mol. Mutagen. 48(2):151-157. Cited in Gonzalez et al. (2008)

Warheit DB, Hoke RA, Finlay C, Donner EM, Reed KL & Sayes CM (2007) Development of a base set of toxicity tests using ultrafine TiO2 particles as a component of nanoparticle risk management. Toxicol Lett 171(3):99-110. Cited in Gonzalez et al. (2008)

Watters GP, Smart DJ, Hravey JS, Austin CA (2009) H2AX phosphorylation as a genotoxicity endpoint. Mutat. Res. 679:50-58

WHO (2000) Crystalline silica, quartz. Geneva, World Health Organization. (Concise International Chemical Assessment Document, CICAD No.24). 50p.

Wiessner JH, Mandel NS, Sohnle PG & Mandel GS (1989) Effect of particle size on quartz-induced hemolysis and on lung inflammation and fibrosis. Exp. Lung Res. 15:801-812

Xia T, Kovochich M, Brant J, Hotze M, Sempf J, Oberley T, Sioutas C, Yeh JI, Wiesner MR & Nel AE (2006) Comparison of the abilities of ambient and manufactured nanoparticles to induce cellular toxicity according to an oxidative stress paradigm. Nano Letters 6:1794-1807. doi: 10.1021/nl061025k

Xu A, Chai Y, Nohmi T & Hei TK (2009) Genotoxic responses to titanium dioxide nanoparticles and fullerene in gpt delta transgenic MEF cells. Part. Fibre Toxicol. 6:3, 13p.

Yang H, Liu C, Yang D, Zhang H & Xi Z (2009) Comparative study of cytotoxicity, oxidative stress and genotoxicity induced by four typical nanomaterials: the role of particle size, shape and composition. J. Appl. Toxicol. 29:69-78

Yu KO & Grabinski CM (2009) Toxicity of amorphous silica nanopartikles in mouse-keratinocytes. J.Nanopart. Res. 11(1):15-24

Zhang FM, Liu BC, Liu HF, Jia XW & Ye M (2009) Role of DNA-dependent protein kinase catalytic subunit in silica-induced DNA double-strand break repair in human embryo lung fibroblasts. Zhonghua Lao Dong Wei Sheng Zhi Ye Bing Za Zhi 27(1):2-6 [Article in Chinese]

Ziemann C, Bürkle A, Kahl GF & Hirsch-Ernst KI (1999) Reactive oxygen species participate in mdr1b mRNA P-glycoprotein overexpression in primary rat hepatocyte cultures. Carcinogenesis 20(3):407-414

Ziemann C, Bellmann B, Serwatzki K, Creutzenberg O, Ernst H, Kolling A, Beneke S & Rittinghausen S (2010) Quantification of Local Genotoxicity in Rat Lungs after 3 Months of Particle Exposure by Immunohistochemical Detection of 8-OH-dG, gamma-H2AX, and Poly(ADP-Ribose). Naunyn Schmiedebergs Arch. Pharmacol. 381:300 Suppl. 1

Appendices

Appendix I Literature Review – Tables

Genotoxicity *in vitro*

Table Appendix I-1 *In vitro* genotoxicity studies with crystalline silica DQ12

NP type	Cell type	Concentration/dose	Assessment of cytotoxicity	Test for genotoxicity	Result	Reference
Crystalline SiO_2 DQ 12						
DQ 12 (batch 6, IUF, Germany) 1.1 µm Surface area, SDM: n.d.	RLE-6TN (rat lung epithelial type II cells)	4 h; 50 and 100 µg/cm^2	n.d.	Comet assay	+ (50 µg/cm^2; *equal to 156,25 µg/ml)*	LI et al., 2007
				8-OH-dG	+ (100 µg/cm^2)	
DQ 12 Surface area, SDM; size; source: n.d	IMR 90 (human lung fibroblasts)	36 h; 15 µg/cm^2 48 h; 5 µg/cm^2 72 h; 1 µg/cm^2	DMPO-OH Generation of OH radicals + (10 µg/cm^2)	Micronucleus assay + (48 h/10 µg/cm^2)	+ (10 µg/cm^2) < 1% quartz negative	GEH et al., 2006
DQ 12 (batch6, IUF; Germany) 1,1 µm Surface area, SDM: n.d.	A549 (human lung epithelial cells)	2, 4 and 24 h; 8, 40; 80 and 200 µg/cm^2	LDH (200 µg/cm^2) MTT (4h / 200 µg/cm^2)	Comet assay	+ (40 µg/cm^2; *equal to 125 µg/ml)*	SCHINS et al., 2002
				8-OH-dG	+ (80 µg/cm^2)	
DQ 12 (batch6, IUF; Germany) 1.1 µm Surface area BET: 3.20 m^2/g SDM: n.d.	A549 (human lung epithelial cells)	1.6; 8; 40 and 200 µg/cm^2	LDH: + (200 µg/cm^2) MTT: + (40 µg/cm^2) Trypan Blue: + (40 µg/cm^2)	Comet assay	+ (200 µg/cm^2; *equal to 625 µg/ml*)	CAKMAK et al., 2004

Table Appendix I-2 *In vitro* genotoxicity studies with crystalline silica nanoparticles

NP type[1]	Cell type	Concentration/dose	Assessment of cytotoxicity	Test for genotoxicity	Result	Reference
Crystalline SiO_2 Nanoparticles						
SiO_2, < 100 nm Sigma Aldrich; Surface area; SDM: 7.1 nm	WIL2-NS (human B-cell Lymphoblastoids)	0; 30; 60 and 120 µg/ml 6; 24 h	MTT (120 µg/ml; 6 h) Population growth assay (decreased at 30 µg/ml; 6 h) FCM (30 µg/ml; 6 h)	CBMN	+ (30 µg/ml; 24 h)	WANG et al., 2007b
				Comet assay	- (120 µg/ml)	
				HPRT	+ (120 µg/ml; 24 h)	
SiO_2 (Runhe; Shanghai) 20.2 nm Surface area, SDM; source: n.d	primary mouse embryo fibroblasts from BALB/c mice	24 h 5, 10, 20; 50 and 100 µg/ml	MTT assay (20 µg/ml) WST assay (50 µg/ml) LDH assay Trypan Blue (viability >90%)	Comet assay	+ (10 µg/ml)	YANG et al., 2009
				ROS (DCFH-DA)	↑ (20 µg/ml)	
				GSH	↓ (10 µg/ml)	
				SOD	↓ (5 µg/ml)	
				MDA	↑ (20 µg/ml)	

Table Appendix I-3 *In vitro* genotoxicity studies with amorphous silica

NP type	Cell type	Concentration/ dose	Assessment of cytotoxicity	Test for genotoxicity	Results	Reference
Amorphous SiO_2						
Glantreo 30 nm; TEM: 33.21 nm SDM, DLS: average size after dialysis 77.9 nm; zeta-potential: -33.7 mV Glantreo 80 nm; TEM: 34.89 nm SDM, DLS: average size after dialysis 65.9 nm; zeta-potential: -10.7 mV	3T3-L1 mouse fibroblasts	4 and 40 µg/mL; 3, 6 and 24 h	MTT and WST-1 LDH assay Highest dose not cytotoxic	Comet assay	- (4 and 40 µg/mL, results confirmed by two independent studies)	BARNES et al., 2008
SiO_2 30 and 48 nm; source: no data DLS: 28,9 nm (water), 39 nm (media) and 52,9 nm (water), 51,9 nm (media); other data not reported	HEL-30 (mouse keratinocytes)	10, 50, 100 and 200 µg/ml; 24 h	LDH (+, 30 and 48 nm); MTT (+, 100 µg/ml	GSH	+ (30 nm; 50 µg/ml)	YU et al., 2009
				ROS	- (200 µg/ml)	

Table Appendix I-4 *In vitro* genotoxicity studies with nanoparticulate carbon black

NP type	Cell type	Concentration/dose	Assessment of cytotoxicity	Test for genotoxicity	Result	Reference
Carbon Black						
14 nm	A549	100 µg/ml, 3 h, -FCS	LDH release, Trypan blue	Alkaline Comet assay	+ (100 µg/ml)	MROZ et al., 2008 (cited from GONZALEZ et al., 2008)
				Neutral Comet assay	- (100 µg/ml)	
14 nm (BaP-coated)	A549	100 µg/ml, 3 h, -FCS	LDH release, Trypan blue	Alkaline Comet assay	(+) (not significant)	MROZ et al., 2008 (cited from GONZALEZ et al., 2008)
				Neutral Comet assay	- (100 µg/ml)	
260 nm	A549	100 µg/ml, 3 h, -FCS	LDH release, Trypan blue	Alkaline Comet assay	+ (100 µg/ml)	MROZ et al., 2008 (cited from GONZALEZ et al., 2008)
				Neutral Comet assay	- (100 µg/ml)	
14 nm (PRINTEX® 90, Degussa)	FE1-MML	75 µg/ml, 3 h, +FCS	LDH (92.8 % cell viability after 24 h)	Alkaline Comet assay	+ (75 µg/ml)[1]	JACOBSEN et al., 2007 (cited from GONZALEZ et al., 2008)
				Alkaline Comet assay + fpg	+ (75 µg/ml)	
		75 µg/ml, 3 passages of 72 h, +FCS		Mutant frequency	+ (*cII* gene and *LacZ* gene)	

[1] Only one dose level tested

NP type	Cell type	Concentration/dose	Assessment of cytotoxicity	Test for genotoxicity	Result	Reference
Carbon Black						
Carbon Black (PRINTEX® 90, Evonik Degussa) 14 nm, 338 m²/g; SDM, DLS: bimodal size, average sizes 98 and 153 nm in culture medium indicating agglomeration to larger particles	FE1-MML	2.08 – 18.75 µg/ml (1.3 – 11.7 µg/cm², 8 – 75 µg/10^6 cells), - FCS, 3 h	LDH release, NucleoCounter	ROS (DCFH-DA)	↑ (2.08 µg/ml)	JACOBSEN et al., 2008
Carbon Black (Nano-Innovation, Shenzhen) 12.3 nm SDM: no data reported	PMEF from BALB/c mice	5 – 100 µg/ml, + FCS, 24 h	MTT, WST, LDH	ROS (DCFH-DA) GSH SOD MDA	↑ ROS (20 µg/ml) ↓ GSH (5 µg/ml) ↓ SOD (5 µg/ml) ↑ MDA (50 µg/ml)	YANG et al., 2008
		5 – 10 µg/ml, + FCS, 24 h	Trypan Blue (viability > 95 %)	Alkaline comet assay	+ (5 µg/ml)	
Carbon Black (PRINTEX® 90, Degussa) 14 nm, 300 m²/g SDM, DLS: average size 232 nm (range 13.6 - 337 nm) in saline + Tween 80, indicating agglomeration to larger particles	A549	3 – 34 µg/ml, + FCS, 6 h	Growth inhibition	Micronucleus formation	+ (all concentrations, no growth inhibition) DLS size distribution indicates presence of non-agglomerated primary particles	TOTSUKA et al., 2009

Table Appendix I-5 *In vitro* genotoxicity studies with C60 fullerene

NP type (source), primary particle size, surface area; data on size distribution (SDM) in medium	Cell type	Concentration or dose	Assessment of cytotoxicity	Test for genotoxicity	Results/remarks	Reference
Fullerene						
C_{60}-Fullerene (Sigma-Aldrich) 0.7 nm, < 20 m²/g; SDM, DLS: average size 311 nm in culture medium indicating agglomeration to larger particles	FE1-MML	100 µg/ml (15 µg/cm², 500 µg/10^6 cells), + FCS, 3 h	LDH release, NucleoCounter (> 90 % viability)	Alkaline comet assay, + fpg	- + (fpg, 15 µg/cm²)	JACOBSEN et al., 2008
		100 µg/ml (15 µg/cm², 213 – 3333 µg/10^6 cells), + FCS, 8 x 72 h	LDH release, NucleoCounter	Mutant frequency (*cII* gene)	-	
		2.78 - 25 µg/ml (1.7 – 15.6 µg/cm², 11 – 100 µg/10^6 cells), - FCS, 3 h	LDH release, NucleoCounter	ROS (DCFH-DA)	-**	
C_{60}-Fullerene (SES Research) No further data reported	PMEF from gpt delta transgenic mice	0.1 – 30 µg/ml, + FCS, 24 h	MTT (cytotoxic at ≥ 1 µg/ml)	Mutant frequency at *red/gam* loci, Spi^- mutation	+ (10 µg/ml), response inhibited by nystatine and NS398	XU et al., 2009
				RNS (DHR123)	+ (1 µg/ml, inhibition by L-NMMA)	

NP type (source), primary particle size, surface area; data on size distribution (SDM) in medium	**Cell type**	**Concentration or dose**	**Assessment of cytotoxicity**	**Test for genotoxicity**	**Results/remarks**	**Reference**
C_{60}-Fullerene (Sigma-Aldrich) 0.7 nm; SDM, DLS: bimodal size, mostly 234 and 857 nm (range 10,5 – 12914 nm) in saline + Tween 80 medium indicating agglomeration to larger particles	A549	3 – 34 µg/ml, + FCS, 6 h	Growth inhibition	Micronucleus formation	+ (all concentrations, no growth inhibition)	TOTSUKA et al., 2009

Table Appendix I-6 *In vitro* genotoxicity studies with nanoparticulate titanium dioxide

NP type	Cell type	Concentration/dose	Assessment of cytotoxicity	Test for genotoxicity	Result	Reference
TiO_2						
6.6 nm	WIL2-NS	26 – 130 µg/ml, 24 h, 48 h, +FCS	MTT, population growth, apoptosis	Alkaline Comet assay	+ (65 µg/ml, 24 h)	WANG et al., 2007a (cited from GONZALEZ et al., 2008)
		26 – 130 µg/ml, +FCS 6 h + 26 h 24 h + 26 h 48 h + 26 h	CBPI	CBMN	 + (65 µg/ml) + (65 µg/ml) + (26 µg/ml)	
		26 – 130 µg/ml, 24 h, 48 h, +FCS		HPRT mutation	+ (65 µg/ml, 24 h)	
≤ 20 nm	SHE fibro-blasts	0.5 – 10 µg/cm², FCS? 12 h 24 h, 66 h, 72 h 48 h	↑ Cytotoxity at > 10 µg/cm²	MN + kinetochore staining	 - + (1 µg/cm²) + (5 µg/cm²)	RAHMANN et al., 2002 (cited from GONZALEZ et al., 2008)
> 200 nm	SHE fibro-blasts	0.5 – 10 µg/cm², FCS? 12, 24, 48, 66, 72 h	↑ Cytotoxity at > 10 µg/cm²	MN	-	
5 nm (anatase)	GFSk-S1 cells	10 µg/ml, 2 h, FCS 10 µg/ml, 2 h + UVA, FCS 1- 100 µg/ml, 24 h, FCS	NRR assay	Comet assay	+ + + (100 µg/ml)	REEVES et al., 2008 (cited from GONZALEZ et al., 2008)
		10 µg/ml, 2 h, FCS 10 µg/ml, 2 h + UVA, FCS 1- 100 µg/ml, 24 h, FCS		Comet assay + fpg	+ + + (1 µg/ml)	
		1- 100 µg/ml, 24 h, FCS		Comet assay + Endo III	-	
10 nm (anatase)	BEAS-2B	10 µg/ml, 1 h, FCS	MTT IC50, 3d: 6.5 µg/ml	Alkaline Comet assay (+ or - fpg)	+/-	GURR et al., 2005
		10 µg/ml, 24 h, FCS		CBMN	+	
20 nm (anatase)	BEAS-2B	10 µg/ml, 1 h, FCS	MTT (50 % after 3d 10 µg/ml apoptosis)	Alkaline Comet assay (+ or - fpg)	+/-	GURR et al., 2005 (cited from GONZALEZ et al., 2008)

NP type	Cell type	Concentration/dose	Assessment of cytotoxicity	Test for genotoxicity	Result	Reference
TiO_2						
60 nm (37 % Al, 12 – 18 % SiO_2-coat)	CHO-WBL	1715 – 5000 µg/ml (3 h + 17 h recovery), + and – UV, - FCS	Cell count	CA	-	THEOGARAJ et al., 2007 (cited from GONZALEZ et al., 2008)
200 nm	BEAS-2B	10 µg/ml, 1 h, FCS	MTT (50 % after 3d < 10 µg/ml)	Alkaline Comet assay (+ or - fpg)	-/-	GURR et al., 2005 (cited from GONZALEZ et al., 2008)
		10 µg/ml, 24 h, FCS		CBMN	-	
> 200 nm	BEAS-2B	10 µg/ml, 1 h, FCS	MTT (50 % after 3d < 10 µg/ml apoptosis)	Alkaline Comet assay (+ or - fpg)	+/-	GURR et al., 2005 (cited from GONZALEZ et al., 2008)
		10 µg/ml, 24 h, FCS		CBMN	-	
14 - 22 nm (Rutile, Al-coat, nd + or – organic coat)	CHO-WBL	348.1 – 5000 µg/ml (3 h + 17 h recovery), + and – UV, - FCS	Cell count	CA	-	THEOGARAJ et al., 2007 (cited from GONZALEZ et al., 2008)
200 nm (rutile)	BEAS-2B	10 µg/ml, 1 h, FCS	MTT (50 % after 3d < 10 µg/ml)	Alkaline Comet assay (+ or - fpg)	+/-	GURR et al., 2005 (cited from GONZALEZ et al., 2008)
		10 µg/ml, 24 h, FCS		CBMN		
21 nm (20 % rutile, 80 % anatase, + or – coated)	CHO-WBL	209.7 – 800 µg/ml (3 h + 17 h recovery), + and – UV, - FCS	Cell count	CA	-	THEOGARAJ et al., 2007 (cited from GONZALEZ et al., 2008)
200 nm (50 % rutile, 50 % ana-	BEAS-2B	10 µg/ml, 1 h, FCS	MTT (50 % after 3d < 10 µg/ml)	Alkaline Comet assay + fpg	+ (synergy)	GURR et al., 2005

NP type	Cell type	Concentration/dose	Assessment of cytotoxicity	Test for genotoxicity	Result	Reference
TiO_2						
tase)						(cited from GONZALEZ et al., 2008)
140 nm (79 % anatase, 21 % rutile)	*Salmonella/ E. coli* CHO cells	100 – 5000 µg/plate 25 – 2500 µg/ml, - FCS, 4, 20 h	Test not mentioned	Ames test CA	- -	WARHEIT et al., 2007 (cited from GONZALEZ et al., 2008)
TiO_2 (Anatas, Degussa), 30 – 50 nm, 20 – 120 m²/g; SDM: no data	V79	1 – 25 µg/cm², + FCS, 24, 48, 72 h	Trypan Blue	Micronucleus formation	- (all exposures)	BHATTACHARYA et al., 2008
		1 – 10 µg/cm², + FCS, 24, 48, 72 h	Trypan Blue	ROS (TBARS)	↑ (1 µg/cm², 48 h)	
TiO_2 (Anatas), V_2O_5-coated prior to study 30 – 50 nm, 20 – 120 m²/g; SDM: no data	V79	1 – 25 µg/cm², + FCS, 24, 48, 72 h	Trypan Blue	Micronucleus formation	+ (1 µg/cm², 48 h)	
		1 – 10 µg/cm², + FCS, 24, 48, 72 h	Trypan Blue	ROS (TBARS)	↑ (1 µg/cm², 48 h)	
TiO_2 (Anatas, Degussa), < 100 nm (average: 91 nm), 49.7 m²/g; SDM: no data	BEAS-2B	5 – 50 µg/cm², + FCS, 6, 12, 24 h	Trypan Blue	ROS (DCFH-DA) 8-Oxo-dG (ELISA)	+ (10 µg/cm²), inhibition bei desferoxamine	BHATTACHARYA et al., 2009
	IMR-90	5 – 10 µg/cm², + FCS, 24 h	Trypan Blue	8-Oxo-dG (ELISA)	+ (5 µg/cm²)	
	IMR-90, BEAS-2B	2 – 50 µg/cm², + FCS, 24 h	Trypan Blue	Alkaline comet assay	- (both cell lines)	

NP type	Cell type	Concentration/dose	Assessment of cytotoxicity	Test for genotoxicity	Result	Reference
TiO_2						
TiO_2 (Anatas, Sigma-Aldrich), 40 - 70 nm; SDM: no data	Peripheral blood lymphocytes	3.73 – 59.7 µg/ml, + FCS, 30 min preincubation (+/- irradiation) + 30 min treatment (+/- irradiation) + TiO_2	Trypan Blue (> 70 % after freezing and thawing, prior to incubation)	Alkaline comet assay, in darkness or UV-irradiated simultaneously (SI) pre-irradiated (PI)	+ (also photogenotoxic: effect SI ≥ PI > dark)	GOPALAN et al., 2009
	Human sperm cells	3.73 – 59.7 µg/ml, - FCS, 30 min preincubation (+/- irradiation) + 30 min treatment (+/- irradiation) + TiO_2	Trypan Blue (> 70 %, fresh samples prior to freezing)	Alkaline comet assay in the dark or with irradiation as indicated above	+ (all concentrations, but no photogenotoxic effect)	
TiO_2 (70 – 85 % anatase, 15 – 30 % rutile) (P25, Degussa) ~ 30 nm, 50 m²/g; SDM: no data	Peripheral blood lymphocytes	20, 50, 100 µg/ml, + FCS, 48 h (+ cytochalasin B after 20 h)	Trypan Blue (viability ≤ 70 % after ≥ 12 h with ≥ 50 µg/ml TiO_2)	Cytokinesis-block micronucleus formation (CBMN)	+ (dose-dependent, significant at ≥ 50 µg/ml)	KANG et al., 2008
		20, 50, 100 µg/ml, + FCS, 0, 6, 12, 24 h		Alkaline comet assay	+ (significant, dose-dependent, all timepoints, effect ↓ by N-acetyl-cysteine)	
		ROS: 50, 100 µg/ml, + FCS, 1 h p53: 50 µg/ml, + FCS, 6, 12, 24 h		ROS (DCFH-DA), p53 (Western blot, antibody assay)	ROS: + p53: + (upregulation of total and phosphor-p53	
TiO_2 (Sigma-Aldrich) 63 nm, 24 m²/g; TEM: 20 – 100 nm, SDM, DLS: average size 300 nm in culture medium	A549 type II lung epithelial cells	2 µg/ml (1 µg/cm²), 40 µg/ml (20 µg/cm²) (fpg), 80 µg/ml (40 µg/cm²) (fpg), + FCS, 4 h	Trypan Blue (no cytotoxicity at tested concentrations)	Alkaline comet assay, +fpg	+ (≥ 40 µg/ml) fpg: - Particle agglomeration in cell culture medium	KARLSSON et al., 2008
		40 µg/ml (20 µg/cm²) , 80 µg/ml (40 µg/cm²), + FCS, 18 h		ROS (DCFH-DA)	- (slight increase, not significant)	

NP type	Cell type	Concentration/dose	Assessment of cytotoxicity	Test for genotoxicity	Result	Reference
TiO_2						
indicating agglomeration to larger particles						
TiO_2 (P25, Degussa-Korea) 21 nm; SDM: no data	BEAS-2B	5, 10, 20, 40 µg/ml; + FCS, 24, 48, 72, 96 h	MTT (viability < 80 % at > 5 µg/ml, 24 – 96 h; 40 % at 40 µg/ml, 96 h)	ROS, GSH, apoptotic cell, death: caspase-3, chromosome condensation, expression of oxidative stress genes: HO1, TRR, GSH-T, catalase	↑ (time and conc. dependent: chromosome condensation, caspase-3, ROS, expression of oxidative stress and inflammation related genes); ↓ (GSH, cell viability)	PARK et al., 2008
TiO_2, (Sigma-Aldrich) 3 types: a) 5 nm, 114.1 m²/g b) 325 mesh, 8.9 m²/g (Inframat Advanced) c) 40 nm, 38.2 m²/g; SDM: no data	PMEF from gpt delta transgenic mice	0.1 – 30 µg/ml, + FCS, 24 h	0 nm: cytotoxic at ≥ 0.1 µg/ml, 5 nm, 325 mesh: no cytotoxicity)	Mutant frequency at *red/gam* loci, Spi^- mutation	+ (0.1 µg/ml; 5 nm and 40 nm sized), inhibition by nystatine & NS-398 - (325 mesh)	XU et al., 2009
				RNS (DHR123)	+ (1 µg/ml; 40 nm sized, 5 nm: non-sign.), inhibition by L-NMMA and NS-398 - (325 mesh)	

Legend and explanations to Tables on Genotoxicity *in vitro*

For better comparison of the studies, doses are provided in µg/cm^2 and µg/ml. If not provided by the author, concentrations/doses were calculated based on the information on the amount of medium per Petri dish in the publications. If the information was not provided, an amount of 0.3 ml/cm^2 was assumed. The value not originally provided by the author is in italics.

↑: increase; ↓: decrease; +: positive response; -: no effect
*: cells first exposed to test substance, then to DCFA-DA in absence of test substance, assay therefore may be affected by reduced cell viability due to cytotoxicity
**: cells first loaded with DCFA-DA, then incubated with test substance

A549: human lung carcinoma cell line;
BEAS-2B: human bronchial epithelial cells;
BET: Brunauer, Emmett, Teller (gas absorption method for determination of specific surface);
CA: chromosome aberration; CBMN: cytokinesis-block micronucleus assay;
CBPI: cytokinesis-block proliferation index;
CBMN:
CHO: Chinese hamster ovarian cells; CHO-WBL: Chinese hamster ovarian cell subclone;
DCFH-DA: 2',7'-Dichlorofluorescein diacetate;
DHR123: dihydrorhodamine 123;
DLS: Dynamic light scattering;
FCS: fetal calf serum;
FE1-MML: MutaTM mouse lung epithelial cells;
fpg: formamidopyrimidine-DNA glycosylase;
GFSk-S1: goldfish skin derived primary cell line;
GSH: glutathione;
GSH-T: glutathione transferase;
HPRT: hypoxanthine guanine phosphoribosyltransferase;
HO1: heme oxygenase 1;
IUF: Institut für Umweltmedizinische Forschung (Düsseldorf, Germany);
LDH: lactate dehydrogenase;
L-NMMA: L- NG-methyl-L-arginine;
MDA: malondialdehyde;
MN: micronucleus;
MTT: 3-(4,5-dimethylthiazol-2-yl)-2,5-diphenyltetrazolium bromide;
NS-398: N-[2-(cyclohexyloxy)-4-nitrophenyl]-methanesulfonamide, a COX-2 inhibitor;
PI: pre-irradiation;
PMEF: primary mouse embryo fibroblast cells;
RNS: reactive nitrogen species (esp. peroxynitrite);
ROS: reactive oxygen species;
SDM: Sauter diameter;
SHE: Syrian hamster embryo;
SOD: superoxide dismutase;
TBARS: thiobarbituric acid reactive substances;
TEM: Transmission electron microscopy;
TRR: thioredoxin reductase;

WIL2-NS: a human lymphoblastoid cell line;
WST: 2-(4-iodophenyl)-3-(4-nitrophenyl)-5-(2,4-disulfophenyl)-2H-tetrazolium bromide

Genotoxicity in vivo

Table Appendix I-7 *In vivo* genotoxicity studies with nanoparticulate amorphous silica

NP type (source), primary particle size, surface area; agglomeration/aggregation	Species Strain No./Sex & group	Cell/tissue type	Test	Exposure Concentration or dose Duration	Results/remarks	Reference
Amorphous SiO_2						
Freshly generated, monodisperse D_{50} = 37 nm D_{50} = 83 nm non aggregated in inhalation chamber	Crl:CD (SD)IGS BR rats 5	Peripheral blood	MN 24 h post exposure	Inhalation, nose only D_{50} = 37 nm 3.1 x 10^7 particles/cm^3 1.8 mg/m^3 D_{50} = 83 nm 1.8 x 10^8 particles/cm^3 86 mg/m^3 1 or 3 days 6 h/day	- no increase in MN for both particle sizes no significant toxicity to bone marrow indicated by the frequence of reticulocytes among the total erythrocytes	SAYES et al., 2010
		BAL	Cells LDH, microprotein, alkaline phosphatise, 24 h, 1 week, 1 month, 2 months post exposure		- no effect	
		Lung tissue	Histopathology, 2 months post exposure		- no effect	

Table Appendix I-8 *In vivo* genotoxicity studies with nanoparticulate carbon black

NP type (source), primary particle size, surface area; agglomeration/aggregation	**Species Strain No./Sex & group**	**Cell/tissue type**	**Test**	**Exposure Concentration or dose Duration**	**Results/remarks**	**Reference**
Carbon Black						
Carbon Black (Monarch 900, Cabot Corp.) 15 nm, 230 m²/g; Agglomeration: no data reported	Rat F344 9 F	Lung (alveolar cells)	HPRT mutation	Intratracheal instillation 0, 10, 100 mg/kg (in 2 equal doses on consecutive days) 15 months	+ (100 mg/kg), also + when alveolar cells *in vitro* exposed to BAL cells from 100 mg/kg treated rats, response inhibited by catalse	DRISCOLL et al., 1997
		BAL	Cells		- (total cell no.), ↓ (percentage macrophages), ↑ (percentage neutrophils, lymphocytes) (both doses)	

NP type (source), primary particle size, surface area; agglomeration/aggregation	**Species Strain No./Sex & group**	**Cell/tissue type**	**Test**	**Exposure Concentration or dose Duration**	**Results/remarks**	**Reference**
Carbon Black						
Carbon Black (Monarch 880, Cabot Corp.) 14 nm; 220 m²/g MMAD: 880 nm (GSD 3300 nm)	Rat F344 4 M	Lung (alveolar cells)	HPRT mutation	Inhalation 0, 1.1, 7.1, 52.8 mg/m³ 6 h/d, 5 d/week, 13 weeks + recovery 12 or 32 weeks	+ (13 w, ≥ 7.1 mg/m³) + (12 and 32 weeks recovery, 52.8 mg/m³)	DRISCOLL et al., 1996
		BAL	Cells and proteins		↑ neutrophils (≥ 7 mg/m³, ≥ 6,5 weeks, with/without recovery) ↑ cell no., macrophages, lymphocytes, LDH, ß-glucuronidase, protein (50 mg/m³, all)	
		Lung tissue	mRNA levels of cytokines: *Mip-2, Mcp-1, IL-6*	Inhalation 0, 1.1, 7.1, 52.8 mg/m³ 6 h/d, 5 d/week, 13 weeks + recovery 12 or 32 weeks	↑ (*Mip-2,* all time points, ≥ 7.1 mg/m³) ↑ (*Mcp-1,* ≥ 7.1 mg/m³ at end of exposure, 50 mg/m³: all time points)	

NP type (source), primary particle size, surface area; agglomeration/aggregation	**Species Strain No./Sex & group**	**Cell/tissue type**	**Test**	**Exposure Concentration or dose Duration**	**Results/remarks**	**Reference**
Carbon Black						
Carbon Black (PRINTEX® 90, Degussa) 16 nm, 300 m²/g; Agglomeration: no data reported	Rats F344 5 F	Lung tissue	8-OH-dG in DNA	Inhalation 0, 1, 7, 50 mg/m³, 6 h/week, 5 d/week, 13 weeks, + or – 44 weeks recovery	+ (prior to recovery, 50 mg/m³) + (after recovery, 7, 50 mg/m³)	GALLAGHER et al., 2003
		BAL	Cells		↑ (total cell no., 50 mg/m³, with/without recovery) ↑ (percentage neutrophils, 7 mg/m³ without, 50 mg/m³ with/without recovery)	
Carbon Black (Sterling V, Degussa) 70 nm, 37 m²/g Agglomeration: no data reported		Lung tissue	8-OH-dG in DNA	0, 50 mg/m³, 6 h/week, 5 d/week, 13 weeks, + or – 44 weeks recovery	- (with/without recovery) Retained dose higher than that of PRINTEX® 90 mass at 50 mg/m³ but equivalent to surface area at 7 mg/m³	
		BAL	Cells		↑ (total cell no., percentage neutrophils, with/without recovery)	

NP type (source), primary particle size, surface area; agglomeration/aggregation	**Species Strain No./Sex & group**	**Cell/tissue type**	**Test**	**Exposure Concentration or dose Duration**	**Results/remarks**	**Reference**
Carbon Black						
Carbon Black (PRINTEX® 90, Degussa) 14 nm, 338 m²/g Size distribution in medium, DLS: bimodal, 1200 nm and 5500 nm, dispersion unstable, agglomerating Size distribution in inhalation study: median no. concentration 45 nm, median mass distribution 331 nm (range 200 – 2750 nm)	Mice C57BL/6 7 F	BAL	Cells and protein content	Intratracheal instillation 54 µg, 3 h or 24 h	- (3 h, all parameters) ↑ (24 h, neutrophils, macrophages)	JACOBSEN et al., 2009
		Lung tissue	mRNA levels of *Mip-2, Mcp-1, IL-6*	Intratracheal instillation 54 µg, 3 h or 24 h	- (3 h, all parameters) ↑ (24 h, all parameters)	
	Mice C57BL/6-ApoE-/- 5 or 7 F	BAL	Cells and protein content	Intratracheal instillation 18 µg, 54 µg 3 h or 24 h	+ (3 h, protein) ↑ (24 h, neutrophils, macrophages, protein) Instillation effects much stronger effects than inhalation	
		Lung tissue	mRNA levels of cytokines: *Mip-2, Mcp-1, IL-6*	Intratracheal instillation 18 µg, 54 µg 3 h or 24 h	↑ (3 h, all parameters) ↑ (24 h, all parameters) Instillation had much stronger effects than inhalation	
	Mice C57BL/6-ApoE-/-, 7 F	BAL cells	Alkaline comet assay (tail length)	Intratracheal instillation 54 µg, 3 h	+	
	Mice C57BL/6-ApoE-/-, 5 F	BAL	Cells and protein content	Inhalation, 60 mg/m³ 30 min or 90 min	+ (30 min, 90 min. protein) + (30 min, *Mcp-1*)	
		Lung tissue	mRNA levels of cytokines: *Mip-2, Mcp-1, IL-6*	Inhalation, 60 mg/m³ 30 min or 90 min	↑ (3 h, all parameters) ↑ (24 h, all parameters)	
Carbon Black (PRINTEX F90, Degussa)	Mice, TNF-/-	BAL cells	Alkaline comet assay (tail length)	Inhalation, 20 mg/m³, 90 min/d, 4 d	+ (effects slightly more pronounced in TNF-/- mice)	SABER et al., 2005

NP type (source), primary particle size, surface area; agglomeration/aggregation	**Species Strain No./Sex & group**	**Cell/tissue type**	**Test**	**Exposure Concentration or dose Duration**	**Results/remarks**	**Reference**
Carbon Black						
65 nm, 295 m²/g Particle size in air: 65 nm (geometric mean), particle no. 8 x 10^{-5}/m³	4/n.r. C57/BL (TNF+/+) 4/n.r.		Percentage of neutrophils		No change (TNF-/- and +/+ mice)	
		Lung tissue	mRNA levels of cytokines: *IL-6, IL-1ß,* TNF		↑ (IL-6, both TNF-/- and +/+ mice) ↑ (TNF+/+) -(IL-1ß, both TNF -/- and +/+))	
Carbon Black PRINTEX® 90, Degussa, 14 nm, 300 m²/g Size distribution, DLS: average size 232 nm (range 13.6 - 337 nm) in saline + Tween 80, indicating agglomeration to larger particles	Mice C57BL/6 5 M	Lung	Alkaline comet assay (tail length)	Intratracheal instillation 50 or 200 µg 3 h or 24 h	+ (200 µg, 3 h and 24 h) ~ control (50 µg)	TOTSUKA et al., 2009
	Mice *gpt* delta 10 M	Lung	Mutant frequency at *gpt* loci, Spi⁻ mutation	Intratracheal instillation 200 µg once or 4 x 200 µg on consecutive days	*gpt,* Spi⁻: - (slight increase not statistically significant)	
			Histopathology	Intratracheal instillation 4 x 200 µg on consecutive days	Test-substance phagocytized macrophages diffusively found, also focal granulomatous formation	

Table Appendix I-9 *In vivo* genotoxicity studies with nanoparticulate titanium dioxide

NP type (source), primary particle size, surface area; agglomeration/aggregation	**Species Strain No./Sex & group**	**Cell/tissue type**	**Test**	**Exposure Concentration or dose Duration**	**Results/remarks**	**Reference**
TiO_2						
TiO_2, 20 nm (P25, hydrophilic surface, Degussa) 20 nm (T805, hydrophobic surface, Degussa) TEM: particles highly aggregated and agglomerated, but no quantitative data reported	Rats Wistar F	Lung parenchyma cells	Formation of 8-OH-dG	Intratracheal instillation 0.15 – 1.2 mg/ml in saline with 0.25 % lecithin, 90 d	- (both materials)	REHN et al., 2003
		BAL	Cells and protein		- (no. total cells and macrophages, TNF-α, fibronectin, lung surfactants, both materials) + (percent. neutrophils, P25)	

NP type (source), primary particle size, surface area; agglomeration/aggregation	**Species Strain No./Sex & group**	**Cell/tissue type**	**Test**	**Exposure Concentration or dose Duration**	**Results/remarks**	**Reference**
TiO_2						
TiO_2 (86 % Anatas/ 14 % Rutile), (NTP, Baker & Collinson) 25.1 nm (range 13 – 71 nm, uncoated, hydrophobic), 51.1 m²/g; TEM: small and large agglomerates in atmosphere MMAD by cascade impactor analysis: 700 – 1100 nm (GSD: 2.3 – 3.4 nm)	Rats Wistar 3 M	BAL	Cells and protein content	Inhalation 2; 10; 50 mg/m³ 6 h/d, 5 d	↑ cell count, protein, enzyme activities: PMN, GGT, MCP-1, MCP-3, M-CSF, MDC, MIP-2, MyP, OSP (10, 50 mg/m³), LDH, ALP, NAG, clusterin, Hp (50 mg/m³)	MA-HOCK et al., 2009
		Lung tissue	Histopathology, cell proliferation (BrdU), apoptosis	Inhalation 2; 10; 50 mg/m³ 6 h/d, 5 d	↑ alveolar macrophages (10, 50 mg/m³), epithelial thickening (50 mg/m³) ↑ lung weight, TiO_2 in mediastinal lymph nodes (50 mg/m³), ↑ cell replication (esp. terminal bronchioli, all doses) - (apoptosis)	
		Blood	Haematology	Inhalation 2; 10; 50 mg/m³ 6 h/d, 5 d	↑ neutrophil gelatinase-associated lipocalin (10, 50 mg/m³)	

NP type (source), primary particle size, surface area; agglomeration/aggregation	**Species Strain No./Sex & group**	**Cell/tissue type**	**Test**	**Exposure Concentration or dose Duration**	**Results/remarks**	**Reference**
TiO_2						
TiO2 (75 % Anatase/ 25 % Rutile), (P25 "Aeroxide, Degussa) 21 nm, 50 ± 15 m²/g DLS (aqueous solution): mean size 160 ± 5 nm (range 21 – 1446 nm)	Mouse C57Bl/6J 5 M	Blood	Alkaline comet assay in WBC	Oral (drinking water) 5 d; 0, 60, 120, 300, 600 µg/ml (total dose: 0, 50, 100, 250, 500 mg/kg b.w.)	↑ at highest dose (no data for other doses)	TROUILLER et al., 2009
			Micronucleus assay in RBC		↑ at highest dose only	
			mRNA of Cyto-kines		↑ (up-regulation) of mRNA for proinflammatory proteins TNF-alpha, IFN-gamma, IL-8 at highest dose (no data for other doses); no effect on mRNA of anti-inflammatory ctokines	
		Bone mar-row	γ-H2-AX (indicat-ing DNA-double strand breaks)		↑ in no. of positive foci at all concentrations (dose-dependent)	
		Liver	8-OH-dG		↑ at highest dose (no data for other doses)	
	Mouse C57Bl/6Jpun/pun Pregnant F (no. not reported), Offspring: 42 (control), 53 (exposed)	Eye of off-springs 20 d after birth	DNA deletion assay (RPE)	Oral (drinking water) 10 d (day 8.5 – 18.5 of gestation); 0, 300 µg/ml (total dose: 0, 500 mg/kg b.w.)	↑ No. of eyespots/RPE indicat-ing DNA deletions	

Table Appendix I-10 *In vivo* genotoxicity studies with nanoparticulate C60 fullerene[1]

NP type (source), primary particle size, surface area; agglomeration/aggregation	Species Strain No./Sex & group	Cell/tissue type	Test	Exposure Concentration or dose Duration	Results/remarks	Reference
Fullerene						
C_{60}-Fullerene (Sigma-Aldrich) 0.7 nm, < 20 m²/g Size distribution in medium, DLS: mostly > 1700 nm, dispersion unstable, agglomerating during analysis	Mice C57BL/6-ApoE-/- 5 or 7 F	BAL cells	Alkaline comet assay (tail length)	Intratracheal instillation 54 µg 3 h	-	JACOBSEN et al., 2009
		BAL	Cells and protein content	Intratracheal instillation 54 µg 3 h or 24 h	↓ (3 h, 24 h, protein)	
		Lung tissue	mRNA levels of cytokines: *Mip-2, Mcp-I, IL-6*	Intratracheal instillation 54 µg 3 h or 24 h	↑ (3 h, *Mcp-1*) ↑ (24 h, all parameters)	
C_{60}-Fullerene (Sigma-Aldrich) 0.7 nm, < 20 m²/g; Size distribution, DLS: in saline 407 nm (low dose), bimodal with 621 and 5117 nm at high dose in corn oil: 234 nm (low dose), trimodal with 40, 713, 3124 nm	Rats F344 8-10 M	Colon, liver. lung cells	8-OH-dG in DNA	Oral (gavage, saline or corn oil), 64 or 640 µg/kg b.w., 24 h	- (colon) + (lung, high dose) + (liver, both doses)	FOLKMANN et al. 2009
		Liver and lung	mRNA level of *HO1, MUTYH, NEIL1, NUDT1, OGG1*	Oral (gavage, saline or corn oil), 64 or 640 µg/kg b.w., 24 h	- (lung, all parameters) - (liver, all parameters except: + (*OGG1,* high dose))	
		Liver	*OGG1* repair activity of enzyme	Oral (gavage, saline or corn oil), 64 or 640 µg/kg b.w., 24 h	-	

NP type (source), primary particle size, surface area; agglomeration/aggregation	**Species Strain No./Sex & group**	**Cell/tissue type**	**Test**	**Exposure Concentration or dose Duration**	**Results/remarks**	**Reference**
Fullerene						
C_{60}-Fullerene 0.7 nm; Size distribution, DLS: bimodal size, mostly 234 and 857 nm (range 10,5 – 12914 nm) in saline + Tween 80 medium indicating agglomeration to larger particles	Mice C57BL/6 5 M	Lung	Alkaline comet assay (tail length)	Intratracheal instillation 50 or 200 µg 3 h or 24 h	+ (200 µg, 3 h, effect decreased at 24 h) ~ control (50 µg)	TOTSUKA et al. 2009
	Mice *gpt* delta 10 M	Lung	Mutant frequency at *gpt* loci, Spi^- mutation	Intratracheal instillation 200 µg, once or 4 x 200 µg on consecutive days	*gpt:* + (single exposure, 12 weeks after treatment) + (multiple exposure, 8 weeks after treatment) Sp^-: -	
			Histopathology	Intratracheal instillation 4 x 200 µg on consecutive days	Test-substance phagocytized macrophages diffusively found, also focal granulomatous formation	

Legend to Tables on Genotoxicity *in vivo*

↑: increase;
↓: decrease;
+: positive response;
-: no effect;
*: cells first exposed to test substance, then to DCFA-DA in absence of test substance, assay therefore may be affected by reduced cell viability due to cytotoxicity;
**: cells first loaded with DCFA-DA, then incubated with test substance; DCFH-DA: 2',7'-Dichlorofluorescein diacetate;

ALP: alkaline phosphatase;
BAL: bronchoalveolar lavage;
BrdU: 5-bromo-2´-deoxyuridine;
DLS: dynamic light scattering;
F: females;
GGT: gammy-glutamyltransferase;
GSD: geometric standard deviation;
GSH: glutathione;
HO1: heme oxygenase 1;
IL: interleukin;
LDH: lactate dehydrogenase;
M: males;
MCP-1 and -3: macrophages/monocyte chemoattractant protein-1 and -3;
M-CSF: macrophage colony stimulating factor;
MDC: macrophage-derived chemoattractant;
MMAD: Mass median aerodynamic diameter;
Mip-2: macrophage inflammatory protein-2;
MUTYH: mutY homolog;
Myp: myeloperoxidase;
NAG: N-acetyl glucosaminidase;
NEIL1: nei endonuclease VIII-like 1;
NUDT1: nucleoside diphosphate linked moiety X-type motif 1;
OGG1: 8-oxoguanine DNA glycosylase;
OSP: osteopontin;
PMN: Polymorphonuclear neutrophils;
RBC: Red blood cells;
RPE: Retinal pigment epithelium

Appendix II
Physico-Chemical Characterisation of Quartz DQ12

INTRODUCTION

DQ12<5µm quartz has been a standard quartz for experimental biological use in Europe for over 25 years. It answered a need expressed in the early 1970's for a standard quartz for biological studies. ROBOCK (1973) describes preparation of the original sample.

PROCESSING

Source sand

The quartz used for the basis of DQ12 is from a kaolinitic sand from the Dörentrup deposit of Tertiary age in Westphalia, Germany. The processor, Dörentrup Sand- und Thonwerke GmbH, presumably extracted the quartz sand from the kaolin, then ground it to <60 µm to provide a product "Ground Product No. 12", also known as "DQ12."

Separations

In 1966, Leiteritz of the Steinkohlenbergbauverein in Essen, Germany, separated a <5 µm from the <60 µm product and provided Dr. Friedrich Pott, University of Düsseldorf, with this sample (6th delivery, called no. 6). He used an air centrifuge made by Walther-Staubtechnik of Cologne, Germany. Technical conditions are the same as published later by ROBOCK (1973).

In 1973 Robock of the Steinkohlenbergbauverein in Essen, Germany, separated a <5 µm from the <60 µm product, and termed this fraction "DQ12<5 µm." He also used an air centrifuge made by Walther-Staubtechnik of Cologne, Germany.

In 1985, Armbruster, a colleague of Robock, made yet another separation at the Steinkohlenbergbauverein. He used the same DQ12, and the same equipment and techniques that Robock had used. Armbruster separated the DQ12 into fine, medium, and coarse fractions. The fine fraction presumably was identical to the original DQ12<5 µm. Fraunhofer ITEM purchased the samples from Bergbauforschung, Essen, Germany.

PROPERTIES

Robock's determination of his DQ12<5µm sample

Robock characterized the sample he prepared, and reported the following information:

Particle size distribution:

- Particle number distribution: ~0.8 µm
- Maximum of the volume or mass distribution: ~1.3 µm
- Upper size of quartz particles: between 5 and 6 µm

(Particle size distribution by Coulter counter)

Appendix II
Physico-Chemical Characterisation of Quartz DQ12 - cont'd

Mineralogy:

- Quartz content: 87 %
- Remainder: amorphous SiO_2 and a small contamination of kaolinite

(Determination by infrared spectrophotometer analysis)

Fraunhofer determination of Armbruster's DQ12<5µm sample:
Particle size:

Sample	Mass median geometric diameter (µm)	Arithmetic mean diameter (µm)	Geometric mean diameter (µm)
Quartz DQ12 coarse	15.2	13.8	12.7
Quartz DQ12 middle size	3.0	3.3	3.0
Quartz DQ12 fine <5µm	**1.3**	**1.3**	**1.3**

Note: longest and shortest dimensions measured by electron microscopy, mean calculated

Surface area:

- 9.4 m^2/g, presumably by BET method

Sorptive Minerals Institute (USA) determination of Armbruster's DQ12<5µm sample
Particle size, electron microscope:

Measurement	**DQ12<5µm, µm**
Mean	**1.0266**
STD	**0.6853**
Geometric Mean	**0.8635**
Geometric STD	**1.7772**
Minimum	**0.1824**
Maximum	**5.8069**
Median	**0.8202**

Note: Particle size from electron microscope measurements of 1000 particles, longest dimension measured (Determination by R. HAMILTON)

Appendix II
Physico-Chemical Characterisation of Quartz DQ12 - cont'd

Particle size laser scattering:

Sample	**D[4,3]**	D[3,2]	D(v,0.1)	D(v,0.5)	D(v,0.9)	Span	Uniformity
DQ12<5 µm	**1.29**	0.65	0.30	0.98	2.63	2.374	0.7682

D[4,3] the mean of the entire particle size distribution
D[3,2] the mean calculated from a surface area assuming spherical particles
v,0.1 the point at 10 percent of the particle size distribution
v,0.5 the point at 50 percent of the particle size distribution
v,0.9 the point at 90 percent of the particle size distribution
span the span of the particle size distribution
uniformity a calculated parameter, the lower the number the more uniform
Determination by Oil-Dri Corporation

Surface area:

Sample	BET (m^2/g)	EGME (m^2/g)
DQ12<5µm	**1.51**	**16.01**

BET: gas adsorption method by Oil-Dri Corporation
EGME: ethylene glycol monoethyl ether method by Oil-Dri Corporation

Chemical analysis:

	DQ12<5µm
SiO_2, %	**99.39**
Al_2O_3, %	**0.10**
Fe_2O_3, %	**0.04**
MnO, %	**-0.001**
MgO, %	**0.04**
CaO, %	**0.14**
Na_2O, %	**0.16**
K_2O, %	**0.05**
TiO_2, %	**0.049**
P_2O_5, %	**0.02**

Analysis done by ACT Laboratories by wet methods

Appendix II
Physico-Chemical Characterisation of Quartz DQ12 - cont'd

Mineralogical characterization:

Mineral	DQ12<5%
quartz, %	**87**
smectite, %	
rutile, %	
undeterminable, %	**13**

Analysis by X-ray diffraction (R. HAMILTON)

Crystallographic properties:

Sample	Murata ratio	FWHM	Domain size µm	Particle size µm, Note 1	Particle size µm, Note 2
DQ12<5µm	**6.8**	**0.1981**	**0.16**	**1.0266**	**1.29**

FWHM: full width of diffraction peak at half maximum
Note 1: Determination by electron microscope measurements (R. HAMILTON)
Note 2: Determination by laser scattering (Oil-Dri Corporation)

REFERENCES
Nolan, Robert P., Arthur M. Langer, and George B. Herson (1988) Physicochemical properties and membranolytic activities of the titanium dioxide polymorphs compared with those of quartz, Proceedings of the workshop on Biological Interaction of Inhaled Mineral Fibers and Cigarette Smoke, 1988, Alfred P. Wehner, ed., Battelle Pacific Northwest Laboratories, Richland, Washington, 391-421.
Robock, K. (1973) Standard quartz DQ12<5µm for experimental pneumoconiosis research projects in the Federal Republic of Germany, Ann. Occup. Hyg., 16, 63-66.
Hamilton R - personal communication

Appendix III
Sources of Data for Correlation

1. Research project of the German Umweltbundesamt FKZ 298 61 273 (UBA I)

The lung paraffin blocks for immunohistochemistry of genotoxicity markers and the data for correlation analysis were taken from the research project titled: “Pathogenetische und immunbiologische Untersuchungen zur Frage: Ist die Extrapolation der Staubkanzerogenität von der Ratte auf den Menschen gerechtfertigt?”

Ernst H, Rittinghausen S, Heinrich U, & Pott F (2005) Pathogenetische und immunbiologische Untersuchungen zur Frage: Ist die Extrapolation der Staubkanzerogenität von der Ratte auf den Menschen gerechtfertigt? Umweltforschungsplan des Bundesministeriums für Umwelt, Naturschutz und Reaktorsicherheit. Förderkennzeichen (FKZ): 298 61 273

2. Reports of research project FKZ 298 61 273 (UBA I)

Interim Report 1: Reported period 01.03.1998-30.09.1998

Relevant contents:

- Summary of results of dose finding test (1-month study)
  - BALF
  - TNF-alpha
  - Necropsy findings
  - Histopathology

Interim Report 2: Reported Period 01.10.1998-31.03.1999

Relevant contents:

- Report for 28-day study
  - Summarized result tables
  - BALF
  - TNF-alpha
  - RNI (=NOx)
  - Necropsy findings
  - Histopathology (extended description of findings and diagrams)

Appendix III
Sources of Data for Correlation - cont'd

Interim Report 3: Reported Period 01.04.1999-31.09.1999
Relevant contents:
- Report for 3-month study
  - Necropsy findings
  - Lung wet-weights
  - BALF (results table)
  - ROS
  - RNI (=NOx)
  - TNF-alpha
  - Comet Assay (table)
  - UDS
  - HPRT

Interim Report 4: Reported Period: 01.10.1999-31.07.2000
Relevant contents:
- Report for animal experiment of 9-month study
  - Necropsy findings
  - BALF (results table)
  - ROS (diagram)
  - RNI (diagram)
  - TNF-alpha (diagram)

Interim Report 5: Reported Period: 01.08.2000-31.01.2001
Relevant contents:
- Report for completed 1-, 3-, and 9-month studies
  - Retention
- Report for running carcinogenicity study
  - Body weight and mortality

Interim Report 6: Reported Period: 01.02.2001-31.08.2001
Relevant contents:
- Report for running carcinogenicity study
  - Body weight and mortality

Final Report August 2002
Relevant contents:
- Report for finalized carcinogenicity study
- Publication 1 (ERNST et al., 2002) is part of this final report.

Appendix III
Sources of Data for Correlation - cont'd

3. Histology Data of the Life Time Study

Table Appendix III-1 Percentage of tumours and precancerous lesions of the carcinogenicity study

Tumours and Preneoplastic Lesions			
Group Life Time Study	**% of Rats with Lung Tumours**	**% of Rats with Precancerous Lung Lesions**	**No. of rats**
10 x 0.3 ml Negative control: 0.9% saline/Tween 80®	0.0	2.0	55
1 x 3 mg Crystalline SiO_2: Quartz DQ12	39,6	43.4	53
30 x 0.5 mg Amorphous SiO_2: AEROSIL® 150	9.3	1.9	53
10 x 0.5 mg Carbon black: PRINTEX® 90	15.0	20.3	59

4. Histology data of the 3-month study from the animals examined for genotoxicity

Table Appendix III-2 Mean inflammation score of the animals from the 3-month study (included are only animals which were also evaluated for genotoxicity marker expression)

Inflammation Score Histology		
Group	**Mean Inflammation Score**	**No. of rats**
Negative control: 0.9% saline	0.3	6
Crystalline SiO_2: Quartz DQ12	3.2	6
Amorphous SiO_2: AEROSIL® 150	1.8	6
Carbon black: PRINTEX® 90	2.2	6

Appendix III
Sources of Data for Correlation - cont'd

Table Appendix III-3 Single animal data for the inflammation score from the 3-month study (included are only the animals which were also evaluated for genotoxicity marker expression, for single animal data see Appendix IV)

Inflammation Score Histology				
Group	**Animal Number**	**Inflammation Score**	**Mean**	**Standard Deviation**
Negative control: 0.9% saline	A020012	0	0.3	0.8
	A020013	2		
	A020014	0		
	A020015	0		
	A020022	0		
	A020023	0		
Crystalline SiO_2: Quartz DQ12	B040012	3	3.2	0.4
	B040013	3		
	B040014	3		
	B040015	3		
	B040021	3		
	B040022	4		
Amorphous SiO_2: AEROSIL® 150	D080012	2	1.8	0.3
	D080013	2		
	D080015	1.5		
	D080021	1.5		
	D080022	2		
	D080023	2		
Carbon black: PRINTEX® 90	H160012	2	2.2	0.4
	H160013	2		
	H160014	2		
	H160021	2		
	H160022	3		
	H160023	2		

Appendix III
Sources of Data for Correlation - cont'd

5. Bronchoalveolar lavage data of the 3-months study

Table Appendix III-4 Bronchoalveolar lavage data of the 3-months study concerning leucocytes and polymorphonuclear granulocyte counts

Bronchoalveolar Lavage - Inflammation	BAL Leucocytes [No./ml]		BAL Polymorphonuclear Granulocytes [No./ml]	
Group	**Mean**	**No. of rats**	**Mean**	**No. of rats**
Negative control: 0.9% saline	98.250	5	2.250	5
Crystalline SiO_2: Quartz DQ12	15130.000	5	5547.500	5
Amorphous SiO_2: AEROSIL® 150	698.500	5	306.000	5
Carbon black: PRINTEX® 90	3785.000	5	2534.000	5

Table Appendix III-5 Bronchoalveolar lavage data of the 3-months study concerning lactic dehydrogenase, alkaline phosphatase and γ-glutamyl transferase measurements

Bronchoalveolar Lavage - Inflammation	BAL Lactic Dehydrogenase [U/l]		BAL Alkaline Phos-phatase [U/l]		BAL γ-Glutamyl Transferase [U/l]	
Group	**Mean**	**No. of rats**	**Mean**	**No. of rats**	**Mean**	**No. of rats**
Negative control: 0.9% saline	44	5	37	5	2.23	5
Crystalline SiO_2: Quartz DQ12	1064	5	105	5	14.88	5
Amorphous SiO_2: AEROSIL® 150	274	5	89	5	6.21	5
Carbon black: PRINTEX® 90	907	5	167	5	13.22	5

Appendix III
Sources of Data for Correlation - cont'd

Table Appendix III-6 Bronchoalveolar lavage data of the 3-months study concerning total protein measurements

Bronchoalveolar Lavage - Inflammation	BAL Total Protein [mg/l]	
Group	**Mean**	**No. of rats**
Negative control: 0.9% saline	95	5
Crystalline SiO_2: Quartz DQ12	1860	5
Amorphous SiO_2: AEROSIL® 150	311	5
Carbon black: PRINTEX® 90	1669	5

Table Appendix III-7 Bronchoalveolar lavage data of the 3-months study concerning lung wet-weights

Bronchoalveolar Lavage		BAL normed[a)]	BAL
Group	**No. of rats**	**Lung Wet-Weight Mean**	
Negative control: 0.9% saline	5	1.00[a)]	1.11
Crystalline SiO_2: Quartz DQ12	5	2.82	3.13
Amorphous SiO_2: AEROSIL® 150	5	1.53	1.7
Carbon black: PRINTEX® 90	5	2.52	2.8

[a)] Negative control scaled to 1.00

APPENDIX III
Sources of Data for Correlation - cont'd

6. Immunobiology data of the 3-months study

Table Appendix III-8 Immunobiology data of the 3-months study for estimation of tumour-necrosis-factor-α (TNF-α) liberation

***Ex vivo* Reactivity of Alveolar Macrophages: TNF-α Liberation**						
	TNF-α Concentration [pg/ml]					
Stimulation	**Control**		**0.1 ng/ml LPS**		**1 ng/ml LPS**	
Group	**Mean**	**No. of rats**	**Mean**	**No. of rats**	**Mean**	**No. of rats**
Negative control: 0.9% saline	285.93	5	334.18	5	1393.13	5
Crystalline SiO_2: Quartz DQ12	18.70	5	27.41	5	362.05	5
Amorphous SiO_2: AEROSIL® 150	213.87	5	282.15	5	997.46	5
Carbon black: PRINTEX® 90	16.26	5	20.09	5	293.99	5

APPENDIX III
Sources of Data for Correlation – cont'd

7. Publication 1

ERNST et al., (2002):
Ernst H, Rittinghausen S, Bartsch W, Creutzenberg O, Dasenbrock C, Gorlitz BD, Hecht M, Kairies U, Muhle H, Müller M, Heinrich U & Pott F (2002) Pulmonary inflammation in rats after intratracheal instillation of quartz, amorphous SiO_2, carbon black, and coal dust and the influence of poly-2-vinylpyridine-N-oxide (PVNO). Exp Toxicol Pathol 54: 109-126
Relevant contents:

- Results of the 1-month and 3-month studies
- BALF
- Histopathology
- Results of RNI -, ROS - und TNF-alpha-production after 9-month (satellite groups of carcinogenicity study).
- Detailed description of methods

Table Appendix III-9 Histopathology data of the 3-month study published by ERNST et al. (2002).

Table 6. Summary of main histopathological findings in the lungs (of females), 3-month study.

Lesions	Incidence of lesions Treatment								
	3× 0,3 ml NaCl	3×2 mg DQ 12	3×2 mg DQ 12+ 20 mg PVNO	3×2 mg Aeros. 150	3×2 mg Aeros. +100mg PVNO	3×6 mg Print. 90	3×6 mg Print. +20 mg PVNO	1× 2 mg Aeros. 150	1×2 mg Aeros. +100mg PVNO
Lungs	(13)	(13)	(13)	(13)	(13)	(13)	(13)	(6)	(6)
Accumulation of particle-laden macrophages	0	13***	13***	13***	13***	13***	13***	6***	6***
Accumulation of multinucleate giant-cells	0	0	0	0	0	13***	13***	0	0
Interstitial fibrotic granulomas	0	0	0	13***	13***	0	0	6***	2
Interstitial fibrosis	0	13***	13***	13***	13***	13***	13***	6***	6***
Bronchiolo-alveolar hyperplasia	0	13***	13***	13***	12***	13***	13***	6***	2
Bronchial/bronchiolar mucus cell hyperplasia	0	7**	2	3	1	0	3	2	0
Alveolar lipoproteinosis	0	13***	13***	0	0	0	0	0	0
Cholesterol granulomas	0	3	0	1	0	0	0	0	0
Alveolar/Interstitial inflammatory cell infiltration	0	13***	13***	13***	13***	13***	13***	6***	6***

Significance of difference in a pairwise Fisher's test between control and treatment groups: *$p < 0.05$,**$p < 0.01$, ***$p < 0.001$; Figures in brackets represent the number of animals from which this tissue was examined microscopically

APPENDIX III
Sources of Data for Correlation – cont'd

Description of Methods
Bronchoalveolar lavage (BAL):
The method described by HENDERSON et al. (1987) was used with minor modifications. Lungs including trachea were prepared from 5 rats per group after anesthetization with an overdose of pentobarbitone sodium. Following cannulation, lungs were lavaged with 2 x 4 ml saline without massage. From this first lavage series the following parameters were investigated. The cell concentration of leukocytes in the lavage fluid was determined by light microscopy using a counting chamber. After preparation of cytoslides for differential cell count (May-Grünwald/Giemsa stain) the lavage fluid was centrifuged at 160 g and 4°C and the supernatant analyzed for biochemical parameters (lactic dehydrogenase - LDH, alkaline phosphatase - AP, γ-glutamyl tranferase - γ-GT, total protein - TP) according to standard routine procedures. A second series of lavage was performed on the same lungs using 5 x 5 ml saline with massage. This technique provided an increased number of leukocytes that were subjected to immunobiological investigations.

Production of tumour-necrosis-factor-α (TNF-α):
The number of macrophages was calculated on the basis of the differential cell count. One x 10^5 macrophages/well were plated in a 96-well micro titer plate. Triplicates of the cells were stimulated with LPS at a final concentration of 0.1, 1, and 10 ng/ml, respectively. The controls received medium. After an incubation period of 24 h at 37 ºC, the supernatants were harvested and stored at –20 ºC until the test was performed. After thawing the supernatants the production of TNF-α was measured in a rat TNF-α ELISA (R&D systems) according to the manufacturer's instructions.

8. Research Project of the German „Umweltbundesamt" FKZ 203 61 21 (UBA II)

Title of the research project: Pathogenetische und immunbiologische Untersuchungen zur Frage: Ist die Extrapolation der Staubkanzerogenität von der Ratte auf den Menschen gerechtfertigt? Teil II: Histologie. Umweltforschungsplan des Bundesministeriums für Umwelt, Naturschutz und Reaktorsicherheit. Förderkennzeichen: 203 61 215.
Autoren der Berichte zum Forschungsvorhaben: Ernst H, Kolling A, Bellmann B, Rittinghausen S, Heinrich U & Pott F.

Interim Report 1: Reported Period: 01.08.2003-31.01.2004
- No relevant results because of running investigations.

Interim Report 2: Reported Period: 31.01.2004-31.07.2004
Relevant contents:
- Carcinogenicity study
- Results of serial sections of 7 animals/group and results of routine sections of 10 animals per group

APPENDIX III
Sources of Data for Correlation – cont'd

Interim Report 3: Reported Period: 01.08.2004-31.01.2005
Relevant contents:
- Results of routine sections of 17 animals per group and of serial sections of 7 animals per group.

Final Report 2005
The final report is accessible in the internet:
[http://www.umweltdaten.de/publikationen/fpdf-l/3033.pdf]
Ernst H, Kolling A, Bellmann B, Rittinghausen S, Heinrich U & Pott F.: Pathogenetische und immunbiologische Untersuchungen zur Frage: Ist die Extrapolation der Staubkanzerogenität von der Ratte auf den Menschen gerechtfertigt? Teil II: Histologie. Abschlussbericht. Umweltforschungsplan des Bundesministeriums für Umwelt, Naturschutz und Reaktorsicherheit. November 2005. Förderkennzeichen (UFOPLAN) 203 61 215
Relevant contents:
- Histopathology of satellite groups (9-months)
- Image analysis of fibrosis on same lungs

9. Publication 2

KOLLING et al., (2008):
Kolling A, Ernst H, Rittinghausen S, Heinrich U & Pott F (2008) Comparison of primary lung tumour incidences in the rat evaluated by the standard microscopy method and by multiple step sections. Exp Toxicol Pathol. 60:281-8. Epub 2008 May 2.

Relevant contents:
Results of tumour diagnostics. animals examined are 55 rats of control group (30 lungs with serial sections), 53 rats of quartz group (7 lungs with serial sections), 56 rats of quartz + PVNO-group (7 lungs with serial sections), 53 rats of AEROSIL®-group (31 lungs with serial sections), 17 rats of PRINTEX®-group (7 lungs with serial sections), 17 rats of coal dust group (17 lungs with serial sections).

APPENDIX III
Sources of Data for Correlation – cont'd

Comment on the method of lung trimming and sectioning:
Lung tissue was trimmed according to the Fraunhofer ITEM Standard Operating Procedures (see drawing in Figure Appendix III-1):
The left lung lobe and the right caudal lobe were trimmed longitudinal along the major bronchi. From each of the two larger lung lobes a dorsal and a ventral portion was received and embedded. From the three other smaller lung lobes cross sections containing the bronchi were taken.

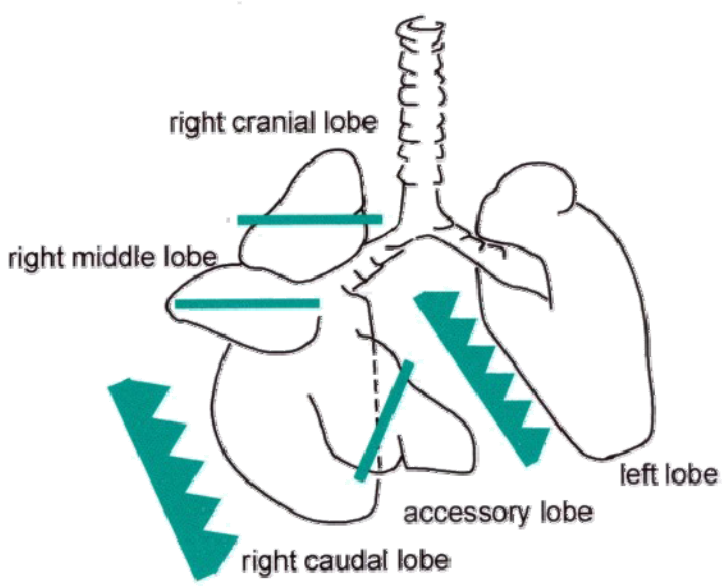

Figure Appendix III-1 Trimming of lung tissue

Seven pieces of lung tissue of all five lung lobes were embedded into six paraffin wax blocks:
8A_d: left lung lobe, dorsal part
8A_v: left lung lobe, ventral part
8B_d: right caudal lung lobe, dorsal part
8B_v: right caudal lung lobe, ventral part
8C: right cranial lobe and right middle lobe
8D: accessory lobe

APPENDIX III
Sources of Data for Correlation – cont'd

From each of the six wax blocks one 3 µm paraffin section was taken and placed on a glass slide (see Figure Appendix III-2). Therefore from each animal six glass slides containing cuts from seven pieces of lung were evaluated routinely.

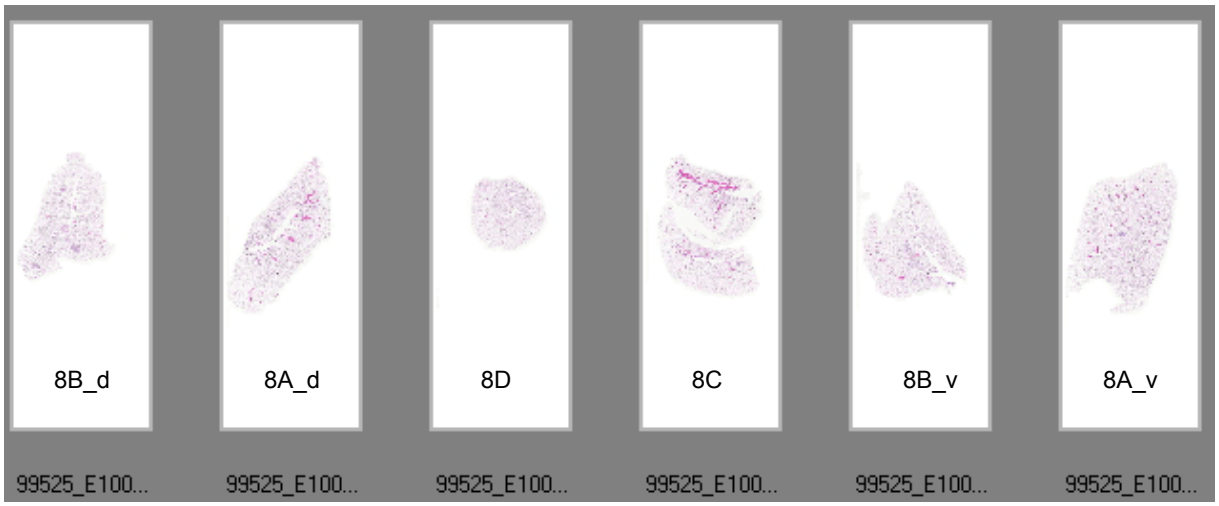

Figure Appendix III-2 Seven pieces of lung tissue from five lung lobes of on glass slides.

For the lung step sections (minimum 60 sections per animal, maximum 78 sections) from every of the six wax blocks at least 10 paraffin sections (3 µm thin) were taken in a distance of 250 µm.

APPENDIX III
Sources of Data for Correlation – cont'd

Data of the research project FKZ 298 61 273 und FKZ 203 61 215 of the German Umweltbundesamt

Table Appendix III-10 Incidences[a)] of tumours and tumour types in the lungs of female Wistar rats after intratracheal instillation of granular dusts (from: KOLLING et al., 2010 in preparation)

	10 x 0.3 ml vehicle NaCl/Tween	1 x 3 mg crystalline SiO_2 quartz DQ 12	30 x 0.5 mg amorphous SiO_2 AEROSIL® 150	10 x 0.5 mg carbon black PRINTEX®
No. of rats examined	55	53	54	59
No. (%) of rats with lung tumours	0 (0%)[a)]	21 (39.6%)	5 (9.3%)	9 (15%)
No. (%) of rats with multiple tumours	0 (0%)	11 (21%)	0 (0%)	2 (3.3%)
Total no. of lung tumours/group	0	46	5	13
No. (%) of rats with precancerous lesions	1 (2%)	23 (43.4%)	1 (1.9%)	12 (20.3%)
No. (%) of rats with:				
Bronchiolo-alveolar carcinoma	0 (0%)	14 (26.4%)	2 (3.7%)	6 (10.2%)
Squamous cell carcinoma	0 (0%)	7 (13.2%)	1 (1.9%)	2 (3.4%)
Adenosquamous carcinoma	0 (0%)	0 (0%)	0 (0%)	0 (0%)
Bronchiolo-alveolar adenoma	0 (0%)	6 (11.3%)	2 (3.7%)	2 (3.4%)
Cystic keratinizing epithelioma	0 (0%)	5 (9.4%)	0 (0%)	1 (1.7%)

[a)] Number of tumour-bearing rats expressed as total number or percentage (in brackets) of the total number of rats examined in this treatment group

Appendix IV
Single Animal Data for Genotoxicity Marker Expression

Genotoxicity Marker Expression						
	Animal No.	Positive Nuclei per mm^2				Positive Cytoplasm
Group	Marker	8-OH-dG	γ-H2AX	PAR	OGG1	OGG1
Negative control: 0.9% saline	A020012	123.7	128.8	458.0	92.0	41.0
	A020013	142.1	153.0	305.1	65.2	42.6
	A020014	160.5	161.5	286.0	79.4	45.1
	A020015	129.6	173.1	226.5	62.7	71.9
	A020022	110.3	136.4	238.3	65.2	71.1
	A020023	122.0	199.8	231.5	66.0	73.6
Crystalline SiO_2: Quartz DQ12	B040012	357.9	388.7	626.9	178.1	166.4
	B040013	454.7	458.2	442.9	165.5	242.4
	B040014	264.4	337.2	466.3	84.4	168.8
	B040015	368.6	347.0	398.6	164.7	232.4
	B040021	335.3	426.5	438.0	57.7	342.7
	B040022	356.0	373.8	408.8	71.9	193.9
Amorphous SiO_2: AEROSIL® 150	D080012	209.0	218.3	628.6	87.8	56.8
	D080013	202.3	222.3	346.8	79.4	137.1
	D080015	191.4	186.5	429.6	41.8	176.4
	D080021	301.8	142.3	321.8	49.3	196.5
	D080022	276.6	286.0	285.8	68.6	209.8
	D080023	295.0	249.2	365.3	57.7	203.9
Carbon black: PRINTEX® 90	H160012	260.1	381.3	431.3	83.6	283.3
	H160013	224.0	264.2	438.0	61.9	186.5
	H160014	306.8	362.2	426.2	83.6	241.6
	H160021	188.9	389.8	345.2	43.5	236.6
	H160022	299.2	301.8	415.3	39.3	251.5
	H160023	157.9	309.3	402.0	63.5	224.8

Appendix V
Presentation of First Project Results at DGPT Congress Mainz

Quantification of Local Genotoxicity in Rat Lungs after 3 Months of Particle Exposure by Immunohistochemical Detection of 8-OH-dG, gamma-H2AX, and Poly(ADP-Ribose)

C. Ziemann[1], B. Bellmann[1], K. Serwatzki[1], O. Creutzenberg[1], H. Ernst[1], A. Kolling[1], S. Beneke[2], and S. Rittinghausen[1]

The mechanisms of genotoxicity in the lung after uptake of low soluble particles are still intensely under debate, as fine and ultrafine particles like carbon black and TiO_2 were shown to induce fibrosis and tumours in lungs of chronically exposed rats. Data on local genotoxicity after particle exposure could aid in resolving mechanistic aspects like the impact of chronic inflammation, types of DNA-damage, or significance of DNA-damage for lung carcinogenesis. Therefore, immunohistochemical methods for quantification of the genotoxicity markers 8-hydroxyguanosine (oxidized base), gamma-H2AX (indicates DNA-double strand breaks) and poly(ADP-ribose) (general DNA-damage marker) in formalin-fixed paraffin-embedded lung tissue samples were established within a BAuA-funded project (F2135) on genotoxic mechanisms of fine and ultrafine particles in the lung. To be able to correlate local genotoxicity with other relevant endpoints, existing rat lung tissue samples of an already published carcinogenicity experiment (UBA grant no. 29861273) were investigated. The rats had been intratracheally exposed at monthly intervals for 3 months to saline (3 x 0.3 ml), quartz DQ12 (average arithmetical diameter ∅ 1.3 µm; 3 x 2 mg), amorphous SiO_2 (Aerosil®150; ∅ 14 nm; 3 x 2 mg) or carbon black (Printex 90®; ∅ 14 nm; 3 x 6 mg). Lung sections were stained, using antigen-specific primary and corresponding secondary antibodies, streptavidine-biotine alkaline phosphatase, Fast Red as chromogen and a counterstain. Markers were quantified by interactive counting of positive nuclei in digital images of 4 regions of 5 bronchioles (= 20 fields at 40-fold magnification) per animal using the image analysis software SIS Analysis Five. Data were expressed per mm^2. In the investigated experimental overload situation, significant and graded increase in genotoxicity was demonstrated in all treatment groups, as compared to the negative controls. Interestingly, the mean increases in marker positive nuclei correlated well with the detected lung tumour incidences after 24 months and the mean inflammation score after 3 months of exposure. As expected, genotoxicity was most profound in DQ12 treated rats. In conclusion, immunohistochemical detection of different genotoxicity markers in lung tissue is feasible, enables integration of local genotoxicity into inhalation studies and seemed to have prognostic value for long-term outcome of particle exposure. For further mechanistic predications respective investigations are also needed for the non-overload situation without inflammation.

[1] Fraunhofer Institute for Toxicology and Experimental Medicine, Hannover, Germany;
[2] Molecular Toxicology, University of Konstanz, Konstanz, Germany

*There were two errors in the original abstract concerning the average arithmetical diameter of DQ12 (1.5 µm) and Aerosil® 150 (4 nm). These errors were corrected (DQ12: 1.3 µm; Aerosil® 150: 14 nm) in the present abstract version.